

2007

A Study of the Stability of Longitudinal Vorticies in a Poiseuille Flow Modulated by Periodic Wall Heating

Matthew L. Fotia
Western University

Follow this and additional works at: <https://ir.lib.uwo.ca/digitizedtheses>

Recommended Citation

Fotia, Matthew L., "A Study of the Stability of Longitudinal Vorticies in a Poiseuille Flow Modulated by Periodic Wall Heating" (2007). *Digitized Theses*. 4478.
<https://ir.lib.uwo.ca/digitizedtheses/4478>

This Thesis is brought to you for free and open access by the Digitized Special Collections at Scholarship@Western. It has been accepted for inclusion in Digitized Theses by an authorized administrator of Scholarship@Western. For more information, please contact wlsadmin@uwo.ca.

**A Study of the Stability of Longitudinal Vortices
in a Poiseuille Flow
Modulated by Periodic Wall Heating**

(Spine title: Stability of a Poiseuille Flow with Periodic Wall Heating)

(Thesis format: Monograph)

By

Matthew L. Fotia
B.E.Sc., Hon. B.Sc.

Graduate Program in Engineering Science
Dept. of Mechanical & Materials Engineering

A thesis submitted in partial fulfilment
of the requirements for the degree of
Master of Engineering Science.

Faculty of Graduate Studies
The University of Western Ontario
London, Ontario, Canada

© Matthew L. Fotia 2007

THE UNIVERSITY OF WESTERN ONTARIO
FACULTY OF GRADUATE STUDIES

Certificate of Examination

Supervisor

Examiners

Dr. J .M. Floryan

Dr. M. Asai

Supervisory Committee

Dr. C. Zhang

Dr. B. Tryggvason

The thesis by

Matthew L. Fotia

entitled

**A Study of the Stability of Longitudinal Vortices in a Poiseuille Flow
Modulated by Periodic Wall Heating**

is accepted in partial fulfilment of the requirements for the degree of Master of
Engineering Science.

Date: _____

Dr. J. Yang
Chair of the Thesis Examination Board

Abstract

The ability to enhance heat-transfer processes with a minimal amount of added energy expenditure has application in many industrial sectors. One avenue to pursue this is in the use of passive controls to trigger the promotion of secondary topological structures in a flow. These structures can be beneficial to the mixing and the transfer of heat into and out of the working fluid. In this instance, the influence of period heating and cooling patterns in the direction of the flow is considered with regard to the linear-stability of longitudinal vortices in a Poiseuille flow. The growth or suppression of these particular structures is investigated over an applicable range of flow parameters. Two physical arrangements are considered, the first case is that of only periodic wall heating being applied to the channel, while the second investigates the periodic heating's impact on the stability of the flow in the instance of a heated lower wall.

Keywords: Hydrodynamic stability, Stratified flow, Poiseuille flow, Passive flow control, Heating modulations, Longitudinal vortices, Longitudinal rolls.

Epigraph

Computers are useless. They can only give you answers.

- Pablo Picasso

Table of Contents

CERTIFICATE OF EXAMINATION	ii
ABSTRACT & KEYWORDS	iii
EPIGRAPH	iv
TABLE OF CONTENTS	v
LIST OF TABLES	vi
LIST OF FIGURES	vii
1 INTRODUCTION	1
2 OVERVIEW OF DENSITY-DRIVEN INSTABILITY.....	4
2.1 THE RAYLEIGH-TAYLOR INSTABILITY.....	4
2.1.1 <i>The Density Driven Problem</i>	4
2.1.2 <i>Thermal Effects on Stability</i>	10
2.1.3 <i>Modern Stability Simulation</i>	14
2.1.3.1 <i>Extension to Three-Dimensions</i>	14
2.1.3.2 <i>The Influence of Phase Change</i>	16
2.2 THE DENSITY-DRIVEN INSTABILITY OF A FLUID IN MOTION	21
3 MATHEMATICAL FORMULATION	28
3.1 MODULATED FLOW FORMULATION	28
3.2 IMPLEMENTATION OF THE NUMERICAL SOLUTION.....	37
3.2.1 <i>The Streamfunction</i>	37
3.2.2 <i>Numerical Solver</i>	41
3.3 FORMULATION OF THE LINEAR-STABILITY PROBLEM.....	43
3.4 NUMERICAL SOLUTION TECHNIQUE	49
3.4.1 <i>Preparation of the Governing Equations for Numerical Solution</i>	49
3.4.2 <i>The Eigenvalue Solver</i>	52
3.4.3 <i>Error and its Control in the Numerical Solution</i>	52
4 DISCUSSION OF THE STABILITY CHARACTERISTICS OF THE FLOW.....	54
4.1 THE TWO CASES	54
4.2 POISEUILLE FLOW SUBJECTED TO PERIODIC HEATING MODULATIONS.....	54
4.2.1.1 <i>Equivalency of Two Flow Arrangements</i>	55
4.2.2 <i>Definition of the 'Critical' Stability Condition</i>	57
4.2.3 <i>Reynolds Number Dependence</i>	59
4.2.4 <i>Prandtl Number Dependence</i>	62
4.2.5 <i>Disturbance Wavenumber Dependence</i>	63
4.3 POISEUILLE FLOW SUBJECTED TO UNSTABLE THERMAL STRATIFICATION AND PERIODIC HEATING MODULATIONS	65
4.3.1 <i>The Influence of the Amplitude of Heating Modulations</i>	65
4.3.2 <i>Reynolds Number & Disturbance Wavenumber Dependence</i>	66
5 SUMMARY AND CONCLUSIONS	68
6 BIBLIOGRAPHY.....	71
7 APPENDIX.....	73
8 CURRICULUM VITAE.....	105

List of Tables

TABLE 1 - THE MODES OF MAXIMUM INSTABILITY FOR THE CASE $v_2 = v_1$ AND $\rho_2 > \rho_1$. [4].....9

List of Figures

FIGURE 1 - PHYSICAL ARRANGEMENT OF RAYLEIGH'S ORIGINAL INVESTIGATION	5
FIGURE 2 - THE DEPENDENCE OF THE RATE OF GROWTH, N (MEASURED IN THE UNIT $(G^2/\nu)^{1/2}$), OF A DISTURBANCE ON ITS WAVE NUMBER, K (MEASURED IN THE UNIT $(G/\nu^2)^{1/2}$), IN THE CASE WHERE THE UPPER FLUID IS MORE DENSE AND THE KINEMATIC VISCOSITIES ARE THE SAME. THE CURVES LABELLED 1, 2, 3 AND 4 ARE FOR VALUES OF	8
FIGURE 3 - THE DEPENDENCE OF THE RATE OF DECAY, $-RE(N)$ (MEASURED IN THE UNIT $(G^2/\nu)^{1/2}$) OR THE REAL COMPONENT OF THE EIGENVALUE, OF A DISTURBANCE ON ITS WAVE NUMBER, K (MEASURED IN THE UNIT $(G/\nu^2)^{1/2}$), IN THE CASE WHERE THE LOWER FLUID IS MORE DENSE AND THE KINEMATIC VISCOSITIES ARE THE SAME. THE CURVES LABELLED 2, 4, 5, 6 AND 7 ARE FOR VALUES OF $(\alpha_1 - \alpha_2) = 0.05, 0.15, 0.25, 0.50$ AND 0.90 RESPECTIVELY.[4]	9
FIGURE 4 - THE INITIAL RATES OF GROWTH, N_1 , FOR DISTURBANCES OF WAVE NUMBER K_1 IN UNSTABLY STRATIFIED LAYERS, PLOTTED IN DIMENSIONLESS FORM FOR A RANGE OF VALUES OF THE RAYLEIGH NUMBER, A_1 , AND FOR PRANDTL NUMBER OF UNITY, $\sigma = 1$. [5].....	12
FIGURE 5 -THE DEPENDENCE OF THE RATE OF GROWTH FACTOR (N_1) ON THE WAVE NUMBER (K_1) FOR VARIOUS VALUES OF THE PRANDTL NUMBER (σ) IN THE CASE OF MARGINAL STABILITY (I.E. $A_{1c} = 27/4$) FOR AN UNSTABLY STRATIFIED LAYER. [5].....	13
FIGURE 6 - SIMULATION OF A RAYLEIGH-TAYLOR INSTABILITY FOR AN INITIAL 2-D PERTURBATION OF THE INTERFACE WITH AN AMPLITUDE OF 10^{-2} WITH ADDITION OF NORMALLY DISTRIBUTED RANDOM NOISE WITH A VARIANCE 5×10^{-4} . NUMBERS AT THE TOP ARE NON-DIMENSIONAL TIMES, SHADING SHOWS RELATIVE HEIGHTS OF THE INTERFACE. [6].....	15
FIGURE 7 - PHASE DIAGRAM PREDICTING THE SURVIVAL OF AN INITIAL SINUSOIDAL 2-D PERTURBATION OVER BACKGROUND NOISE DEPENDING ON ITS INITIAL AMPLITUDE (A_0), INITIAL WAVELENGTH (λ_{2D}) AND THE INITIAL AMPLITUDE OF THE LARGEST DOMINANT NORMAL MODE PRESENT IN THE NOISE A_0^{DOM} . CROSSES SHOW RESULTS OF NUMERICAL SIMULATIONS, WHERE THE INITIAL PERTURBATION SURVIVED, WHEREAS OPEN CIRCLES, X-MARKS AND SQUARES SHOW RESULTS WHERE THE INITIAL PERTURBATION BROKE UP INTO 2-D, INTERMEDIATE OR 3-D STRUCTURES. INSETS SHOW THE INTERFACE AT THE END OF NUMERICAL SIMULATIONS THAT RESULTED IN 3-D, INTERMEDIATE AND 2-D STRUCTURE RESPECTIVELY. [6]	16
FIGURE 8 - OZEN & NARAYANAN'S PHYSICAL MODEL. [7].....	16
FIGURE 9 - THE DEPENDENCE OF THE COEFFICIENT α^* ON THE WAVENUMBER FOR INFINITELY DEEP FLUID LAYERS. [7]	20
FIGURE 10 - THE DEPENDENCE OF THE COEFFICIENT α^* ON THE WAVENUMBER FOR FLUID LAYERS WITH FINITE DEPTHS, WHERE $D^L = 1MM$ AND $D^G = 1MM$. [7].....	20
FIGURE 11 - RELATION BETWEEN THE CRITICAL RAYLEIGH NUMBER AND THE WAVENUMBER. [9].....	21
FIGURE 12 - THE NUSSELT NUMBER AS A FUNCTION OF RAYLEIGH NUMBER, REPRESENTED AS A FRACTION OF THE CRITICAL VALUE. [8]	22
FIGURE 13 - PITCH OF THE VORTEX ROLLS. [8]	22
FIGURE 14 - FLOW PATTERNS FOR VARIOUS PARAMETERS ACROSS CRITICAL CONDITIONS FOR TRANSITION. [8]	23
FIGURE 15 - THE NUSSELT NUMBER OF THE FLOW VERSUS RAYLEIGH NUMBER. [10].....	24
FIGURE 16 - STABILITY BOUNDARIES FOR LONGITUDINAL VORTEX ROLLS, CRITICAL RAYLEIGH NUMBER, R_A , VERSUS HEATING PARAMETER, μ . [14]	24
FIGURE 17 - STABILITY BOUNDARIES FOR LONGITUDINAL VORTEX ROLLS, CRITICAL WAVENUMBER, A , VERSUS HEATING PARAMETER, μ . [14]	25
FIGURE 18 - FORMATION OF SECONDARY FLOW PATTERNS WITH FREE-CONVECTION EFFECT FOR THE CASE OF NEGATIVE μ AND $h = 1$ IN. [13]	25
FIGURE 19 - SECONDARY FLOW PATTERS FOR THE CASE $\mu = 0$ AND $h = 1$ IN. [13].....	26
FIGURE 20 - THE THREE-DIMENSIONAL STABILITY BOUNDARY FOR THE CASE OF UNSTABLE STRATIFICATION. [15]	27
FIGURE 21 - PHYSICAL ARRANGEMENT OF THERMALLY MODULATED FLOW.....	28

FIGURE 22 - NEUTRAL GROWTH-RATE CURVE, RAYLEIGH NUMBER VERSUS DISTURBANCE WAVENUMBER, β , FOR PRANDTL NUMBER, Pr , EQUAL TO 0.71, REYNOLDS NUMBER EQUAL TO 1000 AND HEATING WAVENUMBER, α , EQUAL TO 5 WITH THE CRITICAL RAYLEIGH NUMBER, RA_c , AND CRITICAL VORTEX WAVENUMBER, β_c , INDICATED.58

FIGURE 23 - NEUTRAL GROWTH-RATE CURVES, RAYLEIGH NUMBER VERSUS DISTURBANCE WAVENUMBER, β , FOR PRANDTL NUMBER, Pr , EQUAL TO 0.71, REYNOLDS NUMBER EQUAL TO 2000 AND VARIOUS HEATING WAVENUMBERS, α59

FIGURE 24 - CRITICAL STABILITY CONDITIONS, REYNOLDS NUMBER, Re , VERSUS CRITICAL RAYLEIGH NUMBER, RA_c , FOR PRANDTL NUMBER, Pr , EQUAL TO 0.71 AND SELECTED VALUES OF HEATING WAVENUMBER, α60

FIGURE 25 - STREAMFUNCTION, SOLID LINES, AND ISOTHERMS, DASH-DOTTED LINES, FOR $Re = 1000$, $RA = 50650$, $Pr = 0.71$ AND $\alpha = 1$61

FIGURE 26 - STREAMFUNCTION, SOLID LINES, AND ISOTHERMS, DASH-DOTTED LINES, FOR $Re = 10$, $RA = 3500$, $Pr = 0.71$ AND $\alpha = 1$61

FIGURE 27 - CRITICAL STABILITY CONDITIONS, REYNOLDS NUMBER, Re , VERSUS CRITICAL RAYLEIGH NUMBER, RA_c , FOR A HEATING WAVENUMBER, α , EQUAL TO 1 AND SELECTED VALUES OF PRANDTL NUMBER, Pr62

FIGURE 28 - CRITICAL STABILITY CONDITIONS, HEATING WAVENUMBER, α , VERSUS CRITICAL RAYLEIGH NUMBER, RA_c , FOR PRANDTL NUMBER, Pr , EQUAL TO 0.71 AND SELECTED VALUES OF REYNOLDS NUMBER, Re64

FIGURE 29 - CRITICAL STABILITY CONDITIONS, REYNOLDS NUMBER, Re , VERSUS RAYLEIGH NUMBER, RA , FOR PRANDTL NUMBER, Pr , EQUAL TO 0.71, HEATING WAVENUMBER, α , EQUAL TO 1 AND SELECTED AMPLITUDES OF MODULATED HEATING, T_M66

FIGURE 30 - CRITICAL STABILITY CONDITIONS, HEATING WAVENUMBER, α , VERSUS CRITICAL RAYLEIGH NUMBER, RA , FOR PRANDTL NUMBER, Pr , EQUAL TO 0.71, HEATING MODULATION AMPLITUDE, T_M , EQUAL TO 15% AND VARIOUS REYNOLDS NUMBERS, Re67

1 Introduction

This thesis will consider the promotion or suppression of longitudinal vortices in a Poiseuille flow modulated by periodic heating along the walls of the channel. Two thermal configurations will be examined; the first is where only periodic variations in temperature, in the direction of the flow, are imposed, while the second has an additional mean temperature difference between the two walls of the channel.

The most appropriate place to begin our discussion is to consider the classical Rayleigh-Taylor instability problem. One of the key mechanisms in the flow that will have bearing on its stability characteristics is the interplay between regions of varying fluid density, caused by the non-uniformity of the heating being applied. The Rayleigh-Taylor instability is one of the most basic interactions found in fluid mechanics, with elements of its influence seen across many disciplines. The instability is derived from the behaviour of the equilibrium of an incompressible fluid of variable density. An important special case of this mechanism is the superposition of two fluids of different densities, one over the other, examining the stability of the interface between the layers of fluid.

The first successful attempt to analyse the linear-stability of a variable density fluid was performed by Rayleigh [1], on an inviscid fluid. The procedure given by Rayleigh still forms the basis of such analyses, in that first the base flow is defined and then an eigenvalue problem is posed such that small perturbations are superposed on the flow. The eigenvalues of this problem describe the growth or decay of the perturbations. Chandrasekhar [2] took his investigation to the next level by including viscous effect in his model, while Hide [3] proposed an approximate theory based on Chandrasekhar's work. In his text *Hydrodynamic & Hydromagnetic Stability*, Chandrasekhar [4] provides a comprehensive discussion of the physics of both a heavy fluid overlying a lighter fluid, which is inherently unstable, as well as a light fluid above a heavier one, which is the stabilizing case.

A key ingredient missing in these treatments is the inclusion of the mechanism causing the stratification of the fluids density. Morton [4] proposes that to adequately

model the stability of a variable density fluid, the diffusive nature of the stratification mechanism must be included in the description of the system.

A more modern approach to investigating the Rayleigh-Taylor instability has been to extend the system into three-dimensions. Kaus & Podladchikov [6] undertook this in a two-step iterative process, cycling between Chandrasekhar's [2] stability criteria and then using this information about the model form of the disturbances to update the base flow. They used a hybrid finite-difference/spectral method to solve for the now finite-amplitude disturbances in what would be an otherwise stationary volume of fluid.

Another more recent twist to the classical problem has been to add the effects of a phase change into the model. Ozen & Narayanan [7] included a liquid-gas phase change into their two-dimensional analyse of the Rayleigh-Taylor instability. They found that an important aspect of including such mechanisms in a model meant for a stability analysis is that the solution methods used must reinforce the physics of the system being examined and not impose extraneous constraints on the mechanics of the system.

As might be expected, in moving from the case of an initially stagnant fluid to that of a moving fluid an experimental analysis can most readily be used to investigate the physics of the flow. Mori & Uchida [8] did just this for the instance of a fluid heated from below. They quantified both the critical parameters for the formation of rolls, oriented with their axis in the direction of the flow, and the associated increase in the transfer of heat between the upper and lower walls of the channel due to the improved mixing provided by these rolls.

Pellow & Southwell [9] took an analytical approach to this problem of a unstably stratified flow in a horizontal channel. Their approximation of the increase in heat-transfer was shown to match well with the experimental data available, as well as the critical flow parameters derived for the formation of longitudinal rolls. Ostrach & Kamotani [10] and Silveston [11] undertook further experiments in which the flow was directly observed during the formation of the rolls.

These analytical and experimental results coupled with the numerical work of Hwang & Cheng [12] provide a more than adequate description of the density-driven instability present in a flowing fluid heated from below. This body of work will give a

good source of material to verify the validity of the results for a channel flow subjected to an additional pattern of heating modulations along the walls.

As an extension to the classical case of a flowing fluid heated from below, Akiyama, Hwang & Cheng [13] experimentally investigated this arrangement with an additional thermal gradient in the direction of the flow. Nakayama, Hwang & Cheng [14] provided a numerical analysis of this arrangement. The application of this work to heat exchanger optimization is apparent in the presentation of the result in both cases.

A good summary of the behaviour of the classical case is given by Gage & Reid [15]. It includes a discussion of the form of initial instability, in particular whether rolls or waves will form, as well as treating both the case of heating from below and above. The three-dimensional character of the instabilities is examined spatially with regard to their orientation in channel.

The following chapter contains a more in-depth discussion of the classical work surrounding both the Rayleigh-Taylor instability and the density-driven instability of a flowing fluid. This thesis will build on the classical case of a Poiseuille flow heated from below by applying an alternating pattern of heating, and cooling, to the walls of a horizontal channel, with the particular interest of promoting the formation of longitudinal vortices to improve the quality of the mixing of the fluid.

A mathematical model of the current problem is posed and a numerical solution method implemented which adequately describe both the mechanics and the physics of the flow. A linear-stability analysis is then performed to describe the impact of the applied heating modulations on the formation of longitudinal vortices. A discussion follows on the influence of the various flow parameters on the behaviour of the flow with suggestions for the application this flow mechanism as a method for the improvement of heat-transfer processes.

2 Overview of Density-Driven Instability

This section contains a more in-depth discussion of the Rayleigh-Taylor instability and the density-driven instability of a flowing fluid as a basis for the later investigation of the influence of heating modulations on the formation of longitudinal vortices in a horizontal Poiseuille flow. A focus is placed on the procedures used by the various investigators to obtain the critical flow parameters leading to the instability of the fluid system. The critical conditions themselves will be important, as in future chapters their agreement with the problem posed in this thesis will be examined and used as validation for a portion of the work.

2.1 *The Rayleigh-Taylor Instability*

The classical theory of the Rayleigh-Taylor instability was formed as a direct extension of Lord Rayleigh's original 1883 work on this phenomenon. The inclusion of different fluid properties in the modelling of the instability will be examined with regard to their influence on the ability of the theory to predict the growth of unstable behaviour in the fluid system.

More modern aspects of the Rayleigh-Taylor instability will be examined, particularly the interplay between finite-sized two-dimensional and three-dimensional structures in the instability induced fluid motions; as well as the provisions that may be made for a change in the phase of the fluid under investigation.

2.1.1 The Density Driven Problem

The Rayleigh-Taylor instability arises from an investigation of the character of the equilibrium of a stratified heterogeneous fluid. A static state is considered in which an incompressible fluid of variable density is arranged in horizontal layers. The density and pressure are both functions of the vertical co-ordinate only.

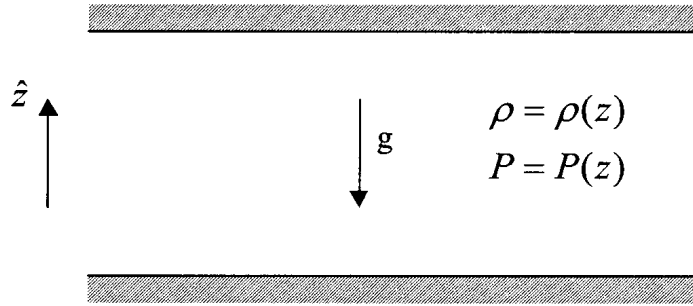


Figure 1 - Physical Arrangement of Rayleigh's Original Investigation

Many of the authors that will be discussed switch readily between the physical case of a continuously stratified fluid and that of two superposed layers of different densities. An effort has been made to focus, where possible, on the case of continuous stratification; however, much useful insight may still be gleaned from the special case of two fluid layers.

The stability of this state can be investigated by supposing that the system is initially at equilibrium and is then perturbed. This problem was first posed mathematically by Lord Rayleigh in his 1883 paper on the "Investigation of the character of the equilibrium of an incompressible heavy fluid of variable density", in which he examined the case of an inviscid fluid [1]. Later, the viscous case was treated formally by Chandrasekhar [2] and Hide [3] in their 1955 complementary papers. The forthcoming derivation is taken from Chandrasekhar but follows directly from Rayleigh's original work.

Let the density at any point in the fluid be $\rho + \delta\rho$, and δP be the corresponding increment in the pressure. The equations of motion and continuity are:

$$\rho \frac{\partial u_i}{\partial t} = -\frac{\partial \delta P}{\partial x_i} + \frac{\partial P_{ik}}{\partial x_k} - g \delta \rho \lambda_i, \quad (1.1)$$

$$\frac{\partial u_i}{\partial x_i} = 0, \quad (1.2)$$

where 'g' is the acceleration due to gravity and the unit vector $\hat{\lambda}$ is in the direction of the vertical. P_{ik} is the viscous stress tensor given by

$$P_{ik} = \mu \left(\frac{\partial u_k}{\partial x_i} + \frac{\partial u_i}{\partial x_k} \right), \quad (1.3)$$

with μ being the coefficient of viscosity.

One further equation is supplied to ensure that the density of every particle remains unchanged,

$$\frac{\partial \delta \rho}{\partial t} + u_i \frac{\partial \rho}{\partial x_i} = 0. \quad (1.4)$$

Inserting (1.3) into (1.1), the equations of motion reduce to:

$$\rho \frac{\partial u_i}{\partial t} = -\frac{\partial \delta P}{\partial x_i} + \mu \nabla^2 u_i + \left(\frac{\partial u_k}{\partial x_i} + \frac{\partial u_i}{\partial x_k} \right) \frac{\partial \mu}{\partial x_k} - g \delta \rho \lambda_i, \quad (1.5)$$

and since $\frac{\partial \mu}{\partial x_k} = \lambda_k \frac{d\mu}{dz}$, this becomes

$$\rho \frac{\partial u_i}{\partial t} = -\frac{\partial \delta P}{\partial x_i} + \mu \nabla^2 u_i + \left(\frac{\partial w}{\partial x_i} + \frac{\partial u_i}{\partial z} \right) \frac{d\mu}{dz} - g \delta \rho \lambda_i, \quad (1.6)$$

where $w = \lambda_i u_i$ is the z-component of the velocity.

The field equations are now, in component form:

$$\rho \frac{\partial u}{\partial t} = -\frac{\partial \delta P}{\partial x_i} + \mu \nabla^2 u + \left(\frac{\partial w}{\partial x} + \frac{\partial u}{\partial z} \right) \frac{d\mu}{dz}, \quad (1.7)$$

$$\rho \frac{\partial v}{\partial t} = -\frac{\partial \delta P}{\partial y} + \mu \nabla^2 v + \left(\frac{\partial w}{\partial y} + \frac{\partial v}{\partial z} \right) \frac{d\mu}{dz}, \quad (1.8)$$

$$\rho \frac{\partial w}{\partial t} = -\frac{\partial \delta P}{\partial z} + \mu \nabla^2 w + 2 \frac{\partial w}{\partial z} \frac{d\mu}{dz} - g \delta \rho, \quad (1.9)$$

$$\frac{\partial u}{\partial x} + \frac{\partial v}{\partial y} + \frac{\partial w}{\partial z} = 0, \quad (1.10)$$

$$\frac{\partial \delta \rho}{\partial t} = -w \frac{\partial \rho}{\partial z}. \quad (1.11)$$

The state of the fluid, as it is currently, is perturbed by a disturbance in the form of normal modes, $e^{(ik_x x + ik_y y + nt)}$. For solutions having this dependence on x , y and t , equations (1.7) through (1.11) become:

$$ik_x \delta P = -n\rho u + \mu(D^2 - k^2)u + (D\mu)(ik_x w + Du), \quad (1.12)$$

$$ik_y \delta P = -n\rho v + \mu(D^2 - k^2)v + (D\mu)(ik_y w + Dv), \quad (1.13)$$

$$D\delta P = -n\rho w + \mu(D^2 - k^2)w + 2(D\mu)(Dw) - g\delta\rho, \quad (1.14)$$

$$ik_x u + ik_y v = -Dw, \quad (1.15)$$

$$n\delta\rho = -wD\rho, \quad (1.16)$$

where $k^2 = k_x^2 + k_y^2$ and $D = \frac{d}{dz}$.

Further reduction is done by multiplying (1.12) and (1.13) by $-ik_x$ and $-ik_y$ respectively and adding;

$$k^2 \delta P = [-n\rho + \mu(D^2 - k^2)]Dw + 2(D\mu)(Dw) + \frac{g}{n}(D\rho)w, \quad (1.17)$$

and combining equation (1.14) and (1.16) gives

$$D\delta P = -n\rho w - \mu(D^2 - k^2)w + 2(D\mu)(Dw) + \frac{g}{n}(D\rho)w. \quad (1.18)$$

The pressure terms are eliminated between these equations producing

$$\begin{aligned} D \left\{ \left[\rho - \frac{\mu}{n}(D^2 - k^2) \right] Dw - \frac{1}{n}(D\mu)(D^2 + k^2)w \right\} \\ = k^2 \left\{ -\frac{g}{n^2}(D\rho)w + \left[\rho - \frac{\mu}{n}(D^2 - k^2) \right] w - \frac{2}{n}(D\mu)Dw \right\}. \end{aligned} \quad (1.19)$$

This single equation now governs the stability of the fluid. For a fluid confined between two rigid surfaces, the no-penetration condition requires that $w = 0$, while the no-slip condition gives $Dw = 0$, through continuity, at the boundary. For a free-surface the

no-slip is replaced by the requirement that the tangential viscous stress vanish on it, providing that $D^2w = 0$ on such a boundary.

In the inviscid limit as $\mu \rightarrow 0$, equation (1.19) reduces to that given by Rayleigh

$$D(\rho Dw) - \rho k^2 w = -\frac{k^2 g}{n^2} (D\rho)w, \quad (1.20)$$

with the boundary conditions requiring only that $w = 0$.

It is at this point that the literature can be split into pre- and post- computer revolution. Many of the earlier authors delve into an analysis of equation (1.19) and the characteristic value problem it poses, through the calculus of variations. The calculus of variations, in short, seeks the minimum energy state of a system given some particular constraints, providing an eigenfunction defining the flow-field, and as such an expression is produced for the eigenvalue n which is necessary for stability to exist.

The more modern literature opts for a numerical analysis of the system either in the form of numerical solutions to the eigenvalue problem posed by (1.19) or full-out direct numerical simulations of the growth of disturbances in the medium. In the latter case a different formulation than has been discussed above is usually used.

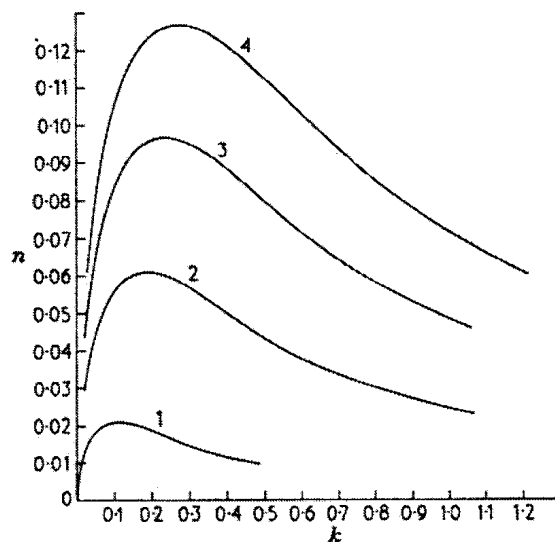


Figure 2 - The dependence of the rate of growth, n (measured in the unit $(g^2/\nu)^{1/2}$), of a disturbance on its wave number, k (measured in the unit $(g/\nu^2)^{1/2}$), in the case where the upper fluid is more dense and the kinematic viscosities are the same. The curves labelled 1, 2, 3 and 4 are for values of

$$(\rho_2 - \rho_1) / (\rho_2 + \rho_1) = (\alpha_2 - \alpha_1) = 0.01, 0.05, 0.10 \text{ and } 0.15 \text{ respectively. [4]}$$

Figure 2 shows the relationship between k and n for the “unstably stratified” (sic) case of a layer of dense fluid above a lighter one, $\rho_2 > \rho_1$, while Figure 3 shows it for the stably stratified case.

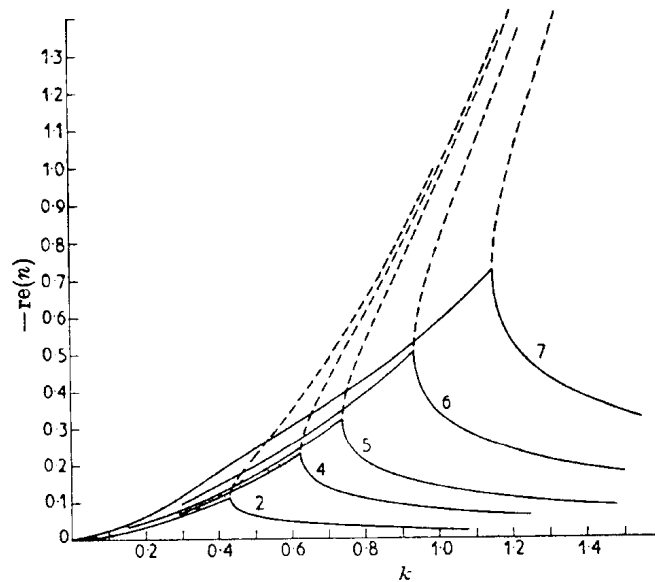


Figure 3 - The dependence of the rate of decay, $-re(n)$ (measured in the unit $(g^2/\nu)^{1/2}$) or the real component of the eigenvalue, of a disturbance on its wave number, k (measured in the unit $(g/\nu^2)^{1/2}$), in the case where the lower fluid is more dense and the kinematic viscosities are the same. The curves labelled 2, 4, 5, 6 and 7 are for values of $(\alpha_1 - \alpha_2) = 0.05, 0.15, 0.25, 0.50$ and 0.90 respectively. [4]

Chandrasekhar also provides a table listing the modes of maximum instability for the unstable case.

Table 1 - The modes of maximum instability for the case $\nu_2 = \nu_1$ and $\rho_2 > \rho_1$. [4]

$\frac{\rho_2 - \rho_1}{\rho_2 + \rho_1}$	$k(\nu^2/g)^{1/3}$	$n(\nu/g^2)^{1/3}$
0.01	0.1134	0.02081
0.05	0.1939	0.06086
0.10	0.2442	0.09663
0.15	0.2793	0.1267
0.25	0.3304	0.1782
0.50	0.4112	0.2842
0.90	0.4806	0.4265
1.00	0.4907	0.4599

Many authors also have examined the superposition of two layers of fluid of different densities with the inclusion of surface tension at the interface between the fluids. Chandrasekhar gives this case a rigorous treatment in his 1961 text *Hydrodynamic & Hydromagnetic Stability* [4], this however is not the focus of the current discussion and is left to the reader's interest.

2.1.2 Thermal Effects on Stability

B.R. Morton [5] points out that although the above derivation satisfactorily describes the stability mechanism present in a continuously stratified heavy viscous fluid, it does not take into account any diffusion of the property causing the variations in density. This means that it cannot be used in the case of continuous stratification without refinement as the stratification mechanism itself, be it thermal, by the dissolution of a solid or any other means, influences the system's stability characteristics.

To address this issue for thermally stratified flows Morton re-derived the governing stability equations, but unlike those discussed above the energy balance equation is included in the analysis,

$$\frac{\partial T}{\partial t} + u_i \frac{\partial T}{\partial x_i} = \kappa \nabla^2 T, \quad (1.21)$$

where $T = T(z)$ is the fluid temperature and κ is the thermal diffusivity.

Following a similar procedure as before, but this time imposing variations of the form $X = \bar{X} + \hat{X}e^{(ik_x x + ik_y y + nt)}$ are used for all the state variables in the problem including temperature, gives the governing equation

$$[-n + \kappa(D^2 - k^2)][-n + \nu(D^2 - k^2)](D^2 - k^2)w = \gamma k^2 w D T, \quad (1.22)$$

once the assumption that any disturbance quantities, for instance \hat{X} , are small is used to linearize the system of field equations, and where $\gamma = \beta g$, with β being the coefficient of volumetric expansion.

This analysis now contradicts Hide's [3] findings, which were that the stability of the system could be characterized in terms of the Grashof number alone. Morton [5]

shows that the characterization of the stability of the fluid must be done in terms of the Rayleigh (or equivalent), Reynolds and Prandtl number.

In this way the importance of the stratifying mechanism is reinforced. Hide acknowledges this but ignores these diffusive effects. The temperature diffusion gives rise to a damping effect in the flow in real fluid. In his analysis, Morton also concludes that the non-linearities in the temperature profile can have little relative effect in modifying the critical value of the Rayleigh number required for marginal stability. He does this by assuming a temperature profile across the layer of fluid and showing that the effects of a non-linear profile have little influence relative to the same profile, less the non-linear components.

This approach is interesting as it is in contrast to applying temperature conditions on the boundaries of the fluid, and solving for the distribution of temperature in between. Instead, the boundary conditions are implied by the profile being examined.

Morton applies a general variational principle to his characteristic value problem that produces an equation for the disturbance growth-rate, N , in an unstable thermally stratified fluid,

$$N = \frac{1}{2}(K^2 + M^2) \left\{ -(\sigma^{1/2} + \sigma^{-1/2}) + \left[(\sigma^{1/2} - \sigma^{-1/2}) - \frac{4K^2 A^*}{(K^2 + M^2)^3} \right]^{1/2} \right\}, \quad (1.23)$$

where: $A = \gamma h^3 \frac{\Delta T}{\kappa \nu}$ - Rayleigh Number,

$$A^* = AB,$$

$$\sigma = \frac{\nu}{\kappa} \quad - \text{Prandtl Number},$$

$$B = \int_{-1/2}^{1/2} b(z) \frac{\cos^2}{\sin^2} MZ dZ \quad - \text{“Entire” Profile Number},$$

$$b\left(\frac{z}{h}\right) = \frac{hDT}{\Delta T} \quad - \text{“Local” Profile Number},$$

$\Delta T = |T_o - T_1|$ - Absolute Temperature difference between upper and lower boundary,

$$M = m\pi,$$

$$\kappa = hk,$$

h - Depth of Fluid,

$$Z = \frac{z}{h}.$$

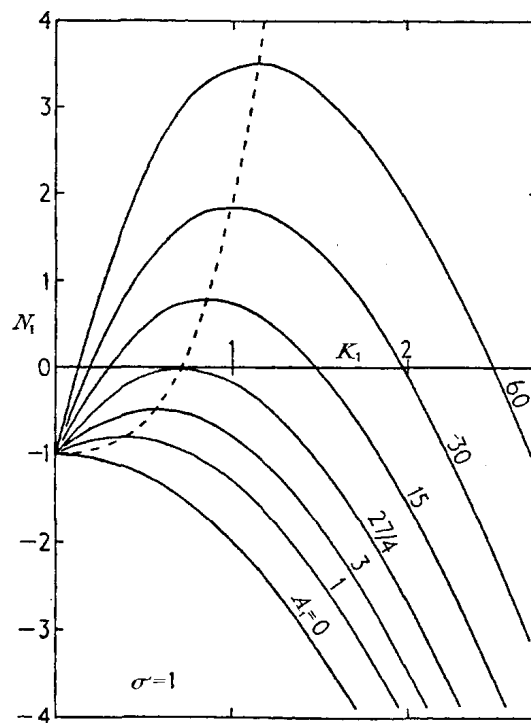


Figure 4 - The initial rates of growth, N_1 , for disturbances of wave number K_1 in unstably stratified layers, plotted in dimensionless form for a range of values of the Rayleigh number, A_1 , and for Prandtl number of unity, $\sigma = 1$. [5]

The resulting family of curves for various Rayleigh numbers is shown in Figure 4 for:

$$M = \pi, \quad K_1 = \frac{K}{\pi}, \quad A_1 = -\frac{A^*}{\pi^4}, \quad N_1 = \frac{N}{\pi^2}.$$

The critical Rayleigh number, below which all wave numbers will be damped out, is $A_{1c} = \frac{27}{4}$. If $A_1 > A_{1c}$, a band of wave numbers exist for which disturbances will be amplified.

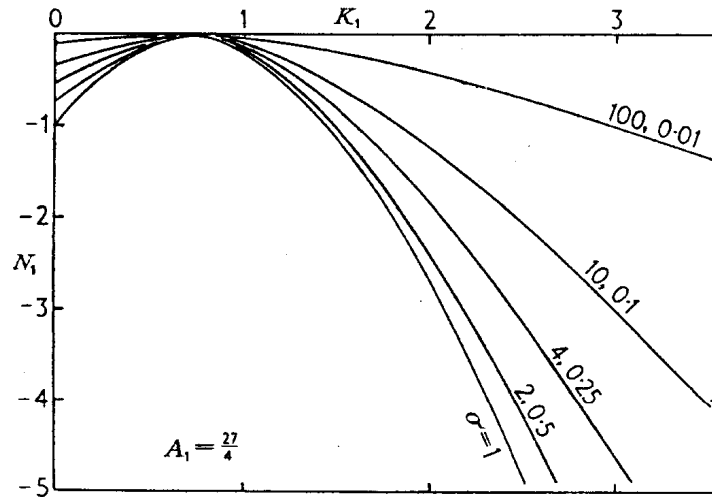


Figure 5 -The dependence of the rate of growth factor (N_1) on the wave number (K_1) for various values of the Prandtl number (σ) in the case of marginal stability (i.e. $A_{1c} = 27/4$) for an unstably stratified layer. [5]

The effects of Prandtl number and wave number on the disturbance growth-rate is illustrated in Figure 5 for the critical Rayleigh number. As the Prandtl number increases the effect of wave number diminishes greatly, a good example of the damping the thermal diffusion provides for the system.

A point that should be discussed is the initial form of the perturbations used by all the authors mentioned so far. They all assume that the disturbances take the form of ‘small’ amplitude plane waves, or ‘normal modes’. Morton, in fact, assumes that the 2-D wave equation provides the eigenfunctions for the eigenvalue problem. The reasoning behind using this form as opposed to one which assumes vorticities, for example, is from experimental observation.

Experimentally, when a denser fluid is placed above one that is less dense, structures referred to as “fingers” of fluid are observed to protrude from one fluid into the other along the fluid-fluid interface. The best mathematical representation of these structures, at small amplitudes, is a plane wave. The second reason for this assumption is that plane waves are convenient to work with when faced with seeking an analytic

solution to an eigenvalue problem, stemming from work already done on many quantum mechanical problems.

2.1.3 Modern Stability Simulation

2.1.3.1 Extension to Three-Dimensions

Much of the modern research into the Rayleigh-Taylor instability is focused on taking the step from predicting the growth-rate of infinitesimally small perturbations to examining finite sized disturbances and their evolution in time. Kaus & Podladchikov [6] undertook the 3-D modelling of the Rayleigh-Taylor instability for a viscous fluid. Their simulation considered the arrangement of a layer of dense fluid above a lighter one. The simulation was broken down into a two-step process in which Chandrasekhar's [2] stability model is used to predict the point of onset of instability and the form of the disturbance through his modal analysis of the problem. This supplied the initial conditions for a combined finite-difference/spectral-method to study the evolution of these initial perturbations, which are now assumed to be of finite size. This takes the form

$$Z(x, y) = 0.5 + dh \cos(k_x, x) \cos(k_y, y), \quad (1.24)$$

where dh is a finite amplitude with the initial 2-D infinitesimal perturbations growing exponentially in the form $A(t) = A_0 e^{qt}$. The growth-rate q is defined as

$$q = \frac{(k^2 + 2)e^{-k} - e^{-2k} - 1}{4k[-2ke^{-k} + e^{-2k} - 1]}. \quad (1.25)$$

Since the classical theory represents the disturbances as plane waves in the horizontal plane, the study of the interplay between these 2-D disturbances and the 3-D disturbances that can be resolved in the finite-difference simulations, in particular the influence of random noise, becomes an important aspect in the study of the behaviour of the fluid. This is important as all the analysis described to this point assumes a pristine initial condition within the fluid.

Kaus & Podladchikov [6] developed a condition under which the initial 2-D perturbations will survive, and not be drowned out by 3-D noise,

$$\frac{\ln\left(\frac{A_o^{2D}}{0,5}\right)}{\ln\left(\frac{A_o^{dom}}{0,5}\right)} < \frac{q}{q_{dom}}, \quad (1.26)$$

with an initial amplitude A_o^{dom} for the largest dominant mode in the noise component. The noise was considered random, with a maximum of $q_{dom} \approx 0.03835$, if $k \approx 4.895$.

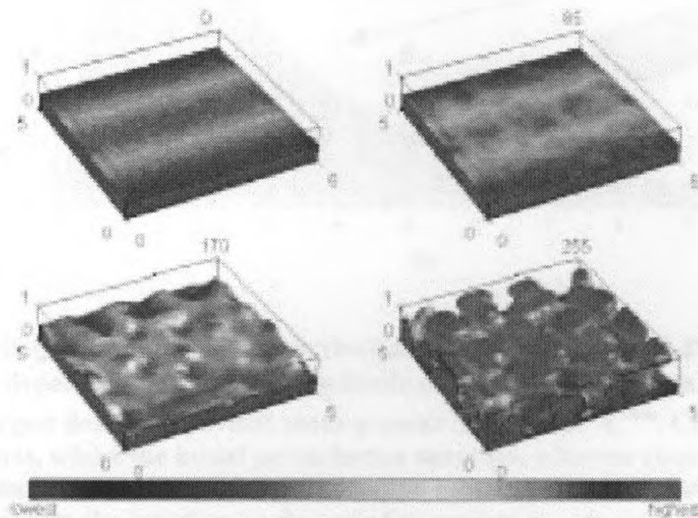


Figure 6 - Simulation of a Rayleigh-Taylor instability for an initial 2-D perturbation of the interface with an amplitude of 10^{-2} with addition of normally distributed random noise with a variance 5×10^{-4} . Numbers at the top are non-dimensional times, shading shows relative heights of the interface. [6]

This analytic condition is found by these authors to match the results of their full numerical simulations. Issues did arise in the numerical simulations when the structures formed in the fluid by the instability mechanism caused inversions or encapsulations in which a fluid of one density became locally both above and below the other. Figure 7 shows the fluid-fluid interface as the instability progresses in time.

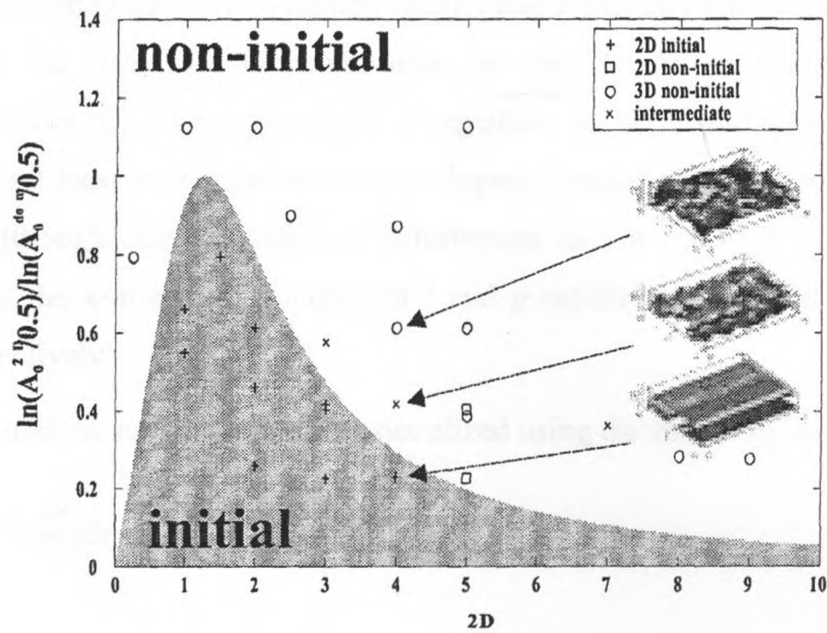


Figure 7 - Phase diagram predicting the survival of an initial sinusoidal 2-D perturbation over background noise depending on its initial amplitude (A_0), initial wavelength (λ_{2D}) and the initial amplitude of the largest dominant normal mode present in the noise A_0^{dom} . Crosses show results of numerical simulations, where the initial perturbation survived, whereas open circles, x-marks and squares show results where the initial perturbation broke up into 2-D, intermediate or 3-D structures. Insets show the interface at the end of numerical simulations that resulted in 3-D, intermediate and 2-D structure respectively. [6]

2.1.3.2 The Influence of Phase Change

Ozen & Narayanan [7] investigate the Rayleigh-Taylor instability from the perspective of its influence on the phase change of a fluid in a multiphase system. The unstable arrangement of a vapour underlying a layer of its own liquid is considered.

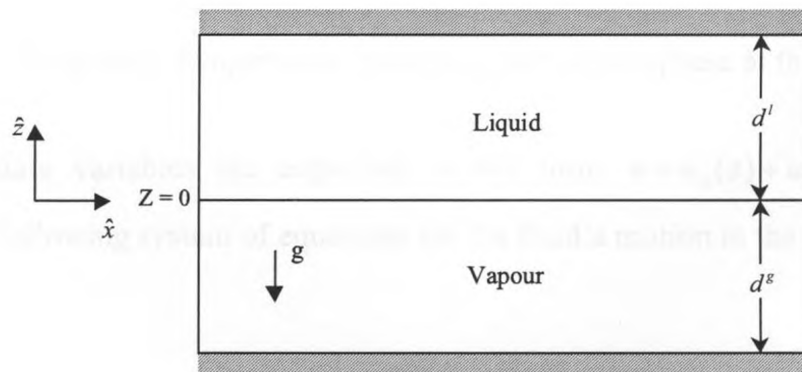


Figure 8 - Ozen & Narayanan's physical model. [7]

By considering the Navier-Stokes, energy and continuity equations in each phase, assuming that the fluids are incompressible, as well as the boundary and interface conditions between the phases, a system of equations is developed which assumes that there is no initial mass exchange between the layers. Linear stability theory is applied as by Morton, although only considering disturbances in the form of 1-D plane waves propagating in the x-direction. Superscript l and g represent the liquid and gas phase variables respectively.

The equations are first non-dimensionalized using the following scales:

$$\text{Length: } d = \frac{\mu^l \kappa^l}{\gamma},$$

$$\text{Velocity: } \bar{v} = \frac{\kappa^l}{d},$$

$$\text{Time: } \bar{t} = \frac{d}{v},$$

$$\text{Temperature: } \tilde{T} = \frac{T}{\frac{dT_o^g}{dz}},$$

where: μ^l - Liquid viscosity,

κ^l - Liquid thermal diffusivity,

γ - Surface tension between phases,

$\frac{dT_o^g}{dz}$ - Base-State temperature gradient in the vapour phase at the interface.

The state variables are expanded in the form $u = u_o(z) + u_1(z)e^{nt} e^{ik_x x}$. This produces the following system of equations for the fluid's motion in the neutral state, (i.e. $n = 0$).

Navier-Stokes:

$$\left(\frac{d^2}{dz^2} - \omega^2\right)^2 v'_{z1} = 0 \quad \text{and} \quad \left(\frac{d^2}{dz^2} - \omega^2\right)^2 v^g_{z1} = 0. \quad (1.27)$$

Energy:

$$\left(\frac{d^2}{dz^2} - \omega^2\right)^2 \tilde{T}'_{z1} = kv'_{z1} \quad \text{and} \quad \left(\frac{d^2}{dz^2} - \omega^2\right)^2 \tilde{T}^g_{z1} = \frac{1}{\kappa} v^g_{z1}, \quad (1.28)$$

subject to no-penetration, no-slip and thermal continuity conditions at the boundaries,

$$v^g_{z1} = 0, \quad \frac{dv^g_{z1}}{dz} = 0, \quad \tilde{T}^g_{z1} = 0 \quad @ \quad z = -d^g, \quad (1.29)$$

$$v^l_{z1} = 0, \quad \frac{dv^l_{z1}}{dz} = 0, \quad \tilde{T}^l_{z1} = 0 \quad @ \quad z = d^l. \quad (1.30)$$

The kinematics of the interface are, mass balance:

$$v^l_{z1} - \rho v^g_{z1} = 0, \quad (1.31)$$

where Z_1 is the perturbed surface deflection, and ρ is the ratio of vapour to liquid densities.

Continuity of temperature:

$$\tilde{T}^l_{z1} + kZ_1 = \tilde{T}^g_{z1} + Z_1. \quad (1.32)$$

No-slip Condition:

$$\frac{dv^g_{z1}}{dz} = \frac{dv^l_{z1}}{dz}. \quad (1.33)$$

Normal / tangential stress balance:

$$\mu \left(\frac{d^3 v^g_{z1}}{dz^3} - 3\omega^2 \frac{dv^g_{z1}}{dz} \right) - \left(\frac{d^3 v^l_{z1}}{dz^3} - 3\omega^2 \frac{dv^l_{z1}}{dz} \right) + \omega^2 (\omega_{RT}^2 - \omega^2) Z_1 = 0 \quad (1.34)$$

and

$$\mu \left(\frac{d^3 v_{z1}^g}{dz^3} + \omega^2 \frac{dv_{z1}^g}{dz} \right) - \left(\frac{d^3 v_{z1}^l}{dz^3} + \omega^2 \frac{dv_{z1}^l}{dz} \right) = 0, \quad (1.35)$$

where μ is the ratio of vapour to liquid viscosity and $\omega_{RT} = \left(\frac{(\rho^l - \rho^g)gd^2}{\gamma} \right)^{1/2}$.

Interfacial Energy balance:

$$v_{z1}^l + E \left(\frac{d\tilde{T}_1^l}{dz} - k \frac{d\tilde{T}_1^g}{dz} \right) = 0, \quad (1.36)$$

where E stands for the evaporation number and is given by $E = \frac{C_p^l \frac{d\tilde{T}_o^g}{dz} d}{\lambda}$.

Equilibrium Condition:

$$\prod_{KE} \left(\frac{d^3 v_{z1}^g}{dz^3} - \omega^2 \frac{dv_{z1}^g}{dz} \right) - \omega^2 \prod_{PE} Z_1 = \omega^2 \eta (\tilde{T}_1^g + Z_1), \quad (1.37)$$

where $\prod_{KE} = \frac{1}{\rho} \frac{v^g \kappa^l}{\lambda d^2}$ and $\prod_{PE} = \frac{gd}{\lambda}$, with η being the inverse of the scaled saturation temperature at the flat interface.

This homogeneous system of equations is usually solved via the introduction of a phenomenological coefficient, α , to reduce the algebraic work. Previous authors had assumed this coefficient to be a constant input. Ozen & Narayanan show that this practise skews the results since α is actually dependent on the system variables.

To make this point, fluid layers of infinite depth are used to allow for an analytic representation of α to be derived from the velocity and temperature fields. The interface mass-balance is replaced with $\rho^g v_{z1}^g = \alpha Z_1$ where the coefficient α takes on the meaning of a perturbed evaporation rate per unit volume. Scaling this equation produces

$$v_{z1}^g = \alpha^* Z_1, \quad (1.38)$$

with $\alpha^* = \frac{\alpha}{\rho^g \kappa^l / d^2}$.

The authors now solve the scaled system and produce Figure 9 and Figure 10 showing the interdependence of evaporation rate, α^* , on disturbance wavenumber. The physical mechanism causing this is the pressure waves from the perturbations due to the Rayleigh-Taylor instability.

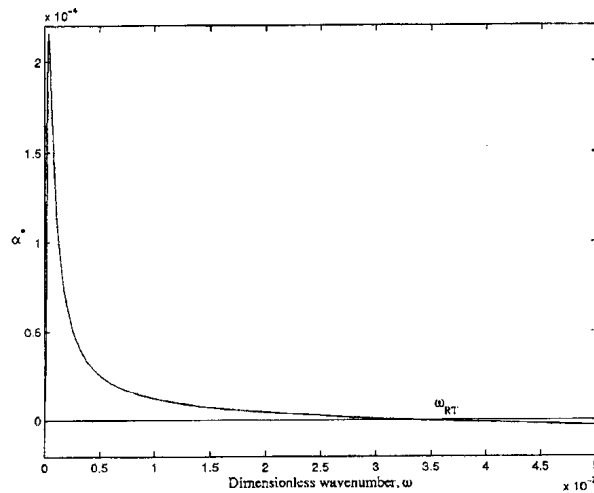


Figure 9 - The dependence of the coefficient α^* on the wavenumber for infinitely deep fluid layers. [7]

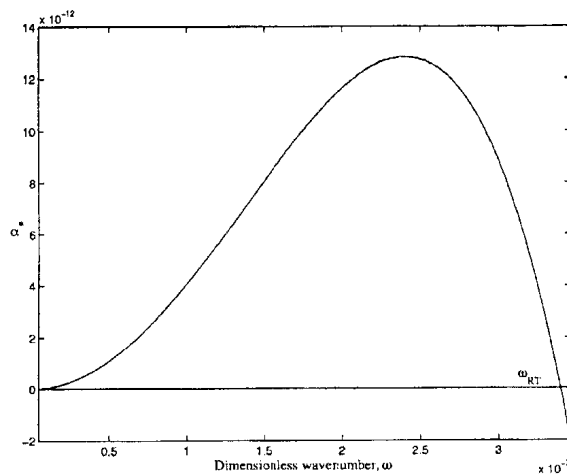


Figure 10 - The dependence of the coefficient α^* on the wavenumber for fluid layers with finite depths, where $d^l = 1mm$ and $d^g = 1mm$. [7]

Both figures show this in that for the classical Rayleigh-Taylor dimensionless critical wavenumber of $3.4 \cdot 10^{-7}$, the values of α^* , or the dimensionless evaporation rate, is zero. A second important observation to be made from these two figures is that there is practically no region on either plot which would allow α^* to be considered a constant in terms of the disturbance wave number.

Stepping back from Ozen & Narayanan's analysis, and examining the impact of the phase change itself on the fluid system's stability it is found that, following Morton's [5] line of thought, the diffusive nature of the phase change delays the onset of instability through the Rayleigh-Taylor mechanism.

2.2 The Density-Driven Instability of a Fluid in Motion

The unstable stratification of a Poiseuille channel flow is the next logical step in complexity from an initially stagnant flow, such as that described by Morton [5]. Mori & Uchida [8] experimentally examined the formation of vortex rolls for the instance of a heated lower wall and a cooled upper wall. They observed that once the temperature difference between the walls increased above a critical value, vortex rolls with their axes parallel to the direction of the flow formed. Figure 11 shows Pellow & Southwell's [9] results for the analytical solution to the problem.

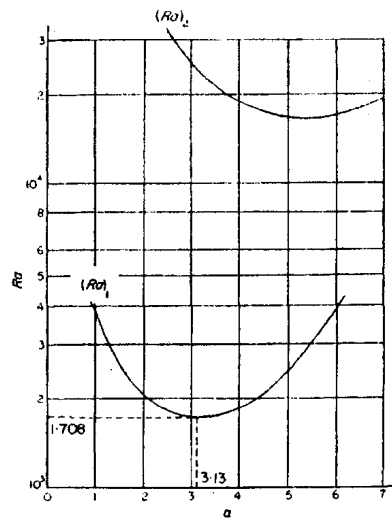


Figure 11 - Relation between the critical Rayleigh number and the wavenumber. [9]

Mori & Uchida's experiments were found to agree well with Pellow & Southwell's analytic predictions. They also showed that there was an improvement in the efficiency of the transfer of heat between the lower and upper walls of the channel. In Figure 12, Mori & Uchida's experimental results and analytical predictions for the Nusselt number achieved by the flow are compared. The Nusselt number is used as a measure of the non-dimensional heat transfer and is defined as $-\partial T/\partial y$ evaluated at the lower wall of the channel.

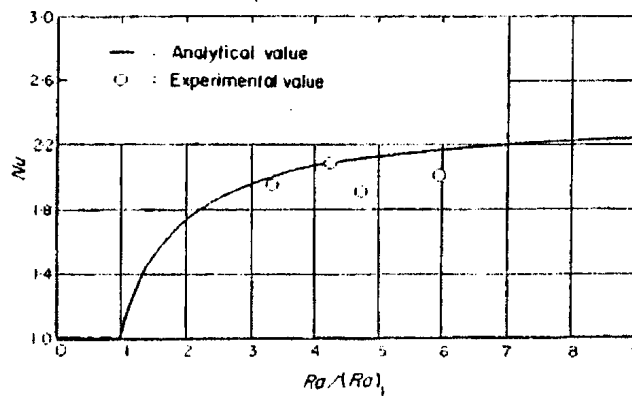


Figure 12 - The Nusselt number as a function of Rayleigh number, represented as a fraction of the critical value. [8]

The analytical expression given for the Nusselt number is

$$Nu = 1 + 1.413 \left(1 - \frac{Ra_{cr}}{Ra} \right). \tag{1.39}$$

Mori & Uchida also found that the linear theory was insufficient to predict the behaviour of the flow past a particular intensity of heating, or Rayleigh number. This is shown in Figure 13, where the pitch of the observed rolls is presented against the analytical value from the linear theory.

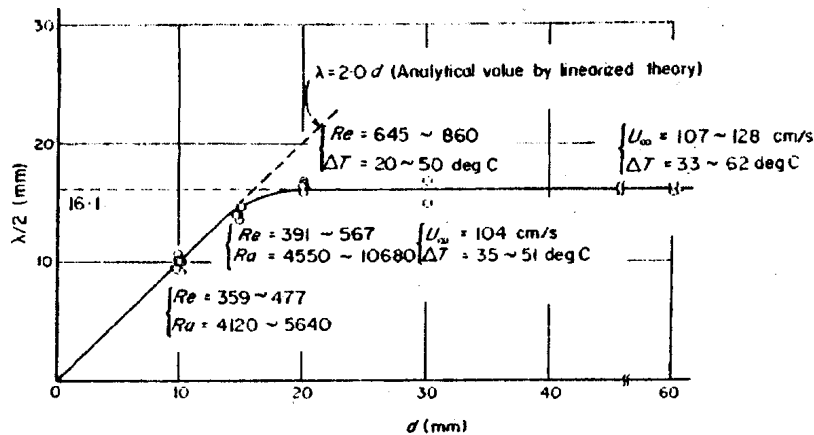


Figure 13 - Pitch of the vortex rolls. [8]

These results emphasize the reasoning behind a more in-depth examination of the critical conditions required to achieve longitudinal rolls in the flow. This will allow an improvement in the flow’s ability to transfer heat, as well as in other important characteristics such as pumping loss reductions.

Further experimental investigations were undertaken by Ostrach & Kamotani [10]. Their experimental arrangement allowed for the direct observation of the flow as the longitudinal rolls formed. Figure 14 shows an image of the transition to instability for a set of critical flow conditions.

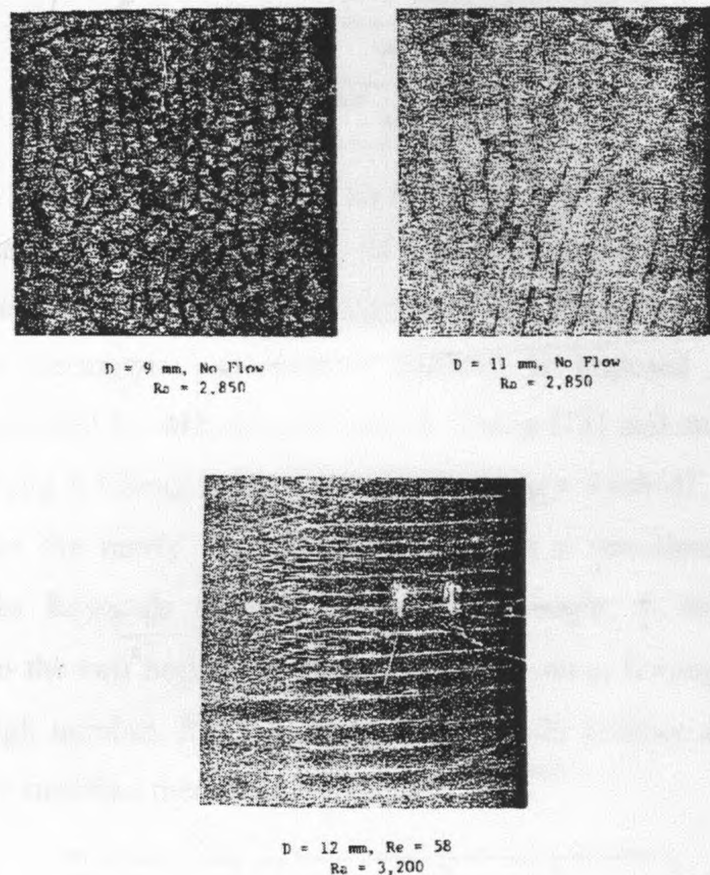


Figure 14 - Flow patterns for various parameters across critical conditions for transition. [8]

They provide a summary of information on the heat transfer present, given in Figure 15, which includes the experimental results of Mori & Uchida [8] and Silveston [11], and the numerical solution of Hwang & Cheng [12], using a finite amplitude approach. The critical conditions found experimentally by Ostrach & Kamotani, and through Hwang & Cheng's finite amplitude simulations, match those predicted by Pellow & Southwell's [9] linear theory. Rayleigh number of 1708 and a longitudinal roll wavenumber of 3.13 were found to be the critical conditions for growth of the instability, where the length scale is taken to be the height of the channel.

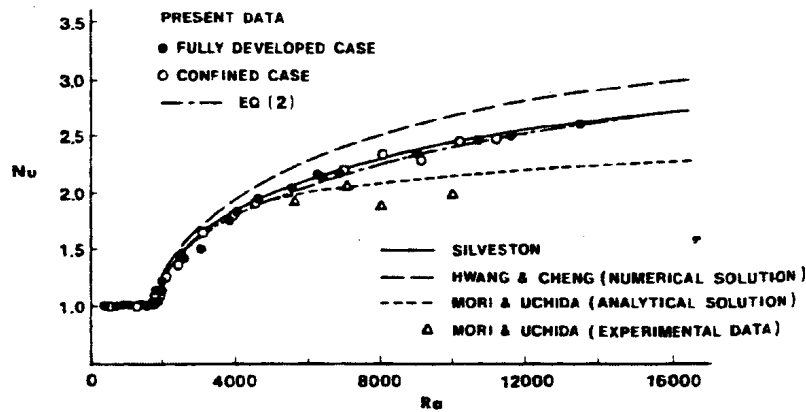


Figure 15 - The Nusselt number of the flow versus Rayleigh Number. [10]

From these fundamental analyses of the basic unstable configuration, other authors have investigated a couple of augmented configurations. In particular, the instance where a streamwise temperature gradient is imposed on the flow was experimentally examined by Akiyama, Hwang & Cheng [13] and analytically modelled by Nakayama, Hwang & Cheng [14]. A new parameter, $\mu = Re \tau h / \Delta T$, is defined by these authors to describe the newly imposed gradient, τ , in a non-dimensional form. The parameters are the Reynolds number, Re , channel height, h , and the temperature difference between the two horizontal plates, ΔT . Nakayama, Hwang & Cheng provide the critical Rayleigh number, Ra^* , as function of Prandtl number and μ , for both the stably and unstably stratified thermal arrangements.

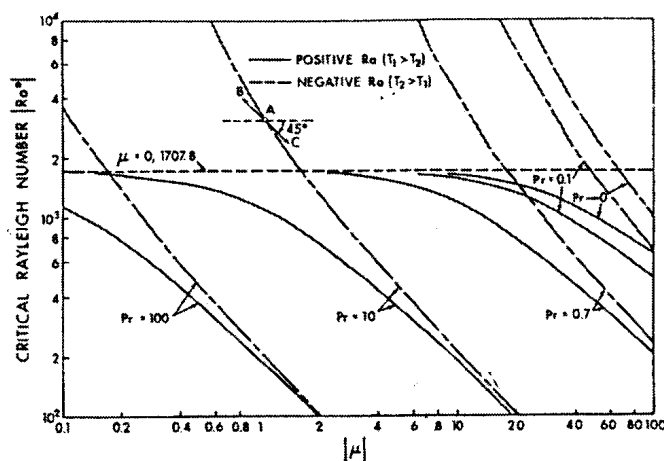


Figure 16 - Stability boundaries for longitudinal vortex rolls, critical Rayleigh number, Ra , versus heating parameter, μ . [14]

The analytical approach used by these authors also gives the critical wavenumber of the flow at which longitudinal vortices will form at the critical Rayleigh number; Figure 17 shows this relationship.

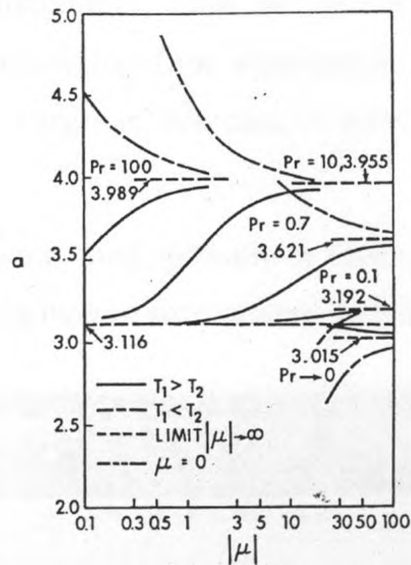


Figure 17 - Stability boundaries for longitudinal vortex rolls, critical wavenumber, a , versus heating parameter, μ . [14]

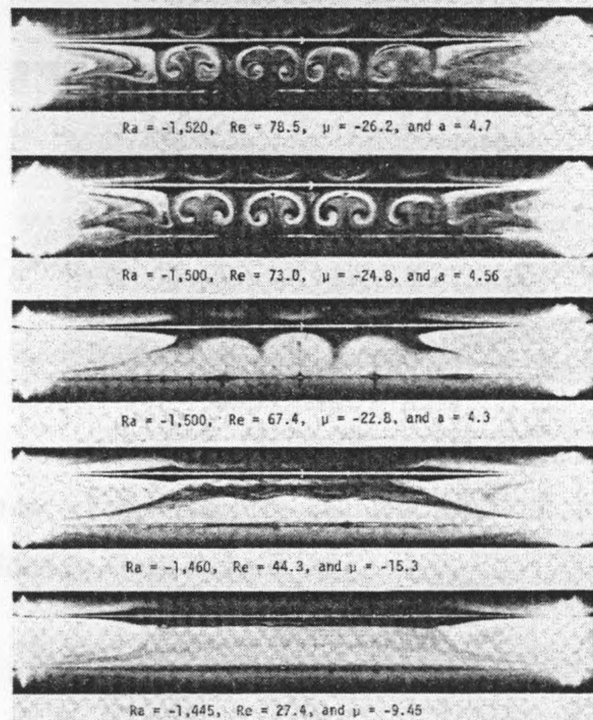


Fig. 8 Formation of secondary flow patterns with free-convection effect for the case of negative μ and $h = 1$ in.

Figure 18 – Formation of secondary flow patterns with free-convection effect for the case of negative μ and $h = 1$ in. [13]

Akiyama, Hwang & Cheng's [13] experiments were shown to agree in principle with the previously discussed analytical work. A comparison of these results is made in Figure 18. Akiyama, Hwang & Cheng conclude that the effects of longitudinal vortices, due to thermally induced instabilities, must be considered in addition to the free-convection effects near the side-walls of the experimental apparatus for large width-to-height aspect ratio channels. Large, in this case, is taken to mean on order of ten or greater.

These effects are shown photographically in Figure 19, and represent a practical limitation of the analytical modelling of such systems as infinite horizontal channels.

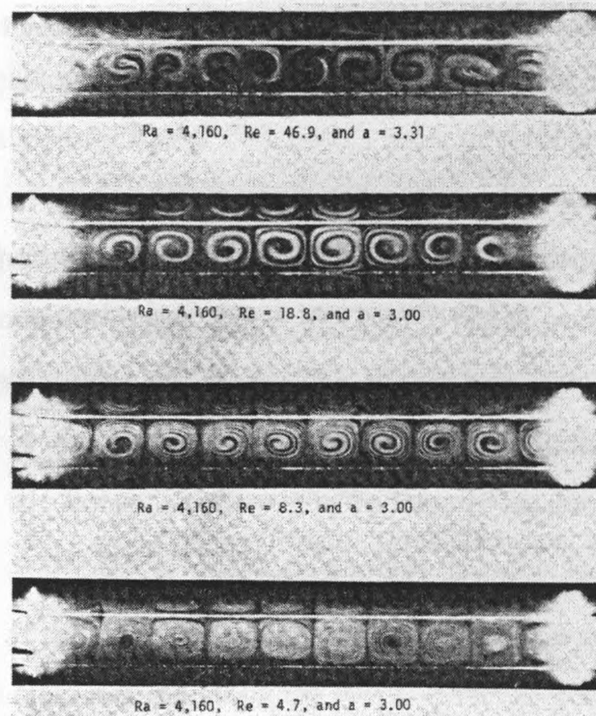


Figure 19 - Secondary flow patterns for the case $\mu = 0$ and $h = 1$ in. [13]

A good overview of the stability characteristics of unstably stratified plane Poiseuille flow is provided by Gage & Reid [15].

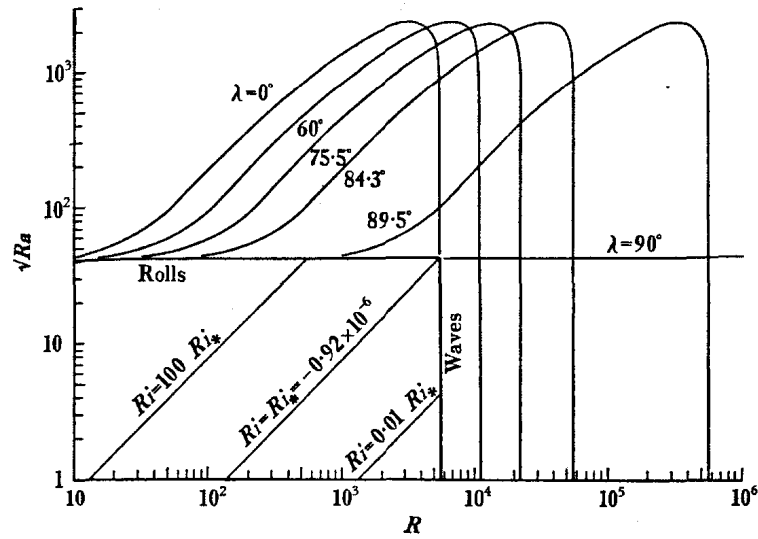


Figure 20 - The three-dimensional stability boundary for the case of unstable stratification. [15]

The three dimensional behaviour of the flow is described, identifying where the initial instability is analytically found to be in the form of rolls or waves. Gage & Reid's description is in terms of the Rayleigh number, Ra , Reynolds number, Re , and the angle λ , which is the angle from the direction of the flow in the horizontal plane of the channel. A unique Richardson number exists, $Ri^* = -0.92 \cdot 10^{-6}$, which marks the abrupt transition from one type of instability to the other. The Richardson number is defined as $Ri = \gamma g d \Delta T / 16 U^2$, where γ is the linear coefficient of volumetric expansion and U is the maximum velocity in the Poiseuille flow profile that would be present in the channel without heating.

The remainder of this thesis will concentrate on the analysis of a plane Poiseuille flow subjected to modulated heating along the walls. An analytical model will be derived that is suitably scaled to capture the critical transition criteria of the flow, as well as the necessary numerical implementation of this model to provide appropriate solutions. A discussion of the results will follow, in which comparisons will be made with previous works and future areas of interest will be identified.

3 Mathematical Formulation

The following two sections have been taken from “A Parametric Study of the Effect of Periodic Wall Heating on a Laminar Channel Flow” by Matthew L. Fotia, a thesis written in partial fulfilment of the requirements for the degree of Honors Bachelors’ of Science in Physics, Department of Physics & Astronomy, The University of Western Ontario. The inclusion of these sections is meant to provide the reader with an adequate description of the methodology used to obtain the base flow present in a channel subjected to spatially-distributed heating. The linear-stability analysis of this base flow is the subject of the present work.

3.1 Modulated Flow Formulation

The approach that will be taken to solve for the flow, a plane Poiseuille flow modulated by periodic heating, will be a direct extension of the technique use by Floryan [16] to simulate roughness effects through an alternating suction and blowing pattern along the walls of the channel.

The problem now being considered is outlined in Figure 21, which is similar to the classical case but with a wall temperature that is spatially-distributed along the walls in the direction of the flow. We will, for the moment, continue to include the mean thermal gradient between the two plates in our derivation for consistency and later validation with the available literature.

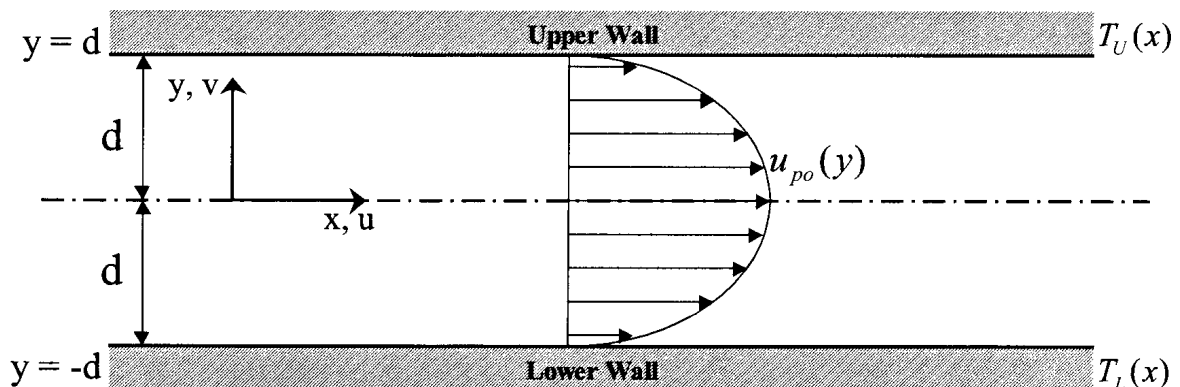


Figure 21 - Physical arrangement of thermally modulated flow.

The wall temperatures are expressed as Fourier expansions, $T_U(x) = \sum_n T_U^{(n)} e^{in\alpha x}$ and

$T_L(x) = \sum_n T_L^{(n)} e^{in\alpha x}$, with wavenumber α .

The basic field equations, of an incompressible fluid, for this situation include the continuity equation, Navier-Stokes equation as well as the energy equation, describing the conservation of mass, momentum and energy in the system respectfully:

$$\nabla \cdot \bar{v} = 0, \quad (2.1)$$

$$\rho_o \frac{\partial \bar{v}}{\partial t} + \rho_o (\bar{v} \cdot \nabla) \bar{v} = -\nabla P - \rho g \hat{j} + \nabla \cdot \left(\frac{4}{3} \mu_o \nabla \cdot \bar{v} \right) - \nabla \times (\mu_o \nabla \times \bar{v}), \quad (2.2)$$

$$\rho_o C_v \frac{\partial T}{\partial t} + \rho_o C_v (\bar{v} \cdot \nabla) T = \nabla \cdot (k_o \nabla T) - P \nabla \cdot \bar{v} + \Phi, \quad (2.3)$$

$$\Phi = \mu_o \left[2 \left(\frac{\partial u}{\partial x} \right)^2 + 2 \left(\frac{\partial v}{\partial y} \right)^2 + \left(\frac{\partial v}{\partial x} + \frac{\partial u}{\partial y} \right)^2 \right] + \lambda \left(\frac{\partial u}{\partial x} + \frac{\partial v}{\partial y} \right)^2. \quad (2.4)$$

Quantities denoted with a subscript zero are evaluated at the reference temperature of the flow, T_{ref} , the temperature at the lower wall, and where:

ρ - Fluid Density

μ - Kinematic Viscosity

k_o - Thermal Conductivity

C_v - Specific Heat at Constant Volume

P - Pressure

T - Fluid Temperature

Φ - Viscous Dissipation Function

λ - Constant Determining Character of Viscosity

$$\text{and } \nabla = \hat{i} \frac{\partial}{\partial x} + \hat{j} \frac{\partial}{\partial y}.$$

The temperature gradients in the channel imply that there should exist a proportional variation in the fluid density as a function of the temperature of the fluid. This is approximated by the Boussinesq expansion for an incompressible fluid, which assumes that the density at any position in the channel can be expressed as a linear variation from the density at a reference temperature. A Taylor expansion of the fluid's density as a function of temperature, retaining only the linear terms,

$$\begin{aligned}\rho &= \rho_o [1 - \gamma(T - T_{ref})] , \\ \frac{\partial \rho}{\partial t} &= -\rho_o \gamma \frac{\partial T}{\partial t} \sim O(\gamma) , \\ \nabla \rho &= -\rho_o \gamma \nabla T \sim O(\gamma) ,\end{aligned}\tag{2.5}$$

with γ being the linear coefficient of volumetric expansion for the fluid in question. [17]

Under this approximation the dimensional fluid field equations become:

Continuity:

$$\begin{aligned}\frac{\partial \rho}{\partial t} + \vec{v} \cdot \nabla \rho + \rho \nabla \cdot \vec{v} &= 0, \\ O(\gamma) + \vec{v} \cdot O(\gamma) + \rho \nabla \cdot \vec{v} &= 0, \\ \therefore \nabla \cdot \vec{v} &= 0\end{aligned}$$

Navier-Stokes:

$$\begin{aligned}\rho_o \frac{\partial \vec{v}}{\partial t} + \rho_o (\vec{v} \cdot \nabla) \vec{v} &= -\nabla P - \rho_o [1 - \gamma(T - T_{ref})] \hat{g} \\ &\quad + \frac{4}{3} \mu_o \nabla (\nabla \cdot \vec{v}) - \mu_o (\nabla (\nabla \cdot \vec{v}) - \nabla^2 \vec{v}) + O(\gamma), \\ \frac{\partial \vec{v}}{\partial t} + (\vec{v} \cdot \nabla) \vec{v} &= -\frac{\nabla P}{\rho_o} - \hat{g} + g\gamma(T - T_{ref}) \hat{j} + \nu_o \nabla^2 \vec{v},\end{aligned}\tag{2.6}$$

once the continuity equation has been applied.

Energy:

$$\rho_o C_v \frac{\partial T}{\partial t} + \rho_o C_v (\vec{v} \cdot \nabla) T = -k_o \nabla^2 T + O(\gamma) - P \nabla \cdot \vec{v} + \Phi ,$$

again applying continuity and making the assumption that the energy loss due to viscous dissipation, i.e. Φ , is small relative to the other terms in the relation,

$$\frac{\partial T}{\partial t} + (\bar{\mathbf{v}} \cdot \nabla)T = -\kappa_o \nabla^2 T \quad (2.7)$$

where $\kappa_o = \frac{k_o}{\rho_o C_v}$, the thermal diffusivity.

The dimensional field equations for a Boussinesq fluid are scaled using two different scales: One to capture the scale of the Poiseuille flow in the channel and the other the convective structures resulting from the modulated heating along the channel walls. The reference temperature for the flow will now be explicitly chosen to be the mean temperature of the upper wall, T_U . The scales are:

Length: $L_* = d$,

Velocity scale for Poiseuille flow: $U_{p*} = U_{Max}$,

Velocity scale for convectively modified flow: $U_{m*} = \text{Re}^{-1} U_{p*} = \frac{v_o}{d}$,

Temperature Scale for mean conduction temperature difference: $T_{p*} = \Delta T = T_L^{(0)} - T_U^{(0)}$,

Temperature Scale for advected temperature difference: $T_{m*} = \text{Pr} T_{p*}$,

Pressure: $P_* = \rho_o U_{m*}^2$,

Time: $t_* = \frac{d}{U_{m*}}$.

Once the definitions of the non-dimensional quantities are given as:

$$\text{Re} = \frac{U_{p*} d}{\nu_o}, \quad \text{Pr} = \frac{\nu_o}{\kappa_o}, \quad \text{Ra} = \frac{g \gamma d^3 \Delta T}{\kappa_o \nu_o}, \quad \text{Fr} = \frac{U_{p*}^2}{g d},$$

this produces:

$$\frac{\partial \hat{u}}{\partial \hat{x}} + \frac{\partial \hat{v}}{\partial \hat{y}} = 0,$$

$$\begin{aligned}
\frac{\partial \hat{u}}{\partial \hat{t}} + \hat{u} \frac{\partial \hat{u}}{\partial \hat{x}} + \hat{v} \frac{\partial \hat{u}}{\partial \hat{y}} &= -\frac{\partial \hat{P}}{\partial \hat{x}} + \nabla^2 \hat{u}, \\
\frac{\partial \hat{v}}{\partial \hat{t}} + \hat{u} \frac{\partial \hat{v}}{\partial \hat{x}} + \hat{v} \frac{\partial \hat{v}}{\partial \hat{y}} &= -\frac{\partial \hat{P}}{\partial \hat{y}} - \frac{1}{Fr} + Ra \hat{\theta} + \nabla^2 \hat{v}, \\
\frac{\partial \hat{\theta}}{\partial \hat{t}} + \hat{u} \frac{\partial \hat{\theta}}{\partial \hat{x}} + \hat{v} \frac{\partial \hat{\theta}}{\partial \hat{y}} &= \frac{1}{Pr} \nabla^2 \hat{\theta},
\end{aligned} \tag{2.8}$$

where again hatted quantities are non-dimensional and the non-dimensional temperature, $\hat{\theta}$, has been introduced such that $\hat{\theta} = \frac{(T - T_{ref})}{\Delta T}$.

Each of the dimensionless parameters represents the interplay of important physical mechanisms in the flow. For instance, Reynolds number is the ratio of inertial to viscous forces in the fluid. The Prandtl number is the ratio of viscous to thermal diffusion, while the Froude number is the ratio of inertia to gravity. The Rayleigh number represents the comparison of the buoyancy forces to the diffusive forces in the fluid.[18]

The standard no-slip and thermal continuity at the wall conditions hold at the boundaries, except that the temperature on the walls is now expanded as a Fourier series in the stream-wise direction, and once appropriately scaled:

$$\begin{aligned}
\hat{v}(x, y = \pm 1) &= 0, \\
\hat{\theta}(y = 1) &= \frac{\left(\sum_n T_U^{(n)} e^{inax} - T_U^{(0)} \right)}{\left(T_L^{(0)} - T_U^{(0)} \right)}, \\
\hat{\theta}(y = -1) &= \frac{\left(\sum_n T_L^{(n)} e^{inax} - T_U^{(0)} \right)}{\left(T_L^{(0)} - T_U^{(0)} \right)}.
\end{aligned} \tag{2.9}$$

Note that superscripts denote the zero mode coefficients of the expansions. This keeps the equivalent temperature scaling, $\Delta T = T_L^{(0)} - T_U^{(0)}$, as used in much of the literature where these zero modes now represent the mean temperature of each wall, about which the rest of the expansion will periodically vary.

The non-dimensional temperature itself may be expanded such that $\hat{\theta}(\hat{x}, \hat{y}) = \sum_n \hat{\theta}^{(n)}(\hat{y})e^{in\hat{x}}$. Substituting this into the boundary conditions in Equation (2.9) gives the new conditions:

$$\hat{v}(\hat{x}, \hat{y} = \pm 1) = 0, \quad (2.10)$$

and $\hat{y} = 1$: $\hat{\theta}(\hat{x}, \hat{y} = 1) = \sum_n \hat{\theta}^{(n)}(\hat{y} = 1)e^{in\hat{x}} = \frac{1}{\Delta T} \left[\sum_n T_U^{(n)} e^{in\hat{x}} - T_U^{(0)} \right]$, with

$$\hat{\theta}^{(n)}(\hat{y} = 1) = \begin{cases} \frac{1}{\Delta T} (T_U^{(0)} - T_U^{(0)}) = 0 & \text{for } n = 0 \\ \frac{T_U^{(n)}}{\Delta T} & \text{for } n \neq 0 \end{cases} \quad (2.11)$$

$\hat{y} = -1$: $\hat{\theta}(\hat{x}, \hat{y} = -1) = \sum_n \hat{\theta}^{(n)}(\hat{y} = -1)e^{in\hat{x}} = \frac{1}{\Delta T} \left[\sum_n T_L^{(n)} e^{in\hat{x}} - T_U^{(0)} \right]$, with

$$\hat{\theta}^{(n)}(\hat{y} = -1) = \begin{cases} \frac{1}{\Delta T} (T_L^{(0)} - T_U^{(0)}) = 1 & \text{for } n = 0. \\ \frac{T_L^{(n)}}{\Delta T} & \text{for } n \neq 0 \end{cases} \quad (2.12)$$

In a similar approach as that taken classically, we will consider the conduction of heat into the fluid from the walls. The conducted temperature distribution in this case will consist of a uniform component, $\hat{\theta}_{o,un}$, imposed by any mean temperature differences between the channel walls and a non-uniform component, $\hat{\theta}_{o,num}$ as a consequence of the variation of the temperature conditions along the walls. The total conducted temperature field is given as

$$\hat{\theta}_o(\hat{x}, \hat{y}) = \hat{\theta}_{o,un}(\hat{y}) + \hat{\theta}_{o,num}(\hat{x}, \hat{y}).$$

This conduction problem has the form of Laplace's equation,

$$\frac{\partial^2 \hat{\theta}}{\partial \hat{y}^2} + \frac{\partial^2 \hat{\theta}}{\partial \hat{x}^2} = 0,$$

subject to the boundary conditions in Equations (2.11) & (2.12).

The uniform component of the conducted temperature field will take a form similar to that of the classical case,

$$\hat{\theta}_{o,un}(\hat{y}) = \frac{1}{2}(1 - \hat{y}), \quad (2.13)$$

while the non-uniform component may be obtained by using the definition of the dimensionless temperature, $\hat{\theta}(\hat{x}, \hat{y}) = \sum_n \hat{\theta}^{(n)}(\hat{y})e^{in\alpha\hat{x}}$, giving

$$\sum_n \left(-n^2 \alpha^2 \hat{\theta}^{(n)} + \frac{\partial^2 \hat{\theta}^{(n)}}{\partial \hat{y}^2} \right) e^{in\alpha\hat{x}} = 0.$$

Once the modes are separated, we find that the solution for each mode is that of a second-order ordinary differential equation,

$$\frac{\partial^2 \hat{\theta}^{(n)}}{\partial \hat{y}^2} - n^2 \alpha^2 \hat{\theta}^{(n)} = 0,$$

where it can be assumed that the solution will take the form: $\hat{\theta}^{(n)} = Ce^{\lambda\hat{y}}$ providing that:

$$\begin{aligned} \lambda^2 - n^2 \alpha^2 &= 0, \\ \lambda &= \pm n\alpha, \end{aligned}$$

allowing

$$\hat{\theta}^{(n)}(\hat{y}) = C_1 \sinh(n\alpha) + C_2 \cosh(n\alpha).$$

Solving for these two constants, using the temperature boundary conditions in Equations (2.11) & (2.12):

$$\begin{aligned} \hat{\theta}^{(n)}(\hat{y} = 1) &= C_1 \sinh(n\alpha) + C_2 \cosh(n\alpha), \\ \hat{\theta}^{(n)}(\hat{y} = -1) &= -C_1 \sinh(n\alpha) + C_2 \cosh(n\alpha), \end{aligned}$$

and after adding and subtracting between equations it is found that:

$$C_1 = \frac{\hat{\theta}^{(n)}(\hat{y} = 1) - \hat{\theta}^{(n)}(\hat{y} = -1)}{2 \sinh(n\alpha)}, \quad C_2 = \frac{\hat{\theta}^{(n)}(\hat{y} = 1) + \hat{\theta}^{(n)}(\hat{y} = -1)}{2 \cosh(n\alpha)}.$$

This results in a temperature distribution where:

$$\begin{aligned}
 \hat{\theta}_{o,num}(\hat{x}, \hat{y}) &= \sum_n \hat{\theta}_{o,num}^{(n)}(\hat{y}) e^{in\hat{x}} \\
 &= \sum_n \left[\frac{\hat{\theta}^{(n)}(\hat{y}=1) - \hat{\theta}^{(n)}(\hat{y}=-1)}{2 \sinh(n\alpha)} \sinh(n\alpha\hat{y}) \right. \\
 &\quad \left. + \frac{\hat{\theta}^{(n)}(\hat{y}=1) + \hat{\theta}^{(n)}(\hat{y}=-1)}{2 \cosh(n\alpha)} \cosh(n\alpha\hat{y}) \right] e^{in\hat{x}}.
 \end{aligned} \tag{2.14}$$

A solution is now sought by separating the basic flow-state of the Poiseuille flow and the conducted temperature modulations from the convective component of the modulations imposed on the flow by the periodic heating.

$$\begin{aligned}
 \hat{u}(\hat{x}, \hat{y}) &= \text{Re} \hat{u}_{po}(\hat{y}) + \hat{u}_1(\hat{x}, \hat{y}), \\
 \hat{v}(\hat{x}, \hat{y}) &= \hat{v}_1(\hat{x}, \hat{y}), \\
 \hat{\theta}(\hat{x}, \hat{y}) &= \text{Pr}^{-1} \hat{\theta}_o(\hat{x}, \hat{y}) + \hat{\theta}_1(\hat{x}, \hat{y}), \\
 \hat{P}(\hat{x}, \hat{y}) &= \text{Re}^2 \hat{P}_o(\hat{x}, \hat{y}) + \hat{P}_1(\hat{x}, \hat{y}).
 \end{aligned} \tag{2.15}$$

The Poiseuille flow in the channel is given by

$$\hat{u}_{po}(\hat{y}) = 1 - \hat{y}^2,$$

and the conducted temperature distribution in the channel is defined as above,

$$\begin{aligned}
 \hat{\theta}_o(\hat{x}, \hat{y}) &= \hat{\theta}_{o,un}(\hat{y}) + \hat{\theta}_{o,num}(\hat{x}, \hat{y}) \\
 &= \frac{1}{2}(1 - \hat{y}) + \sum_n \left[\frac{\hat{\theta}^{(n)}(\hat{y}=1) - \hat{\theta}^{(n)}(\hat{y}=-1)}{2 \sinh(n\alpha)} \sinh(n\alpha\hat{y}) \right. \\
 &\quad \left. + \frac{\hat{\theta}^{(n)}(\hat{y}=1) + \hat{\theta}^{(n)}(\hat{y}=-1)}{2 \cosh(n\alpha)} \cosh(n\alpha\hat{y}) \right] e^{in\hat{x}}.
 \end{aligned} \tag{2.16}$$

The pressure field is defined as

$$\hat{P}_o(\hat{x}, \hat{y}) = -\frac{2}{\text{Re}} \hat{x} - \frac{\text{Ra}}{\text{Re}^2 \text{Pr}} \left(\frac{\hat{y}^2}{4} - \frac{\hat{y}}{2} \right) - \frac{\hat{y}}{\text{Re}^2 \text{Fr}}, \tag{2.17}$$

noting that the pressure term does not include the pressure contribution due to the conduction of the temperature fluctuations in the flow, but only the contribution due to the continuous stratification between the channel walls. That is, the \hat{P}_1 term in Equation

(2.15) contains the total, conducted and convected, pressure influence of these fluctuations.

Once this separation is made in the field equations, and the unmodulated classical flow and conduction terms are cancelled from each side of each equation:

$$\begin{aligned}\frac{\partial u_1}{\partial \hat{x}} + \frac{\partial v_1}{\partial \hat{y}} &= 0, \\ \frac{\partial u_1}{\partial \hat{t}} + (\text{Re}u_{po} + u_1)\frac{\partial u_1}{\partial \hat{x}} + v_1\frac{\partial(\text{Re}u_{po} + u_1)}{\partial \hat{y}} &= -\frac{\partial P_1}{\partial \hat{x}} + \nabla^2 u_1, \\ \frac{\partial v_1}{\partial \hat{t}} + (\text{Re}u_{po} + u_1)\frac{\partial v_1}{\partial \hat{x}} + v_1\frac{\partial v_1}{\partial \hat{y}} &= -\frac{\partial P_1}{\partial \hat{y}} + \text{Ra}(\text{Pr}^{-1}\theta_{o,nun} + \theta_1) + \nabla^2 v_1, \\ \frac{\partial \theta_1}{\partial \hat{t}} + (\text{Re}u_{po} + u_1)\frac{\partial(\text{Pr}^{-1}\theta_{o,nun} + \theta_1)}{\partial \hat{x}} + v_1\frac{\partial(\text{Pr}^{-1}(\theta_{o,un} + \theta_{o,nun}) + \theta_1)}{\partial \hat{y}} &= \frac{1}{\text{Pr}}\nabla^2 \theta_1,\end{aligned}\tag{2.18}$$

where ∇^2 denotes the Laplace operator and the hatted notation for dimensionless quantities is dropped. The assumption that the flow is steady removes the leading derivatives with respect to time.

The separation of states is applied to the boundary conditions, first to the fluid's velocity at the walls:

$$\begin{aligned}u(\hat{y} = \pm 1) &= \text{Re}u_{po} + u_1 = \text{Re}(1 - (\pm 1)^2) + u_1 = 0, \\ \Rightarrow u_1(\hat{y} = \pm 1) &= 0,\end{aligned}\tag{2.19}$$

$$\begin{aligned}v(\hat{y} = \pm 1) &= v_1 = 0, \\ \Rightarrow v_1(\hat{y} = \pm 1) &= 0,\end{aligned}\tag{2.20}$$

and then to the temperature of the fluid at the walls:

$$\begin{aligned}\theta(\hat{y} = 1) &= \theta^{(0)}(\hat{y} = 1) + \sum_{n \neq 0} \theta^{(n)}(\hat{y} = 1)e^{in\alpha\hat{x}} \\ &= -1 + \sum_{n \neq 0} \theta(\hat{y} = 1)e^{in\alpha\hat{x}} = \theta_{o,un}(\hat{y} = 1) + \theta_{o,nun}(\hat{x}, \hat{y} = 1) + \theta_1(\hat{y} = 1) \\ &= -\frac{1}{2}(1+1) + \theta_1(\hat{y} = 1) \\ \Rightarrow \theta_1(\hat{y} = 1) &= 0\end{aligned}\tag{2.21}$$

$$\theta(\hat{y} = -1) = \theta^{(0)}(\hat{y} = -1) + \sum_{n \neq 0} \theta^{(n)}(\hat{y} = -1)e^{in\alpha\hat{x}}$$

$$\begin{aligned}
 &= 0 + \sum_{n \neq 0} \theta(\hat{y} = -1) e^{in\alpha\hat{x}} = \theta_{o,un}(\hat{y} = -1) + \theta_{o,mun}(\hat{x}, \hat{y} = -1) + \theta_1(\hat{y} = -1) \\
 &= -\frac{1}{2}(1-1) + \theta_1(\hat{y} = -1) \\
 &\Rightarrow \theta_1(\hat{y} = 1) = 0
 \end{aligned} \tag{2.22}$$

To summarize the current problem, the system of coupled field equations, Equation (2.18), under the boundary conditions in Equations (2.19) to (2.22), must now be solved. The following sections constitute the methods that will be used to simplify and find a solution to this flow problem, as well as pose and solve the eigenvalue problem which will govern the stability of longitudinal vorticities in this flow.

3.2 Implementation of the Numerical Solution

3.2.1 The Streamfunction

In an effort to simplify the form of Equation (2.18) into one that is more tractable, the concept of a streamfunction is introduced, where the modulated velocities become $u_1 = \frac{\partial \psi}{\partial \hat{y}} = \psi_y$ and $v_1 = -\frac{\partial \psi}{\partial \hat{x}} = -\psi_x$. The scalar ψ is a function of position and may be introduced here only due to the two-dimensional nature of the flow. Once the modulated temperature function is renamed, $\theta_1 = \varphi$, to simplify the notation in the future, the field equations of (2.18) can now be written:

$$\psi_{xy} - \psi_{yx} = 0, \tag{2.23}$$

$$(\text{Re}u_{po} + \psi_y)\psi_{xy} - \psi_x(\text{Re}u'_{po} + \psi_{yy}) = -\frac{\partial P_1}{\partial \hat{x}} + \psi_{xxy} + \psi_{yyy}, \tag{2.24}$$

$$-(\text{Re}u_{po} + \psi_y)\psi_{xx} + \psi_x\psi_{yx} = -\frac{\partial P_1}{\partial \hat{y}} + \text{Ra}(\theta_{o,mun} + \varphi) - \psi_{xxx} + \psi_{yyx}, \tag{2.25}$$

$$(\text{Re}u_{po} + \psi_y) \left(\frac{\partial \theta_{o,mun}}{\partial \hat{x}} + \varphi_x \right) - \psi_x \left(\theta'_{o,un} + \frac{\partial \theta_{o,mun}}{\partial \hat{y}} + \varphi_{yy} \right) = \frac{1}{\text{Pr}} (\varphi_{xx} + \varphi_{yy}) \tag{2.26}$$

The continuity equation, Equation (2.23), is self-satisfied by the introduction of the streamfunction. The pressure terms can be eliminated from this system of equations by taking the derivative of Equation (2.25) with respect to \hat{x} and the derivative of Equation (2.24) with respect to \hat{y} , and then subtracting the results to produce

$$\begin{aligned}
& (\text{Re}u_{po} + \psi_y)(\psi_{xyy} + \psi_{xxx}) - \psi_x(\text{Re}u'_{po} + \psi_{yyy} - \psi_{yxx}) \\
& = -\text{Ra} \left(\frac{\partial \theta_{o,nn}}{\partial \hat{x}} + \varphi_x \right) + \psi_{xxxx} + 2\psi_{xxyy} + \psi_{yyyy}, \tag{2.27}
\end{aligned}$$

while still coupled with Equation (2.26).

These two coupled differential equations are still subject to the boundary condition of Equations (2.19) – (2.22), which can be rewritten using the definition of the streamfunction:

$$\begin{aligned}
\psi_y(\hat{y} = \pm 1) &= 0, \\
\psi_x(\hat{y} = \pm 1) &= 0, \\
\varphi(\hat{y} = \pm 1) &= 0.
\end{aligned} \tag{2.28}$$

Due to the periodicity of the flow, the streamfunction can be represented as a Fourier expansion in the streamwise direction,

$$\psi(\hat{x}, \hat{y}) = \sum_{n=-\infty}^{\infty} \Phi_n(\hat{y}) e^{in\hat{x}}, \tag{2.29}$$

with a wavelength defined as $\lambda_{\hat{x}} = 2\pi/\alpha$. Similarly, the temperature function can be expanded in the form

$$\varphi(\hat{x}, \hat{y}) = \sum_{n=-\infty}^{\infty} \eta_n(\hat{y}) e^{in\hat{x}}. \tag{2.30}$$

Since we are seeking only real solutions to our flow, the added relations that $\Phi_n = \Phi_{-n}^*$ and $\eta_n = \eta_{-n}^*$ are stated to enforce this requirement, where the ‘*’ denotes the complex conjugate.

Using these expansions Equations (2.25) & (2.26) become, respectively:

$$\begin{aligned}
 & \left(\text{Re}u_{po} + \sum_k \Phi'_k e^{ik\alpha\hat{x}} \right) \sum_l \left(il\alpha\Phi_l'' - il^3\alpha^3\Phi_l \right) e^{il\alpha\hat{x}} \\
 & \quad - \sum_k ik\alpha\Phi_k e^{ik\alpha\hat{x}} \left[\text{Re}u_{po}'' + \sum_l \left(\Phi_l''' - l^2\alpha^2\Phi_l' \right) e^{il\alpha\hat{x}} \right] \quad (2.31) \\
 & = -Ra \sum_n \left(in\alpha\theta_{o,nun} + in\alpha\eta_n \right) e^{in\alpha\hat{x}} \\
 & \quad + \sum_n \left(n^4\alpha^4\Phi_n - 2n^2\alpha^2\Phi_n'' + \Phi_n^{IV} \right) e^{in\alpha\hat{x}},
 \end{aligned}$$

and

$$\begin{aligned}
 & \left(\text{Re}u_{po} + \sum_k \Phi'_k e^{ik\alpha\hat{x}} \right) \sum_l il\alpha \left(\eta_l + \theta_{o,nun}^{(l)} \right) e^{il\alpha\hat{x}} \\
 & \quad - \sum_k ik\alpha\Phi_k e^{ik\alpha\hat{x}} \left[\theta'_{o,un} + \sum_l \left(\theta_{o,nun}^{(l)'} + \eta_l' \right) e^{il\alpha\hat{x}} \right] \quad (2.32) \\
 & = \frac{1}{\text{Pr}} \sum_n \left(\eta_n'' + n^2\alpha^2\eta_n \right) e^{in\alpha\hat{x}},
 \end{aligned}$$

noting that the definition of $\theta_{o,nun}$ in Equation (2.16) has been used.

The coupled differential equations for a single mode of the system can be obtained by rearranging the summations, taking $k = n - l$ and separating the resulting equations summed over mode n . We can now write:

$$\begin{aligned}
 & \Phi_n^{IV} - 2n^2\alpha^2\Phi_n'' + n^4\alpha^4\Phi_n + in\alpha \left[\text{Re}u_{po}'' \Phi_n - \text{Re}u_{po} \left(\Phi_n'' - n^2\alpha^2\Phi_n \right) \right] \\
 & \quad + \sum_l i(n-l)\alpha\Phi_{n-l} \left[\Phi_l''' - l^2\alpha^2\Phi_l' \right] - \sum_l il\alpha\Phi_{n-l}' \left[\Phi_l'' - l^2\alpha^2\Phi_l \right] \quad (2.33) \\
 & \quad - in\alpha Ra \left[\theta_{o,nun}^{(n)} + \eta_n \right] = 0,
 \end{aligned}$$

$$\begin{aligned}
 & \eta_n'' - n^2\alpha^2\eta_n - in\alpha \text{Pr} \left[\text{Re}u_{po} \eta_n + \text{Re}u_{po} \theta_{o,nun}^{(n)} - \Phi_n \theta'_{o,un} \right] \\
 & \quad - \text{Pr} \sum_l il\alpha\Phi_{n-l}' \left(\eta_l + \theta_{o,nun}^{(l)} \right) + \text{Pr} \sum_l i(n-l)\alpha\Phi_{n-l} \left(\eta_l' + \theta_{o,nun}^{(l)'} \right) = 0. \quad (2.34)
 \end{aligned}$$

The Fourier expansions of the streamfunction and temperature function can also be applied to the boundary condition in Equation (2.28), giving:

$$\begin{aligned}
 & \psi_y(\hat{y} = \pm 1) = 0 = \sum_n \Phi_n'(\hat{y} = \pm 1) e^{in\alpha\hat{x}}, \\
 & \quad \therefore \Phi_n'(\hat{y} = \pm 1) = 0, \quad n = 0, \pm 1, \pm 2... \quad (2.35)
 \end{aligned}$$

$$\begin{aligned} \psi_x(\hat{y} = \pm 1) = 0 &= \sum_n in\alpha\Phi_n(\hat{y} = \pm 1)e^{in\alpha\hat{x}}, \\ \therefore \Phi_n(\hat{y} = \pm 1) &= \begin{cases} \text{Undefined}, & n = 0 \\ 0, & n \neq 0 \end{cases} \end{aligned} \quad (2.36)$$

$$\begin{aligned} \varphi(\hat{y} = \pm 1) = 0 &= \sum_n \eta_n(\hat{y} = \pm 1)e^{in\alpha\hat{x}}, \\ \therefore \eta_n(\hat{y} = \pm 1) &= 0, \quad n = 0, \pm 1, \pm 2 \dots \end{aligned} \quad (2.37)$$

These conditions, however, are now inadequate to properly confine our system of equations. A fourth order differential equation coupled with a second order differential equation, requires six boundary conditions for each mode of the solution. The conditions supplied by Equations (2.35), (2.36) & (2.37) provide all the required conditions except two, those for the $n = 0$ mode from Equation (2.36). An additional closure condition is therefore required. From Equation (2.36) we find that $\Phi_0(\hat{y} = \pm 1)$ may have arbitrary values, for instance:

$$\begin{aligned} \Phi_0(y = 1) &= C_5, \\ \Phi_0(y = -1) &= C_6, \end{aligned}$$

and if we are to require as a constituent relation that there be a constant mass flux, Q_1 , through the channel we can write:

$$\begin{aligned} Q_1 &= \int_{-1}^1 u_1 d\hat{y} = \int_{-1}^1 \frac{\partial \psi}{\partial \hat{y}} d\hat{y} \\ &= \int_{-1}^1 d\psi = \psi(\hat{y} = 1) - \psi(\hat{y} = -1) \\ &= \Phi_0(\hat{y} = 1) + \sum_n \Phi_n(\hat{y} = 1)e^{in\alpha\hat{x}} + \Phi_0(\hat{y} = -1) + \sum_n \Phi_n(\hat{y} = -1)e^{in\alpha\hat{x}} \\ &= \Phi_0(\hat{y} = 1) + \Phi_0(\hat{y} = -1) \\ &= C_5 - C_6 \end{aligned}$$

where the conditions from Equation (2.36) were used to remove the higher order Fourier components. We can now require $Q_1 = C_5 - C_6 = 0$, such that mass is conserved in the channel, allowing an arbitrary choice of constants,

$$\Phi_0(\hat{y} = \pm 1) = 0, \quad n = 0. \quad (2.38)$$

The final form of the flow problem that must be solved numerically is, restating Equations (2.33) – (2.38):

$$\begin{aligned} & \Phi_n^{IV} - 2n^2 \alpha^2 \Phi_n'' + n^4 \alpha^4 \Phi_n + in\alpha [\text{Re}u_{po}'' \Phi_n - \text{Re}u_{po} (\Phi_n'' - n^2 \alpha^2 \Phi_n)] \\ & + \sum_l i(n-l)\alpha \Phi_{n-l} [\Phi_l'' - l^2 \alpha^2 \Phi_l'] - \sum_l il\alpha \Phi_{n-l}' [\Phi_l'' - l^2 \alpha^2 \Phi_l] \\ & - in\alpha Ra [\theta_{o,num}^{(n)} + \eta_n] = 0, \\ & \eta_n'' - n^2 \alpha^2 \eta_n - in\alpha \text{Pr} [\text{Re}u_{po} \eta_n + \text{Re}u_{po} \theta_{o,num}^{(n)} - \Phi_n \theta_{o,un}'] \\ & - \text{Pr} \sum_l il\alpha \Phi_{n-l}' (\eta_l + \theta_{o,num}^{(l)}) + \text{Pr} \sum_l i(n-l)\alpha \Phi_{n-l} (\eta_l' + \theta_{o,num}^{(l)'}) = 0, \end{aligned}$$

subject to the boundary conditions:

$$\begin{aligned} \Phi_n(\hat{y} = \pm 1) &= 0 \\ \Phi_n'(\hat{y} = \pm 1) &= 0, \quad n = 0, \pm 1, \pm 2, \dots \\ \eta_n(\hat{y} = \pm 1) &= 0 \end{aligned} \tag{2.39}$$

This system of coupled equations must now be solved for each mode of the flow included in the solution. The summations in Equations (2.33) & (2.34) should be noted as they allow for interaction to occur between modes in the flow.

3.2.2 Numerical Solver

To solve the system of equations given in (2.33), (2.34) & (2.39) we will use a standard Matlab solver called ‘bvp4c’ which solves a system of ordinary differential equations subject to two-point boundary conditions, or more specifically:

$$\begin{aligned} y' &= f(x, y), \\ 0 &= bc(y(a), y(b)). \end{aligned}$$

For the current case, Equations (2.32) & (2.33) can be rewritten as a system of ordinary differential equations:

$$\frac{d}{dy} \begin{Bmatrix} f_n \\ f_n' \\ f_n'' \\ f_n''' \end{Bmatrix} = \begin{Bmatrix} \Phi_n' \\ \Phi_n'' \\ \Phi_n''' \\ \Phi_n^{IV} = 2n^2 \alpha^2 \Phi_n'' - n^4 \alpha^4 \Phi_n - in\alpha [\text{Re}u_{po}'' \Phi_n - \text{Re}u_{po} (\Phi_n'' - n^2 \alpha^2 \Phi_n)] \\ - \sum_l i(n-l)\alpha \Phi_{n-l} [\Phi_l''' - l^2 \alpha^2 \Phi_l'] + \sum_l il\alpha \Phi_{n-l}' [\Phi_l'' - l^2 \alpha^2 \Phi_l] \\ + in\alpha Ra [\theta_{o,nun}^{(n)} + \eta_n] \end{Bmatrix}$$

$$\frac{d}{dy} \begin{Bmatrix} g_n \\ g_n' \end{Bmatrix} = \begin{Bmatrix} \eta_n' \\ \eta_n'' = n^2 \alpha^2 \eta_n + in\alpha \text{Pr} [\text{Re}u_{po} \eta_n + \text{Re}u_{po} \theta_{o,nun}^{(n)} - \Phi_n \theta_{o,un}'] \\ + \text{Pr} \sum_l il\alpha \Phi_{n-l}' (\eta_l + \theta_{o,nun}^{(l)}) - \text{Pr} \sum_l i(n-l)\alpha \Phi_{n-l} (\eta_l' + \theta_{o,nun}^{(l)'}) \end{Bmatrix}.$$

The above system of ordinary differential equations must be set up for each mode included in the solution. This will now require that the summations from positive to negative infinity over l , which constitute internal modal coupling, be truncated such that a finite sized system of equations is being considered.

The last complication in using the standard Matlab solver is that it cannot handle complex variables and the system we want to solve is complex. This will require that the real and imaginary components of the system be separated whenever we are returning information to the solver. However, we are able to reassemble the correct complex quantities when being polled by the solver to return information about the system. The complete implementation of the 'bvp4c' solver to this system is included in the appendix; the name of the program is 'Basic_Flow_Mk4sf.m'.

The 'bvp4c' solver implements an iterative collocation method that seeks to fit a Simpson's rule, cubic polynomial to each subinterval of the mesh. This polynomial satisfies the differential equations at both ends and the mid-point of each subinterval, producing a series of non-linear algebraic equations that are iteratively solved by linearization. An initial guess is required for the solution since boundary-value problems can have more than one solution. The solver seeks to control the error in the solution through the residuals in the boundary conditions, for each subinterval and at the system boundaries. Provisions are made for the specification of absolute error in the solutions and the relative error allowed to propagate between iterations.[8]

Through a series of computational experiments, the best solution parameters were determined to be a system truncated to solving modes $-2..0..2$, with both relative and absolute errors of 1.0×10^{-6} . The reasoning for only using $-2..0..2$ modes in the solution is that the magnitude of the coefficients of the -3 and 3 modes is on the order of numerical zero, i.e. 10^{-12} , independent of the level of error specified between values of 10^{-5} to 10^{-10} . The allowable levels of error were chosen to optimize the code in two areas, the accuracy of the solution and the time required to find the solution. Solutions were sought for error levels between 10^{-5} and 10^{-10} . Solutions for error levels of 10^{-6} and lower were found to vary with the 10^{-10} solution on the order of machine zero, and as might be expected, the 10^{-6} case ran in the least amount of time.

3.3 Formulation of the Linear-Stability Problem

To this point, we have described the base flow present in a channel subjected to periodic heating in the streamwise direction. Beginning with the non-dimensional field equations, scaled as in Equations (2.8), but now considering the system in three dimensions:

$$\begin{aligned}
 \frac{\partial \hat{u}}{\partial \hat{x}} + \frac{\partial \hat{v}}{\partial \hat{y}} + \frac{\partial \hat{w}}{\partial \hat{z}} &= 0, \\
 \frac{\partial \hat{u}}{\partial \hat{t}} + \hat{u} \frac{\partial \hat{u}}{\partial \hat{x}} + \hat{v} \frac{\partial \hat{u}}{\partial \hat{y}} + \hat{w} \frac{\partial \hat{u}}{\partial \hat{z}} &= -\frac{\partial \hat{P}}{\partial \hat{x}} + \left(\frac{\partial^2 \hat{u}}{\partial \hat{x}^2} + \frac{\partial^2 \hat{u}}{\partial \hat{y}^2} + \frac{\partial^2 \hat{u}}{\partial \hat{z}^2} \right), \\
 \frac{\partial \hat{v}}{\partial \hat{t}} + \hat{u} \frac{\partial \hat{v}}{\partial \hat{x}} + \hat{v} \frac{\partial \hat{v}}{\partial \hat{y}} + \hat{w} \frac{\partial \hat{v}}{\partial \hat{z}} &= -\frac{\partial \hat{P}}{\partial \hat{y}} - \frac{1}{Fr} + Ra \hat{\theta} + \left(\frac{\partial^2 \hat{v}}{\partial \hat{x}^2} + \frac{\partial^2 \hat{v}}{\partial \hat{y}^2} + \frac{\partial^2 \hat{v}}{\partial \hat{z}^2} \right), \\
 \frac{\partial \hat{w}}{\partial \hat{t}} + \hat{u} \frac{\partial \hat{w}}{\partial \hat{x}} + \hat{v} \frac{\partial \hat{w}}{\partial \hat{y}} + \hat{w} \frac{\partial \hat{w}}{\partial \hat{z}} &= -\frac{\partial \hat{P}}{\partial \hat{z}} + \left(\frac{\partial^2 \hat{w}}{\partial \hat{x}^2} + \frac{\partial^2 \hat{w}}{\partial \hat{y}^2} + \frac{\partial^2 \hat{w}}{\partial \hat{z}^2} \right), \\
 \frac{\partial \hat{\theta}}{\partial \hat{t}} + \hat{u} \frac{\partial \hat{\theta}}{\partial \hat{x}} + \hat{v} \frac{\partial \hat{\theta}}{\partial \hat{y}} + \hat{w} \frac{\partial \hat{\theta}}{\partial \hat{z}} &= \frac{1}{Pr} \left(\frac{\partial^2 \hat{\theta}}{\partial \hat{x}^2} + \frac{\partial^2 \hat{\theta}}{\partial \hat{y}^2} + \frac{\partial^2 \hat{\theta}}{\partial \hat{z}^2} \right).
 \end{aligned} \tag{2.40}$$

The flow is now defined to be the sum of the base flow, discussed in the previous sections, and small disturbances that are dependent on both space and time.

$$\begin{aligned}
\hat{u}(x, y, z, t) &= \text{Re} \hat{u}_{po}(\hat{y}) + \hat{u}_1(\hat{x}, \hat{y}) + u_2(x, y, z, t) \\
&= u_b(x, y) + u_2(x, y, z, t), \\
\hat{v}(x, y, z, t) &= \hat{v}_1(x, y) + v_2(x, y, z, t) \\
&= v_b(x, y) + v_2(x, y, z, t), \\
\hat{w}(x, y, z, t) &= w_2(x, y, z, t), \\
\hat{\theta}(x, y, z, t) &= \text{Pr}^{-1} \hat{\theta}_o(\hat{x}, \hat{y}) + \hat{\theta}_1(\hat{x}, \hat{y}) + \theta_2(x, y, z, t) \\
&= \theta_b(x, y) + \theta_2(x, y, z, t), \\
\hat{P}(x, y, z, t) &= \text{Re}^2 \hat{P}_o(\hat{x}, \hat{y}) + \hat{P}_1(\hat{x}, \hat{y}) + P_2(x, y, z, t) \\
&= P_b(x, y) + P_2(x, y, z, t).
\end{aligned} \tag{2.41}$$

Once this definition is substituted into Equation (2.40), the base flow quantities are cancelled and the resulting equations are linearized we find that:

$$\frac{\partial u_2}{\partial x} + \frac{\partial v_2}{\partial y} + \frac{\partial w_2}{\partial z} = 0, \tag{2.42}$$

$$\begin{aligned}
\frac{\partial u_2}{\partial t} + u_b \frac{\partial u_2}{\partial x} + u_2 \frac{\partial u_b}{\partial x} + v_b \frac{\partial u_2}{\partial y} + v_2 \frac{\partial u_b}{\partial y} &= -\frac{\partial P_2}{\partial x} \\
&+ \left(\frac{\partial^2 u_2}{\partial x^2} + \frac{\partial^2 u_2}{\partial y^2} + \frac{\partial^2 u_2}{\partial z^2} \right),
\end{aligned} \tag{2.43}$$

$$\begin{aligned}
\frac{\partial v_2}{\partial t} + u_b \frac{\partial v_2}{\partial x} + u_2 \frac{\partial v_b}{\partial x} + v_b \frac{\partial v_2}{\partial y} + v_2 \frac{\partial v_b}{\partial y} &= -\frac{\partial P_2}{\partial y} \\
&+ \left(\frac{\partial^2 v_2}{\partial x^2} + \frac{\partial^2 v_2}{\partial y^2} + \frac{\partial^2 v_2}{\partial z^2} \right) + \text{Ra}(\theta_2),
\end{aligned} \tag{2.44}$$

$$\frac{\partial w_2}{\partial t} + u_b \frac{\partial w_2}{\partial x} + v_b \frac{\partial w_2}{\partial y} = -\frac{\partial P_2}{\partial z} + \left(\frac{\partial^2 w_2}{\partial x^2} + \frac{\partial^2 w_2}{\partial y^2} + \frac{\partial^2 w_2}{\partial z^2} \right), \tag{2.45}$$

$$\begin{aligned}
\frac{\partial \theta_2}{\partial t} + u_b \frac{\partial \theta_2}{\partial x} + u_2 \frac{\partial \theta_b}{\partial x} + v_b \frac{\partial \theta_2}{\partial y} + v_2 \frac{\partial \theta_b}{\partial y} \\
= \frac{1}{\text{Pr}} \left(\frac{\partial^2 \theta_2}{\partial x^2} + \frac{\partial^2 \theta_2}{\partial y^2} + \frac{\partial^2 \theta_2}{\partial z^2} \right),
\end{aligned} \tag{2.46}$$

where we have dropped the non-dimensional hatted notation for simplicity.

In the present case, we are interested in examining the growth or decay of longitudinal vortices in the flow. This assumption of disturbance form allows for the explicit functional dependence of the disturbance quantities to be stated as:

$$\begin{aligned}
 u_2(x, y, z, t) &= u(x, y) \cos(\beta z) e^{\sigma t}, \\
 v_2(x, y, z, t) &= v(x, y) \cos(\beta z) e^{\sigma t}, \\
 w_2(x, y, z, t) &= w(x, y) \sin(\beta z) e^{\sigma t}, \\
 \theta_2(x, y, z, t) &= \theta(x, y) \cos(\beta z) e^{\sigma t}, \\
 P_2(x, y, z, t) &= P(x, y) \cos(\beta z) e^{\sigma t},
 \end{aligned} \tag{2.47}$$

and once substituted into Equations (2.42) through (2.46) provides:

$$\frac{\partial u}{\partial x} + \frac{\partial v}{\partial y} + \beta w = 0, \tag{2.48}$$

$$\sigma u + u_b \frac{\partial u}{\partial x} + u \frac{\partial u_b}{\partial x} + v_b \frac{\partial u}{\partial y} + v \frac{\partial u_b}{\partial y} = -\frac{\partial P}{\partial x} + \left(\frac{\partial^2 u}{\partial x^2} + \frac{\partial^2 u}{\partial y^2} - \beta^2 u \right), \tag{2.49}$$

$$\begin{aligned}
 \sigma v + u_b \frac{\partial v}{\partial x} + u \frac{\partial v_b}{\partial x} + v_b \frac{\partial v}{\partial y} + v \frac{\partial v_b}{\partial y} &= -\frac{\partial P}{\partial y} \\
 &+ \left(\frac{\partial^2 v}{\partial x^2} + \frac{\partial^2 v}{\partial y^2} - \beta^2 v \right) + \text{Ra} \theta,
 \end{aligned} \tag{2.50}$$

$$\sigma w + u_b \frac{\partial w}{\partial x} + v_b \frac{\partial w}{\partial y} = \beta P + \left(\frac{\partial^2 w}{\partial x^2} + \frac{\partial^2 w}{\partial y^2} - \beta^2 w \right), \tag{2.51}$$

$$\sigma \theta + u_b \frac{\partial \theta}{\partial x} + u \frac{\partial \theta_b}{\partial x} + v_b \frac{\partial \theta}{\partial y} + v \frac{\partial \theta_b}{\partial y} = \frac{1}{\text{Pr}} \left(\frac{\partial^2 \theta}{\partial x^2} + \frac{\partial^2 \theta}{\partial y^2} - \beta^2 \theta \right). \tag{2.52}$$

From Equation (2.48), the w disturbance function can be expressed as a function of the other two velocity functions, u and v .

$$w = -\frac{1}{\beta} \left(\frac{\partial u}{\partial x} + \frac{\partial v}{\partial y} \right) \tag{2.53}$$

The pressure disturbance, P , can be defined in terms of u and v by combining Equations (2.51) & (2.53), and rearranging,

$$\begin{aligned}
 P &= -\frac{\sigma}{\beta^2} \left(\frac{\partial u}{\partial x} + \frac{\partial v}{\partial y} \right) - \frac{u_b}{\beta^2} \left(\frac{\partial^2 u}{\partial x^2} + \frac{\partial^2 v}{\partial x \partial y} \right) - \frac{v_b}{\beta^2} \left(\frac{\partial^2 u}{\partial x \partial y} + \frac{\partial^2 v}{\partial y^2} \right) \\
 &+ \frac{1}{\beta^2} \left(\frac{\partial^3 u}{\partial x^3} + \frac{\partial^3 v}{\partial x^2 \partial y} + \frac{\partial^3 u}{\partial x \partial y^2} + \frac{\partial^3 v}{\partial y^3} \right) - \left(\frac{\partial u}{\partial x} + \frac{\partial v}{\partial y} \right).
 \end{aligned} \tag{2.54}$$

This may now be used to eliminate the pressure terms for Equations (2.49),

$$\begin{aligned}
& \sigma \left(u - \frac{1}{\beta^2} (u_{xx} + v_{xy}) \right) + u_b \left(u_x - \frac{1}{\beta^2} (u_{xxx} + v_{xxy}) \right) \\
& + \frac{\partial u_b}{\partial x} \left(u - \frac{1}{\beta^2} (u_{xx} + v_{xy}) \right) + v_b \left(u_y - \frac{1}{\beta^2} (u_{xxy} + v_{xyy}) \right) \\
& + v \frac{\partial u_b}{\partial y} - \frac{1}{\beta^2} \frac{\partial v_b}{\partial x} (u_{xy} + v_{yy}) \\
& = -\frac{1}{\beta^2} (u_{xxxx} + v_{xxyy} + u_{xxyy} + v_{yyxx}) + 2u_{xx} + v_{xy} + u_{yy} - \beta^2 u,
\end{aligned} \tag{2.55}$$

and Equation (2.50),

$$\begin{aligned}
& \sigma \left(v - \frac{1}{\beta^2} (u_{xy} + v_{yy}) \right) + u_b \left(v_x - \frac{1}{\beta^2} (u_{xxy} + v_{yyx}) \right) \\
& + \frac{\partial v_b}{\partial y} \left(v - \frac{1}{\beta^2} (u_{xy} + v_{yy}) \right) + v_b \left(v_y - \frac{1}{\beta^2} (u_{xyy} + v_{yyy}) \right) \\
& + u \frac{\partial v_b}{\partial y} - \frac{1}{\beta^2} \frac{\partial u_b}{\partial y} (u_{xx} + v_{xy}) \\
& = -\frac{1}{\beta^2} (u_{xxyy} + v_{xxyy} + u_{xxyy} + v_{yyyx}) \\
& + 2v_{yy} + v_{xx} + u_{xy} - \beta^2 v + \text{Ra}\theta,
\end{aligned} \tag{2.56}$$

where the subscript x 's and y 's denote the corresponding partial derivatives.

Due to the periodicity of the flow, the base flow and disturbance terms can be expanded as Fourier series in the streamwise direction:

$$\begin{aligned}
u_b(x, y) &= \text{Re} u_{p0}(y) + \sum_{n=-\infty}^{\infty} \tilde{u}_n(y) e^{in\alpha x}, & u(x, y) &= \sum_{n=-\infty}^{\infty} u_n(y) e^{in\alpha x}, \\
v_b(x, y) &= \sum_{n=-\infty}^{\infty} \tilde{v}_n(y) e^{in\alpha x}, & v(x, y) &= \sum_{n=-\infty}^{\infty} v_n(y) e^{in\alpha x}, \\
\theta_b(x, y) &= \sum_{n=-\infty}^{\infty} \tilde{\theta}_n(y) e^{in\alpha x}, & \theta(x, y) &= \sum_{n=-\infty}^{\infty} \theta_n(y) e^{in\alpha x}.
\end{aligned}$$

Once these expansions have been used in Equations (2.55), (2.56) & (2.52), and the resulting nested summations simplified such that $s = m + n$, we obtain a system of three coupled differential equations that form an eigenvalue problem, in terms of σ , that describes the linear-stability of the system.

$$\begin{aligned}
& \sum_{s=-\infty}^{\infty} \left\{ \left[\operatorname{Re} u_{po} \left(is\alpha + \frac{is^3\alpha^3}{\beta^2} \right) + \frac{s^4\alpha^4}{\beta^2} - \frac{s^2\alpha^2}{\beta^2} D^2 + 2s^2\alpha^2 - D^2 + \beta^2 \right] u_s \right. \\
& + \left[\operatorname{Re} u_{po} \left(\frac{s^2\alpha^2}{\beta^2} D \right) + \operatorname{Re} Du_{po} - \frac{is^3\alpha^3}{\beta^2} D + \frac{is\alpha}{\beta^2} D^3 - is\alpha D \right] v_s \\
& + \sum_{m=-\infty}^{\infty} \left[is\alpha \tilde{u}_{s-m} \left(1 + \frac{m^2\alpha^2}{\beta^2} \right) + \tilde{v}_{s-m} \left(\left(1 + \frac{m^2\alpha^2}{\beta^2} \right) - i(s-m)\alpha \left(\frac{im\alpha}{\beta^2} \right) \right) D \right] u_m \\
& + \sum_{m=-\infty}^{\infty} \left[\tilde{u}_{s-m} \left(\frac{m^2\alpha^2}{\beta^2} \right) D - i(s-m)\alpha \tilde{u}_{s-m} \left(\frac{im\alpha}{\beta^2} \right) D - \tilde{v}_{s-m} \left(\frac{im\alpha}{\beta^2} \right) D^2 \right. \\
& \left. - i(s-m)\alpha \tilde{v}_{s-m} \left(\frac{1}{\beta^2} \right) D^2 + D\tilde{u}_{s-m} \right] v_m \left. \right\} \\
& = \sigma \sum_{s=-\infty}^{\infty} \left\{ \left[- \left(1 + \frac{s^2\alpha^2}{\beta^2} \right) u_s + \left(\frac{is\alpha}{\beta^2} \right) Dv_s \right] \right\},
\end{aligned} \tag{2.57}$$

$$\begin{aligned}
& \sum_{s=-\infty}^{\infty} \left\{ \left[\operatorname{Re} u_{po} \left(\frac{s^2\alpha^2}{\beta^2} D \right) + \operatorname{Re} Du_{po} \left(\frac{s^2\alpha^2}{\beta^2} \right) + \frac{is\alpha}{\beta^2} D^3 - \frac{is^3\alpha^3}{\beta^2} D - is\alpha D \right] u_s \right. \\
& + \left[\operatorname{Re} u_{po} \left(is\alpha \left(1 - \frac{D^2}{\beta^2} \right) \right) - \operatorname{Re} Du_{po} \left(\frac{is\alpha}{\beta^2} D \right) + \frac{D^4}{\beta^2} - \frac{s^2\alpha^2}{\beta^2} D^2 \right. \\
& \left. - 2D^2 + s^2\alpha^2 + \beta^2 \right] v_s - \operatorname{Ra}\theta_s + \sum_{m=-\infty}^{\infty} \left[\tilde{u}_{s-m} \left(\frac{m^2\alpha^2}{\beta^2} D \right) - D\tilde{v}_{s-m} \left(\frac{im\alpha}{\beta^2} \right) D \right. \\
& + i(s-m)\alpha \tilde{v}_{s-m} - \tilde{v}_{s-m} \left(\frac{im\alpha}{\beta^2} D^2 \right) + D\tilde{u}_{s-m} \left(\frac{m^2\alpha^2}{\beta^2} \right) \left. \right] u_m \\
& + \sum_{m=-\infty}^{\infty} \left[\tilde{u}_{s-m} \left(im\alpha \left(1 - \frac{D^2}{\beta^2} \right) \right) + D\tilde{v}_{s-m} \left(1 - \frac{D^2}{\beta^2} \right) + \tilde{v}_{s-m} \left(1 - \frac{D^2}{\beta^2} \right) D \right. \\
& \left. - D\tilde{u}_{s-m} \left(\frac{im\alpha}{\beta^2} \right) D \right] v_m \left. \right\} = \sigma \sum_{s=-\infty}^{\infty} \left\{ \left[\left(\frac{is\alpha}{\beta^2} \right) Du_s - \left(1 - \frac{D^2}{\beta^2} \right) v_s \right] \right\}
\end{aligned} \tag{2.58}$$

and

$$\begin{aligned}
& \sum_{s=-\infty}^{\infty} \left\{ \left[\operatorname{Re} u_{po}(is\alpha) + \frac{1}{\operatorname{Pr}} (s^2 \alpha^2 - D^2 + \beta^2) \right] \theta_s \right. \\
& \quad \left. + \sum_{m=-\infty}^{\infty} [i(s-m)\alpha \tilde{\theta}_{s-m}] u_m + \sum_{m=-\infty}^{\infty} [D \tilde{\theta}_{s-m}] v_m + \sum_{m=-\infty}^{\infty} [im\alpha \tilde{u}_{s-m} + \tilde{v}_{s-m} D] \theta_m \right\} \\
& = \sigma \sum_{s=-\infty}^{\infty} \{-\theta_s\},
\end{aligned} \tag{2.59}$$

where the notation $D = \frac{d}{dy}$ has been used.

The boundary conditions for this system of equations follow from Equation (2.41), once Equations (2.21) & (2.22) have been used to supply the boundary conditions from the base flow. The no-slip conditions for the flow field become

$$\begin{aligned}
\hat{u}(x, y = \pm 1, z, t) &= \operatorname{Re} \hat{u}_{po}(\hat{y} = \pm 1) + \hat{u}_1(\hat{x}, \hat{y} = \pm 1) + u_2(x, y = \pm 1, z, t) = 0 \\
&= 0 + u_2(x, y = \pm 1, z, t) = 0 \\
&= u(x, y = \pm 1) \cos(\beta z) e^{\sigma t} = 0 \\
\Rightarrow u(x, y = \pm 1) &= \sum_{n=-\infty}^{\infty} u_n(y = \pm 1) e^{in\alpha x} = 0 \\
\therefore u_n(y = \pm 1) &= 0, \quad n = -\infty \dots 0 \dots \infty,
\end{aligned} \tag{2.60}$$

and

$$\begin{aligned}
\hat{v}(x, y = \pm 1, z, t) &= \hat{v}_1(x, y = \pm 1) + v_2(x, y = \pm 1, z, t) = 0 \\
&= 0 + v_2(x, y = \pm 1, z, t) = 0 \\
&= v(x, y = \pm 1) \cos(\beta z) e^{\sigma t} = 0 \\
\Rightarrow v(x, y = \pm 1) &= \sum_{n=-\infty}^{\infty} v_n(y = \pm 1) e^{in\alpha x} = 0 \\
\therefore v_n(y = \pm 1) &= 0, \quad n = -\infty \dots 0 \dots \infty.
\end{aligned} \tag{2.61}$$

Using Equation (2.53), and the appropriate Fourier expansions, we find that

$$\begin{aligned}
 \hat{w}(x, y = \pm 1, z, t) &= w_2(x, y = \pm 1, z, t) = 0 \\
 &= w(x, y = \pm 1) \sin(\beta z) e^{\sigma t} = 0 \\
 \Rightarrow w(x, y = \pm 1) &= \sum_{n=-\infty}^{\infty} [i \alpha u_n(y = \pm 1) e^{i n \alpha x} + D v_n(y = \pm 1) e^{i n \alpha x}] = 0 \quad (2.62) \\
 &= 0 + \sum_{n=-\infty}^{\infty} D v_n(y = \pm 1) e^{i n \alpha x} = 0 \\
 &\therefore D v_n(y = \pm 1) = 0, \quad n = -\infty \dots 0 \dots \infty.
 \end{aligned}$$

The temperature continuity conditions at the boundary similarly require that

$$\begin{aligned}
 \hat{\theta}(x, y = \pm 1, z, t) &= \text{Pr}^{-1} \hat{\theta}_o(x, y = \pm 1) + \hat{\theta}_1(x, y = \pm 1) + \theta_2(x, y = \pm 1, z, t) = 0 \\
 &= 0 + \theta_2(x, y = \pm 1, z, t) = 0 \\
 &= \theta(x, y = \pm 1) \cos(\beta z) e^{\sigma t} = 0 \quad (2.63) \\
 \Rightarrow \theta(x, y = \pm 1) &= \sum_{n=-\infty}^{\infty} \theta_n(y = \pm 1) e^{i n \alpha x} = 0 \\
 &\therefore \theta_n(y = \pm 1) = 0, \quad n = -\infty \dots 0 \dots \infty.
 \end{aligned}$$

Equations (2.57) through (2.59) constitute an eigenvalue problem, subject to the boundary conditions contained in Equations (2.60) through (2.63). The remainder of this thesis will focus on finding an appropriate numerical solution to this problem and the presentation of results. This will include a discussion of the resulting flow dynamics in terms of its agreement with previous investigations and its implication for applications.

3.4 Numerical Solution Technique

This section will describe the numerical techniques used to find an adequate solution to the characteristic value problem posed in Section 3.3, which describes the linear-stability of vortices in a channel subjected to periodic heating modulations along the walls of the channel. The preparation of the equations, the techniques used for their solution and the control of error will be described.

3.4.1 Preparation of the Governing Equations for Numerical Solution

The nature of the channel flow being studied requires that any discretization scheme used across the channel must be able to sufficiently capture the shear layers along the walls. For uniformly spaced collocation points to adequately capture the mechanics

close to the walls a dense distribution of points must be used. This, however, adds a great deal of computation time since a number of points are now located in the centre of the channel where such precise description is not required. To address this issue the roots of Chebyshev polynomials were used. This particular class of polynomial is well behaved within the bounds $[-1,1]$, providing dense distributions of points approaching either wall and a rarefied distribution in the centre of the channel. By reducing the number of computations there will also be a reduction in the accumulation of error as the calculations progress.

Chebyshev polynomials have the added advantage that if a grid function, $p(x_j) = v_j, 0 \leq j \leq N$, is defined on the Chebyshev root points, then the discrete derivative, $w_j = p'(x_j)$, maybe be represented as

$$w = D_N v, \quad (3.1)$$

from the fact that the operation is linear and as such may be represented by a multiplication of an $(N+1) \times (N+1)$ sized matrix. Here N denotes the order of the Chebyshev polynomial being used. This matrix, D_N , is defined as follows:

$$(D_N)_{00} = \frac{2N^2 + 1}{6} \quad (3.2)$$

$$(D_N)_{NN} = -\frac{2N^2 + 1}{6} \quad (3.3)$$

$$(D_N)_{jj} = \frac{-x_j}{2(1-x_j^2)}, \quad j = 1, \dots, N-1 \quad (3.4)$$

$$(D_N)_{ij} = \frac{c_i}{c_j} \frac{(-1)^{i+j}}{(x_i - x_j)}, \quad i \neq j, \quad i, j = 0, \dots, N \quad (3.5)$$

where

$$c_i = \begin{cases} 2, & i = 0 \text{ or } N, \\ 1, & \text{otherwise.} \end{cases} \quad (3.6)$$

In this manner higher order derivatives may be obtained through successive applications of this matrix, and following the notation introduced in the previous section, will be denoted as:

$$D = D_N,$$

$$D^2 = D_N D_N,$$

$$D^3 = D_N D_N D_N,$$

and

$$D^4 = D_N D_N D_N D_N.$$

Following this discretization, Equations (2.57), (2.58) & (2.59) may be numerically constructed in a linear algebraic form such that a generalized eigenvalue problem is obtained,

$$\vec{A} \begin{pmatrix} u_{-n} \\ v_{-n} \\ \theta_{-n} \\ \vdots \\ u_s \\ v_s \\ \theta_s \\ \vdots \\ u_n \\ v_n \\ \theta_n \end{pmatrix} = \sigma \vec{B} \begin{pmatrix} u_{-n} \\ v_{-n} \\ \theta_{-n} \\ \vdots \\ u_s \\ v_s \\ \theta_s \\ \vdots \\ u_n \\ v_n \\ \theta_n \end{pmatrix},$$

where \vec{A} and \vec{B} are matrices built through the summation of the linear operations applied to the eigenvectors and the infinite summations have been arbitrarily truncated such that only modes $-n \dots 0 \dots n$ are considered [19]. In constructing these matrices, care must be taken to respect the modal organization of the eigenvectors, i.e. u_{-1} , u_0 , u_1 etc., and the coupling terms between the three equations being expressed.

The boundary conditions are applied through the substitution, or elimination, of the appropriate rows and columns in these matrices. Equations (2.60) and (2.63) are applied by removing the rows and columns associated with the u and θ eigenfunctions at the boundary points. Meanwhile, Equations (2.61) and (2.62) are applied together by replacing the rows associated with the v eigenfunctions at the boundary points in the \bar{A} matrix with the appropriate lines from the derivative matrix, and the corresponding rows in the \bar{B} matrix with zeros.

3.4.2 The Eigenvalue Solver

Solutions to this numerical eigenvalue problem may now be sought using a standard solver. In this case the Matlab ‘eig’ routine is used, providing as many eigenvalues as the length of the eigenvectors. This routine is adaptive to the properties of the matrices being considered, i.e. Diagonal, Hermitian, etc., and can provide the associated eigenvectors to allow for the proper enforcement of the boundary conditions to be confirmed. If any of the eigenvalues returned are positive in sign then infinitesimal vortices will grow in the channel, while if the eigenvalue is negative in sign the vortices will be damped out.

The script called ‘Wall_Temp_Vort_Stab_NL_FloryanForm.m’ which is used to solve this eigenvalue problem is included in the appendix, along with the supplemental scripts called as procedures.

3.4.3 Error and its Control in the Numerical Solution

The error obtained in the eigenvalues and eigenfunctions returned by the solver may be controlled by varying the number of Fourier modes used in the streamwise expansion and the order of the Chebyshev polynomial used in the spanwise discretization of the disturbance flow and temperature fields.

The number of Fourier modes, n , used to obtain a given solution to the problem was determined through a process of trial and error, in which the number of unchanging significant digits in the returned eigenvalues is monitored. An accuracy of 4 significant digits was sought as a blanket accuracy for the analysis discussed in the remainder of this

thesis, with the number of Fourier modes being considered changing as needed to reflect this accuracy.

Chebyshev polynomials of order $N = 51$ were used as they provided a good balance between accuracy, with regard to discretization error, and computation time. Through trial and error fifty-one collocation points were found to provide between 7-10 digits of accuracy, depending on the particular physical parameters being considered. An odd number of points is used to allow a collocation point to fall on the centre line of the channel.

4 Discussion of the Stability Characteristics of the Flow

To this point we have analytically derived the equations that describe the Poiseuille flow present in a channel while subjected to periodic heating modulations in the streamwise direction. The numerical solution of these coupled equations will be used as an input to a linear-stability analysis. The governing equations for this analysis have been outlined in previous sections, and a numerical technique for the solution of this eigenvalue problem has been implemented. The subject of this section will be the analysis of the growth or decay of longitudinal vortices in the flow, examined over a range of flow and heating parameters.

4.1 The Two Cases

This thesis will focus on two particular cases of heating arrangement. The first is the case where there exists heating applied sinusoidally along one wall of the channel, while for the other case a mean temperature gradient is applied across the channel in addition to these heating modulations. For the second case, the unstable instance of heat from below will be focused on since this is the basis of the classical study presented by Chandrasekhar [4], providing a good asymptotic check for the numerical solutions.

Classically, the heating of the fluid from above stabilizes the Poiseuille flow in the channel. As such, a dramatically different approach will be required since the heating modulations needed to cause instability in this arrangement were found to be substantial fractions of the thermal gradient applied across the channel. This casts doubt on whether the numerical methods used here are adequate to capture the requisite physics found in the flow for a useful analysis to be conducted. The primary concern with the numerical methods used were their stability as the relative magnitudes of the different terms in the equations were varied.

4.2 Poiseuille Flow Subjected to Periodic Heating Modulations

The physical arrangement that will be considered in this section is that of a Poiseuille flow modulated by a sinusoidal heating pattern in the direction of the flow. A point of note is the definition of the Rayleigh number for this flow. The temperature

difference, ΔT , that this parameter will be based on is that of the peak-to-peak amplitude of the sinusoidal heating imposed on the wall.

This arrangement will also require that the uniform component of heating, $\hat{\theta}_{o,un}$, be set to zero as, for the moment, there is only a non-uniform thermal condition along the boundary of the channel.

4.2.1.1 Equivalency of Two Flow Arrangements

To this point the specification of which wall, the upper or the lower, will be heating in a sinusoidal pattern has been deliberately left vague. This is because it is analytically possible to show the equivalency of these two physical arrangements. This allows for the analysis of only one particular case, with a generalization to the other being available. We begin by considering Equations (2.58), (2.59) and the last two equations in (2.8), which govern the linear-stability of the fluid system and the definition of the basic state respectfully. We restate the definition of the Rayleigh number for this problem,

$$Ra = \frac{g\gamma d^3 \Delta T}{\kappa_o \nu_o}.$$

For our purposes we will consider un-primed quantities to represent variables in the case of the lower wall of the channel being heated, and primed quantities for the case of upper wall heating. This gives the definition of the Rayleigh number for the upper wall heating as

$$Ra' = \frac{g'\gamma d^3 \Delta T}{\kappa_o \nu_o}, \quad (4.1)$$

noting that this definition requires that the equality $g = -g'$ hold such that the case of upper wall heating is the same as the case of lower wall heating with the direction of gravity inverted. The fact that $Ra = -Ra'$ follows as well.

This equality is substituted into Equation (2.58):

$$Au_s + Bv_s - [Ra]\theta_s + \sum_m Cu_m + \sum_m Ev_m = \sigma(Fu_s + Gv_s),$$

$$\begin{aligned}
&\Rightarrow Au_s + Bv_s - [-Ra']\theta_s + \sum_m Cu_m + \sum_m Ev_m = \sigma(Fu_s + Gv_s), \\
&\Rightarrow Au_s + Bv_s - [Ra']\theta'_s + \sum_m Cu_m + \sum_m Ev_m = \sigma(Fu_s + Gv_s), \tag{4.2}
\end{aligned}$$

where placeholders have been used to simplify the operations present in the lengthy expression. This gives that $\theta_s = -\theta'_s$ and similarly from the third of (2.8):

$$\begin{aligned}
\frac{\partial \hat{v}}{\partial \hat{t}} + \hat{u} \frac{\partial \hat{v}}{\partial \hat{x}} + \hat{v} \frac{\partial \hat{v}}{\partial \hat{y}} &= -\frac{\partial \hat{P}}{\partial \hat{y}} - \frac{1}{Fr} + Ra\hat{\theta} + \nabla^2 \hat{v}, \\
\Rightarrow \frac{\partial \hat{v}}{\partial \hat{t}} + \hat{u} \frac{\partial \hat{v}}{\partial \hat{x}} + \hat{v} \frac{\partial \hat{v}}{\partial \hat{y}} &= -\frac{\partial \hat{P}}{\partial \hat{y}} - \frac{1}{Fr} + Ra'\hat{\theta}' + \nabla^2 \hat{v},
\end{aligned}$$

we find that $\hat{\theta} = -\hat{\theta}'$. Substituting this equality into the fourth of (2.8):

$$\begin{aligned}
\frac{\partial \hat{\theta}}{\partial \hat{t}} + \hat{u} \frac{\partial \hat{\theta}}{\partial \hat{x}} + \hat{v} \frac{\partial \hat{\theta}}{\partial \hat{y}} &= \frac{1}{Pr} \nabla^2 \hat{\theta}, \\
\Rightarrow \frac{\partial \hat{\theta}'}{\partial \hat{t}} + \hat{u} \frac{\partial \hat{\theta}'}{\partial \hat{x}} + \hat{v} \frac{\partial \hat{\theta}'}{\partial \hat{y}} &= \frac{1}{Pr} \nabla^2 \hat{\theta}',
\end{aligned}$$

and Equation (2.59)

$$H\theta_s + \sum_m [i(s-m)\alpha\tilde{\theta}_{s-m}]\mu_m + \sum_m [D\tilde{\theta}_{s-m}]v_m + \sum_m J\theta_m = -\sigma\theta_s,$$

using a Fourier expansion in the direction of the flow,

$$\begin{aligned}
\hat{\theta}(x, y) &= \sum_{n=-\infty}^{\infty} \tilde{\theta}_n(y)e^{in\alpha x} = -\hat{\theta}', \\
\Rightarrow \hat{\theta}'(x, y) &= \sum_{n=-\infty}^{\infty} -\tilde{\theta}_n(y)e^{in\alpha x} = \sum_{n=-\infty}^{\infty} \tilde{\theta}'_n(y)e^{in\alpha x} \Rightarrow \tilde{\theta}'_n = -\tilde{\theta}_n,
\end{aligned}$$

gives

$$\begin{aligned}
H(-\theta'_s) + \sum_m [i(s-m)\alpha(-\tilde{\theta}'_{s-m})]\mu_m \\
+ \sum_m [D(-\tilde{\theta}'_{s-m})]v_m + \sum_m J(-\theta'_m) &= -\sigma(-\theta'_s),
\end{aligned}$$

again using placeholders for the operations, and finally

$$\begin{aligned}
 H\theta'_s + \sum_m [i(s-m)\alpha\tilde{\theta}'_{s-m}] \mu_m \\
 + \sum_m [D\tilde{\theta}'_{s-m}] \nu_m + \sum_m J\theta'_m = -\sigma\theta'_s.
 \end{aligned}
 \tag{4.3}$$

We find that Equations (4.2) & (4.3) have the same algebraic structure as (2.58) and (2.59), showing that we are examining both heating cases at the same time and as such the results discussed in the following section hold for both instances.

4.2.2 Definition of the 'Critical' Stability Condition

Before the stability of the flow can be discussed, we must first define what will be considered the 'critical' condition at which vortices will grow in the channel. Figure 22 shows a curve tracking the position in parameter space where vortices are neither suppressed nor enhanced by the dynamics of the flow. This is called a neutral growth-rate curve and in this instance is given for an arbitrary Reynolds number and heating wavenumber, α , which specifies the spatial distribution of heating on the wall. All points below the neutral curve are considered stable, damping the growth of vortices. While for those above the curve, the vortices will grow leading to an unstable condition.

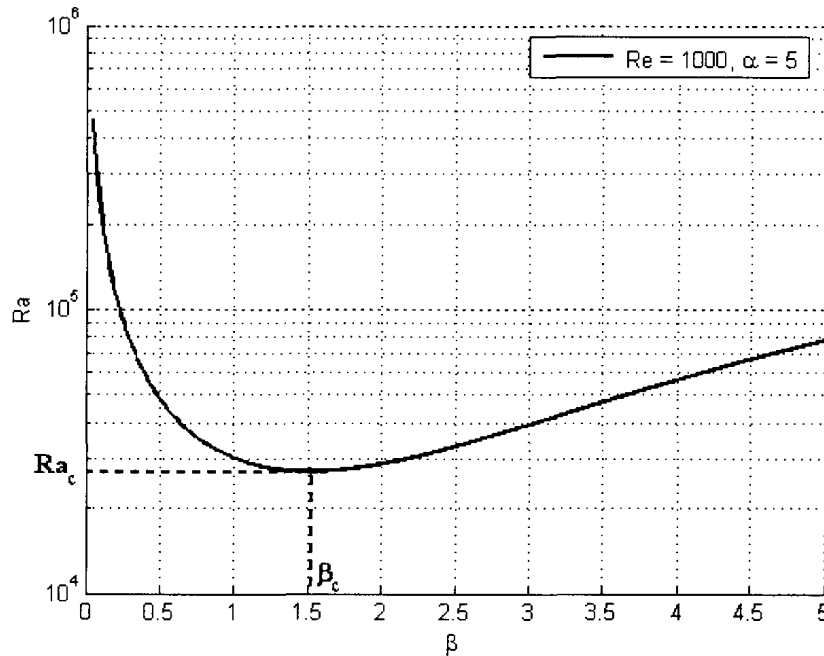


Figure 22 - Neutral growth-rate curve, Rayleigh number versus disturbance wavenumber, β , for Prandtl number, Pr , equal to 0.71, Reynolds number equal to 1000 and heating wavenumber, α , equal to 5 with the critical Rayleigh number, Ra_c , and critical vortex wavenumber, β_c , indicated.

The disturbance wavenumber, β , provides a physical scale for the vortices and we find that the stability characteristics of the vortices vary dependent on this wavenumber. The neutral curve shows a linear behaviour with increasing wavenumber, while at lower values the curve asymptotically approaches an infinite Rayleigh number. This is to be expected, as an infinite wavelength vortex should take an infinite potential, provided by the alternating heating, to overcome the inertia of the fluid and drive the system to instability. However, we are at the moment only particularly interested in studying the growth or decay of the vortices in general, and are not preferential as to which wavenumber of vortex is the most likely to first become unstable with increasing Rayleigh number. It is this first point of instability that we will refer to as the critical stability condition for a particular flow arrangement.

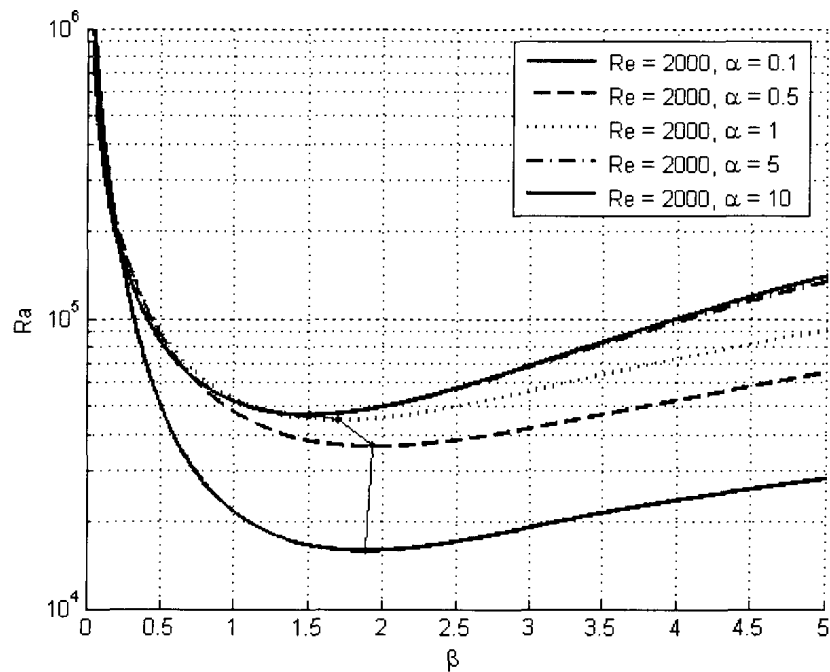


Figure 23 - Neutral growth-rate curves, Rayleigh number versus disturbance wavenumber, β , for Prandtl number, Pr , equal to 0.71, Reynolds number equal to 2000 and various heating wavenumbers, α .

This critical point is seen to vary with flow parameters, but remains in the neighbourhood of the height dimension of the channel, approximately $\pi/2 = 1.5707$. Figure 23 shows this for a range of spatial distributions of the heating. Once these critical conditions are plotted with respect to the flow parameters the problem becomes much more physically intuitive. These relationships are discussed in the following sections.

4.2.3 Reynolds Number Dependence

The critical stability conditions obtained from a particular spatial distribution of heating is of interest as this information has the potential for application to heat-transfer processes. Figure 24 shows the critical stability data arranged by the wavenumber of the heating applied along the channel. As the Reynolds number is increased a linear asymptotic behaviour is displayed by the flow, with the influence of heating wavenumber reducing as the Reynolds number is increased. The increased inertia of the flow has a stabilizing influence with respect to longitudinal vortices.

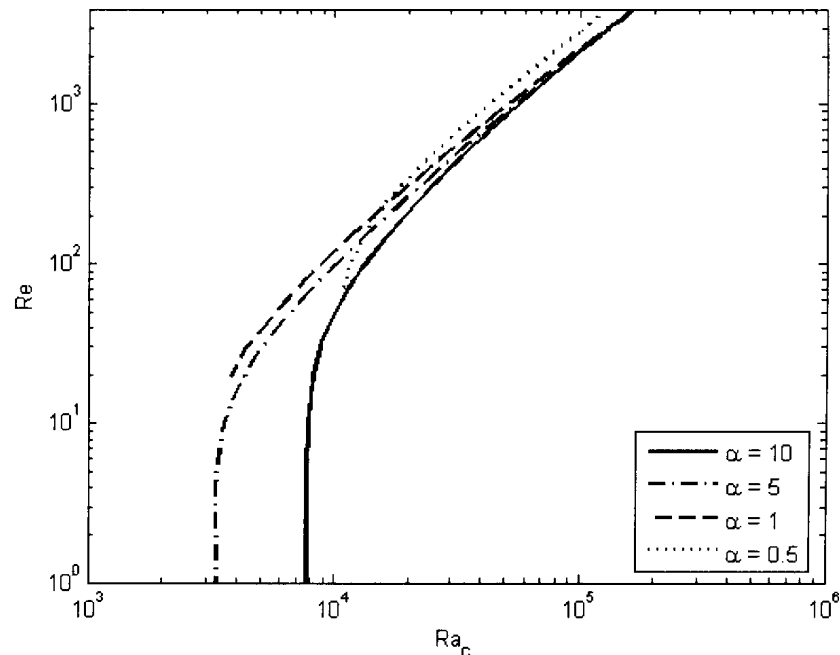
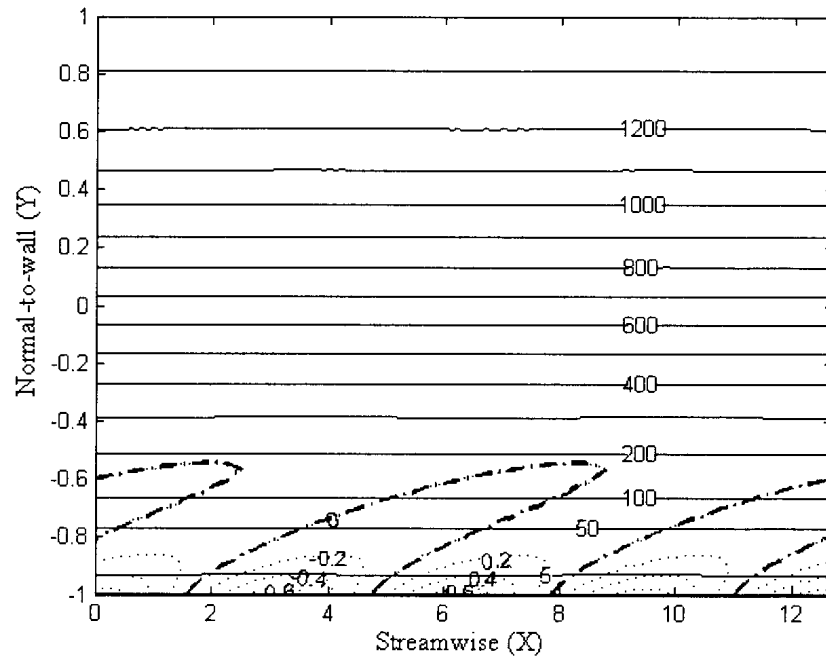


Figure 24 - Critical stability conditions, Reynolds number, Re , versus critical Rayleigh number, Ra_c , for Prandtl number, Pr , equal to 0.71 and selected values of heating wavenumber, α .

In the other Reynolds number limit, as it approaches zero, a minimum critical Rayleigh number is reached in which the forcing wavelength of the heating dominates the dynamics of the flow. These two limiting behaviours can be observed in the base flow present in the channel before the formation of vortices. An inertially dominated, high-Reynolds number flow is shown in Figure 25. The influence of the alternating heating is nearly imperceptible for this combination of flow parameters. A small variation in the streamline, denoted by the value 5, is noticeable along the lower wall.



this limiting case. The influence of heating wavenumber is examined further in a later section.

4.2.4 Prandtl Number Dependence

In examining the dependence of the flows' stability on the Prandtl number, we are really taking into account the possibility of different working fluids in the channel. To this point all the information presented has been for a Prandtl number of 0.71, which corresponds to air. Figure 27 gives the critical stability conditions for three different fluids, or Prandtl numbers. If a more viscous fluid such as water, $Pr = 7.01$, is used, then the curve for a particular spatial distribution shifts downward compared to that for air. Such viscous fluids require higher amplitudes of heating modulations to drive the system to instability.

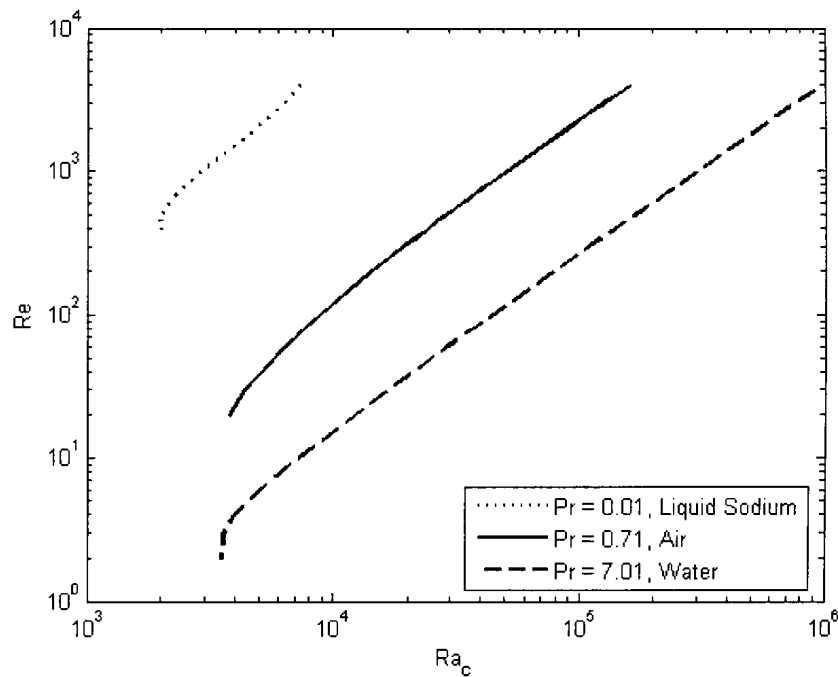


Figure 27 - Critical stability conditions, Reynolds number, Re , versus critical Rayleigh number, Ra_c , for a heating wavenumber, α , equal to 1 and selected values of Prandtl number, Pr .

We do find that the limiting Reynolds number cases behave in a similar manner, with a minimum critical Rayleigh number reached for lower Reynolds number flows and a linear asymptotic behaviour for high values.

For a more conductive fluid such as liquid sodium, $Pr = 0.01$, the opposite occurs. The critical conditions for a given wavenumber of heating shift upward on the graph, showing that the increase in conductivity enables the heating to penetrate further into the centre of the channel, allowing the Poiseuille flow to be influenced more greatly by the modulated heating along the boundary.

The minimum critical Rayleigh number is also effected by varying the Prandtl number, allowing a reduction of this value with lower Prandtl number fluids. This effect, however, is found to be smaller than that achieved by varying the wavelength of the applied heating as can be seen by comparing the curves in Figure 27 with those given in Figure 24.

4.2.5 Disturbance Wavenumber Dependence

As has already been mentioned, the wavenumber of the heating modulations is a key parameter in the critical stability conditions of the flow. Figure 28 shows this relationship in a much clearer manner than previously. For short wavelengths of heating, or high wavenumbers, the stability of vortices in the flow become much more highly dependent on the Reynolds number and the amplitude of heating being applied.

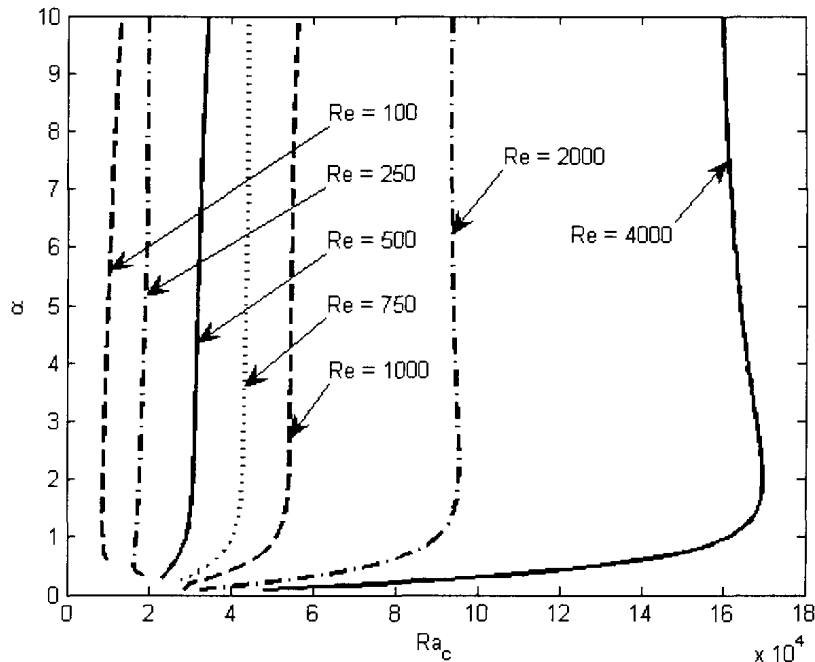


Figure 28 - Critical stability conditions, heating wavenumber, α , versus critical Rayleigh number, Ra_c , for Prandtl number, Pr , equal to 0.71 and selected values of Reynolds number, Re .

This holds true until the wavelength of the heating becomes approximately equal to the height of the channel. It is at this point that further increases in wavelength cause a dramatic reduction in the amplitude of heated, the critical Rayleigh number, required to drive the system to instability.

For example, if the flow has a base Reynolds number of 4000, an order of magnitude increase in the wavelength of heating, from $\alpha = 1$ to 0.1, will reduce the critical Rayleigh number required for vortices to form proportionally by an order of magnitude, from $Ra_c = 1.607 \cdot 10^5$ to $4.784 \cdot 10^4$. Such a change in Rayleigh number would mean that either the channel height may be reduced by a factor of $10^{1/3}$ (≈ 2.154) or the amplitude of heating may be reduced by a factor of 10 while achieving the same result.

This increased dependence on heating wavenumber is reduced as the flow is slowed, with the opposite effect on critical Rayleigh number being observed for flows of Reynolds number of approximately 300 or less. Unfortunately, the solver used to obtain the base flow became inadequate to obtain an acceptable precision for such cases as the wavenumber was reduced. This occurred even after allowing the iterative solver to subdivide the solution space into more than 10,000 segments across the channel.

4.3 Poiseuille Flow subjected to Unstable Thermal Stratification and Periodic Heating Modulations

The physical arrangement of a channel subjected to modulated heat along the lower wall, as well as a mean temperature gradient between the walls, will now be examined. This particular case is an extension of the classical case of a Poiseuille flow heated from below, presented by many authors. The Rayleigh number for this problem will now be based on the temperature difference between the upper and lower walls, which then necessitates the introduction of a new parameter, T_m , to describe the amplitude of the heating modulations. This new heating parameter will measure the absolute peak-to-peak temperature difference of the modulations as a percentage of the temperature difference imposed across the channel.

Pellow & Southwell [9] give a critical Rayleigh number of 1708 and disturbance wavenumber of 3.13 in their analytical investigation of the classical case of the unstable stratification of a Poiseuille flow. These critical parameters must be scaled appropriately to allow a comparison with the current problem, giving a critical Rayleigh number of 213.5 and a wavenumber of 1.565. This result is insensitive to the Reynolds number of the base flow. These values match the limiting case as the amplitude of the heating modulation approaches zero, as obtained numerically from the linear-stability analysis.

4.3.1 The Influence of the Amplitude of Heating Modulations

As might be expected, the impact of the modulated heating on the stability characteristics of the flow is directly tied to the amplitude of the heating modulations. The range of periodic heating amplitudes that will be considered is limited by the numerical techniques being used to analyse the stability of the system. The higher the amplitude of the modulations, the more unstable the numerical methods become, effecting the accuracy of the results. For this reason, a maximum amplitude of 25% of the temperature difference between the walls will be examined. This value was chosen by monitoring the asymptotic behaviour of the system as the amplitude of the heating modulations were increased. For values over 40%, the limiting classical critical values were unobtainable, indicating the need for further investigation into a different solver for the base flow or at the least a verification of these values through the use of a finite-

amplitude time-dependent stability analyse. This is not pursued in this thesis, but is recommended as an avenue for future research.

Figure 29 shows the critical stability conditions, found in a similar manner as that described in Section 4.2.2, for a selection of heating amplitudes.

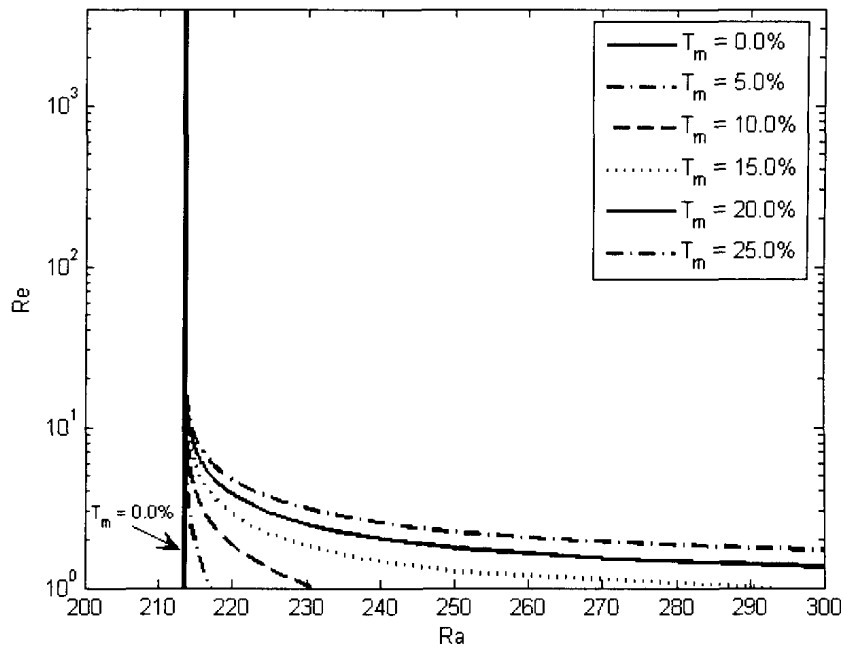


Figure 29 – Critical stability conditions, Reynolds number, Re , versus Rayleigh number, Ra , for Prandtl number, Pr , equal to 0.71, heating wavenumber, α , equal to 1 and selected amplitudes of modulated heating, T_m .

These results are consistent with those for the case with no mean thermal gradient across the channel. As the Reynolds number of the flow increases, the inertia of the flow dominates the buoyancy forces from the heating and we recover the classical critical stability conditions for longitudinal vortices, or 213.47 to be particular. However, for lower Reynolds number flows the effects of the periodic heating become evident, delaying the onset of instability in the flow and requiring either large modulations of heating or a higher mean thermal gradient across the channel to promote the growth of vortices.

4.3.2 Reynolds Number & Disturbance Wavenumber Dependence

In a similar manner to that discussed for the heating modulation-only case, flows with high heating wavenumbers show an asymptotic behaviour. In this case these flows

recover the classical critical conditions and are consistently independent of the Reynolds number examined.

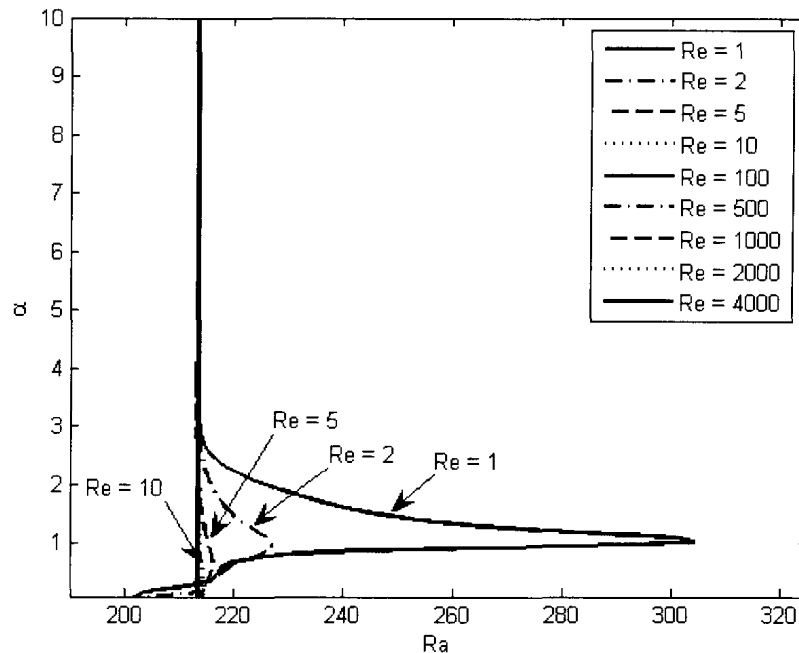


Figure 30 - Critical stability conditions, heating wavenumber, α , versus critical Rayleigh number, Ra , for Prandtl number, Pr , equal to 0.71, heating modulation amplitude, T_m , equal to 15% and various Reynolds numbers, Re .

A heating modulation amplitude of 15% was chosen to provide a representative description of the stability characteristics of the flow. Higher or lower amplitudes will respectively have an increased or decreased impact on the flow. These proportional differences can be read off of Figure 29 given a particular arrangement for the flow.

A sensitivity to a heating wavelength on order of the dimension of the channel can be seen in Figure 30, with this sensitivity enhanced as the Reynolds number of the flow is decreased. For very long wavelengths of heating the critical conditions for these lower Reynolds number flows is actually decreased, promoting the growth of heat-transfer enhancing vortices in the channel at reduced heating conditions as compared to the zero-amplitude heating modulation case. This may be practical for applications relating to heat-transfer in narrow channels or even for dimension down to the micro-scale, so long as the continuous media assumption holds.

5 Summary and Conclusions

The age-old axiom of working smarter and not harder holds true for many things. In the context of the current investigation into the formation of longitudinal vortices in a Poiseuille flow between two horizontal plates, we are seeking to increase the mixing in the flow to better promote the heat-transfer process. The fact that longitudinal vortices provide an increase in the mixing of the flow has been well documented by previous investigators. The use of periodic heating modulations along the walls of the channel to promote or suppress such vortical structures is the primary focus of this research.

A mathematical model for the laminar flow present in the channel subjected to periodic heating loads along the channel walls has been presented, and an adequately accurate numerical solver implemented to provide a description of the base flow. This flow field information is then used as a parameter in a linear-stability analysis of the flow with respect to longitudinal vortices, for which an eigenvalue problem has been derived. This eigenvalue problem is solved using a spectral-collocation method based on Chebyshev polynomials, and provides solutions to the problem which sufficiently account for the dynamic properties of the fluid system.

Two physical arrangements have been examined in detail. The first is that of a Poiseuille flow subjected to a sinusoidal heating, and cooling, pattern along one of the channel walls in the direction of the flow. A proof has been provided to show the mathematical equivalency of applying this heating to either the upper or lower wall of the channel.

It was found that for large wavenumber, short wavelength, heating patterns the critical stability conditions for the flow were primarily influenced by the Reynolds number of the flow and the Rayleigh number of the periodic heating along the wall. This is in contrast to long wavelength patterns, as the stability characteristics of the flow become more greatly dominated by the wavenumber of the periodic heating, creating substantial reductions in the Rayleigh number required for the exponential growth of longitudinal vortices in the flow. The transition point between these two behaviours is

approximately where the wavelength of the heating matches the vertical height of the channel.

The impact of the Prandtl number of the fluid in the channel was also examined, with the result that lower Prandtl number, either more highly conductive or less viscous fluids, show a greater ability to be influenced by the heating modulations.

The second physical arrangement examined was that of a horizontal Poiseuille flow where the lower wall has been heated, or alternatively the upper wall cooled, while again being subjected to period heating modulations in the direction of the flow. In the limit of a decreasing amplitude of heating modulations, the classical stability conditions derived by previous investigators are recovered, independent of the Reynolds number of the flow.

The influence of the ratio of the magnitude of the heating modulations to the temperature difference applied across the channel was examined with the expected results; that the larger the amplitude of the modulations, the more dramatic their influence on the dynamics of the flow. Short wavelengths, large wavenumbers, of heating do not cause the critical flow conditions to vary from the classical results. However, as the wavelength is increased the flow is shown to be much more sensitive to heating patterns with wavelengths of approximately the height of the channel. Around this value the flow is stabilized by the presence of the heating modulations, with the effects more greatly observable for lower Reynolds number flows. As the wavelength of the heating continues to be increased, longitudinal vortices are seen to be promoted by the periodic heating, however, as with the earlier mentioned stabilization of the flow this effect is enhanced as the Reynolds number is decreased.

There is the potential for further research into the effects of large amplitude heating modulations on the flow in the channel. This investigation will require a more robust solver for the base flow in the channel and as such makes the current computationally intense problem even more involved to approach. There is also the potential for the implementation of this variety of passive flow control into actual heat-transfer processes, with the most promising application, presently, being to micro-cooling channel on integrated circuits.

It has been shown that by applying periodic heating and cooling patterns to the walls of a channel containing a Poiseuille flow, the dynamics of the formation of longitudinal vortices in that channel may be manipulated. Cases have been examined both with and without mean thermal stratification across the channel. The critical stability criteria for the promotion or suppression of longitudinal vortices have been identified and the behavioural trends of the flow discussed over the applicable range of flow parameters.

6 Bibliography

- [1] Rayleigh, L., "Investigation of the character of the equilibrium of an incompressible heavy fluid of variable density." *Proc. Lon. Math. Soc.*, **XIV**, pp. 170, 1883.
- [2] Chandrasekhar, S., "The character of the equilibrium of an incompressible heavy viscous fluid of variable density." *Proc. Camb. Phil. Soc.*, **51**, pp. 162, 1955.
- [3] Hide, R., "The character of the equilibrium of an incompressible heavy viscous fluid of variable density: an approximate theory." *Proc. Camb. Phil. Soc.*, **51**, 179, 1955.
- [4] Chandrasekhar, S., *Hydrodynamics & Hydromagnetic Stability*, Oxford University Press, London, U.K., 1961, Chap. 10.
- [5] Morton, B.R., "On the equilibrium of a stratified layer of fluid." *J. Mech. & Appl. Math.*, **10**, pp. 433, 1957.
- [6] Kaus, J.P. & Podladchikov, Y.Y., "Forward and reverse modelling of the three-dimensional viscous Rayleigh-Taylor instability." *Geophysical Research Letters*, **28**, 6, 11095-098, March 15th, 2001.
- [7] Ozen, O. & Narayanan, R., "A note on the Rayleigh-Taylor instability with phase change." *Phys. of Fluids*, **18**, 042110, 2006.
- [8] Mori, Y. & Uchida, Y., "Forced convective heat transfer between horizontal flat plates." *Int. J. Heat Mass Transfer*, **9**, pp. 803, 1966.
- [9] Pellow, A. & Southwell, R.V., "On maintained convective motion in a fluid heated from below." *Proc. R. Soc.*, **A176**, pp. 312, 1940.
- [10] Ostrach, S. & Kamotani, Y., "Heat transfer augmentation in laminar fully developed channel flow by means of heating from below." *J. Heat Transfer: Trans ASME*, **97**, Ser. C, no. 2, pp. 220, 1975.
- [11] Silveston, P.L., "Warmedurchgang in waagerechten Flüssigkeitsschichten." *Forschung auf dem Gebiete des Ingenieurwesens*, **24**, no. 2, pp. 59, 1958.
- [12] Hwang, G.J. & Cheng, K.C., "A boundary vorticity method for finite amplitude convection in plane Poiseuille flow." *Developments in Mechanics*, Proceedings of the 12th Midwestern Mechanics Conference, **6**, pp. 207, 1971.
- [13] Akiyama, M., Hwang, G.J. & Cheng, K.C., "Experiments on the onset of longitudinal vortices in laminar forced convection between horizontal plates." *J. Heat Transfer: Trans ASME*, **93**, Ser. C, no. 4, pp. 335, 1971.
- [14] Nakayama, W., Hwang, G.J. & Cheng, K.C., "Thermal instability in plane Poiseuille flow." *J. Heat Transfer: Trans ASME*, **92**, Ser. C, no. 1, pp. 61, 1970.
- [15] Gage, K.S. & Reid, W.H., "The stability of thermally stratified plane Poiseuille flow." *J. Fluid Mech.*, **33**, part 1, pp. 21, 1968.
- [16] Floryan, J.M., "Stability of wall-bounded shear layers in the presence of simulated distributed surface roughness." *J. Fluid Mech.* **335**, pp. 29, 1997.
- [17] Schlichting, H. & Gersten, K. *Boundary Layer Theory*, 8th Edition. Springer, 2003.

[18] White, F.M. *Viscous Fluid Flow*, 3rd Edition. McGraw-Hill, 2006

[19] Trefethen, L. N. *Spectral Methods in Matlab*. Society of Industrial & Applied Mathematics, 2000.

7 Appendix

Numerical Solution Scripts for Matlab

Basic_Flow_Mk4sf.m

```

function [x,uout,Duout,vout,Dvout,tout,Dtout,plx,yy,T_mod,T_modD] =
Basic_Flow_Mk4sf(at, Ret, Rat, Prt, ct, no_modest, no_ptst, tempt,
vsuct,InitFn);
%Non-linear solution to a channel with Temperature variation at its
boundary

%a - Heating wavenumber
%Re - Reynolds Number
%Ra - Rayleigh Number
%Pr - Prandtl Number
%c - Phase speed of conditions along boundary
%no_modes - Number of additional +/- modes to add to zero mode in
solution
%no_pts - Number of colocation points across channel in solution
%temp - Temperature applied at boundary (Fourier Coefficients) [Rows:
%Upper, Lower wall  Columns: -no_modes..0..no_modes]
%vsuc - Suction applied at boundary (Fourier Coefficients) [Rows:
%Upper, Lower wall  Columns: -no_modes..0..no_modes]
%InitFn - Initial guess for solver (Structure: .x .y)

%Error Tolerances
Rel_Tol = 10^(-6); %Relative Error
Abs_Tol = 10^(-6); %Absolute Error

global no_modes a Re Ra Pr c no_pts temp assump vsuc tempscale
no_modes = no_modest;
a = at;
Re = Ret;
Ra = Rat;
Pr = Prt;
c = ct;
no_pts = no_ptst;
temp = tempt;
vsuc = vsuct;
clear no_modest
clear at
clear Ret
clear Rit
clear Prt
clear ct
clear no_ptst
clear tempt
clear vsuct

%Check for Proper Temperature Scalling
% tsum = 0;
% if temp(1,no_modes+1)==0 && temp(2,no_modes+1)==0
%     for n=-no_modes:1:no_modes
%         if n~=0
%             npos=n+no_modes+1;
%             tsum = tsum + temp(1,npos)-temp(2,npos);
%         end
%     end
%     if tsum~-=-1

```

```

%          error('Temperature Fourier Coefficients in Non-Zero modes are
not Consistent with Scalling of 1');
%      end
% elseif temp(1,no_modes+1)==0 && temp(2,no_modes+1)~=1
%      error('Temperature Fourier Coefficients in Mode Zero are not
Consistent with Scalling of 1');
% end
tempscale = -1;
clear n tsum;

%Initialize
% no_modes = 3;
% a = 1.2;
% Re = 2500;
% Ri = 0;
% Pr = 1;
% c = 0;
% no_pts = 10;
%
% Tm = 0.00000001;
% temp = [zeros(1,2*no_modes+1); ([zeros(1,no_modes-1) i/2*Tm 4 -i/2*Tm
zeros(1,no_modes-1)])];
% S = 0.02;
% vsuc = [zeros(1,2*no_modes+1); ([zeros(1,no_modes-1) -i*S 0 i*S
zeros(1,no_modes-1)])];
% InitFn.x = 0;

%Initialize solver iterations and tolerances...etc
options =
bvpset('RelTol',Rel_Tol,'Abstol',Abs_Tol,'Nmax',5000,'Stats','off','Vec
torized','on');

if InitFn.x == 0
    %Load initial guess as solution from Linear Solution of problem
    [solinit.x, solinit.y] = Alttempnit_Mk4s_Mk3sf(no_modes, a, Re,
Ra, Pr, c, no_pts, temp, vsuc,tempscale);
else
    %Load initial guess as other data
    solinit.x = InitFn.x;
    solinit.y = InitFn.y;
end
solinit.y = [solinit.y((no_modes)*6+1:(2*no_modes+1)*6,:);
solinit.y((3*no_modes+1)*6+1:(2*no_modes+1)*12,:)] ;
%Solve
sol = bvp4c(@alttemp,@alttempbc,solinit,options);

%Display
mode_size = (no_modes+1);
indr = [];
indi = indr;
indtr = indi;
indti = indtr;

%Display Non-linear Streamfunction
%for n = 0:no_modes
%    moder = (n)*6+1;
%    modei = moder+mode_size*6;

```

```

%   modetr = (n)*6+5;
%   modeti = modetr+mode_size*6;
%   indr = [indr moder];
%   indi = [indi modei];
%   indtr = [indtr modetr];
%   indti = [indti modeti];
%end
%   x = solinit.x;
%   xx = sol.x;
%Nomalization
%flmax = max(max(sol.y([1],:)));
%sol.y([indr indi],:) = sol.y([indr indi],:)./flmax;
%tempmax = max(max(sol.y([indtr],:)));
%sol.y([indtr indti]) = sol.y([indtr indti])./tempmax;
%   fr = sol.y([indr indtr],:);
%   fi = sol.y([indi indti],:);
%display_modes(x,fr,fi,xx,mode_size,no_modes,1,'Non-Linear Solution');

%Process Velocity Distribution Data for Output
x = solinit.x;
xx = sol.x;
YY = [];
xd = zeros(no_pts,1);
D = zeros(no_pts,no_pts,4);
[xd,D] = chebdif(no_pts,4);
u = zeros(no_pts,1);
uout = zeros(no_pts,no_modes+1);
v = zeros(no_pts,1);
vout = zeros(no_pts,no_modes+1);
tout = zeros(no_pts,no_modes+1);
for n=0:no_modes
    moder = (n)*6+1;
    modei = moder+mode_size*6;
    str =
interpl(xx,sol.y([moder],:),x,'nearest')+i*interpl(xx,sol.y([modei],:),
x,'nearest');
    Dstr =
interpl(xx,sol.y([moder+1],:),x,'nearest')+i*interpl(xx,sol.y([modei+1]
,:),x,'nearest');
    D2str =
interpl(xx,sol.y([moder+2],:),x,'nearest')+i*interpl(xx,sol.y([modei+2]
,:),x,'nearest');
    D3str =
interpl(xx,sol.y([moder+3],:),x,'nearest')+i*interpl(xx,sol.y([modei+3]
,:),x,'nearest');
    tstr
=interpl(xx,sol.y([moder+4],:),x,'nearest')+i*interpl(xx,sol.y([modei+4]
,:),x,'nearest');
    Dtstr
=interpl(xx,sol.y([moder+5],:),x,'nearest')+i*interpl(xx,sol.y([modei+5]
,:),x,'nearest');
    xpos = 0;
    expo = exp(i*n*a*xpos);

    u = u + (Dstr)*expo;
    uout(:,n+1) = (Dstr)*expo;
    Duout(:,n+1) = (D2str)*expo;

```

```

v = v - (i*a*n*str)*expo;
vout(:,n+1) = -(i*a*n*str)*expo;
Dvout(:,n+1) = -(i*a*n*Dstr)*expo;

tout(:,n+1) = tstr;
Dtout(:,n+1) = Dtstr;

yy = [yy str Dstr D2str D3str];
end

uout = [conj(flipdim(uout(:,2:end),2)) uout];
Duout = [conj(flipdim(Duout(:,2:end),2)) Duout];
vout = [conj(flipdim(vout(:,2:end),2)) vout];
Dvout = [conj(flipdim(Dvout(:,2:end),2)) Dvout];
tout = [conj(flipdim(tout(:,2:end),2)) tout];
Dtout = [conj(flipdim(Dtout(:,2:end),2)) Dtout];
yyt = yy;
for n = 1:1:no_modes
    npos=(n)*4+1;
    yyt = [conj(yy(:,npos:npos+3)) yyt];
end
yy = yyt;
%norm = max(u);
%u = u/norm;
%v = v/norm;
%display_velocities(x,u,v,1,'Flow Velocity');

%Computer Streamwise Pressure Loss
ppstr =
interp1(xx,sol.y([3],:),x)+i*interp1(xx,sol.y([3+6*mode_size],:),x);
plx = 1/(2)*(ppstr(1)-ppstr(no_pts));

function dydx = alttemp(x, fn);
%Loads System of First Order Differential Equations
%x - Colocation Points
%fn - Sets of functions and derivative values for each mode
global no_modes a Re Ra Pr c no_pts temp vsuc tempscale

mode_size = (no_modes+1);
%T_Mod = Temperature Distribution due to conduction of modulated
heating
T_mod = zeros(size(x,2),no_modes+1);
T_modD = T_mod;
T_sinh = zeros(size(T_mod));
T_cosh = zeros(size(T_mod));
for n = 0:no_modes
    if n~=0
        for m = 1:size(x,2)
            T_sinh(m,n+1) = sinh(n*a*x(m));
            T_cosh(m,n+1) = cosh(n*a*x(m));
        end
    end
end
end
for n = 0:no_modes
    if n ~= 0

```

```

        T_mod(:,n+1) = (1/Pr)*((temp(1,(n+no_modes)+1)-
temp(2,(n+no_modes)+1))*0.5*T_sinh(:,n+1)/sinh(n*a)+(temp(1,(n+no_modes
)+1)+temp(2,(n+no_modes)+1))*0.5*T_cosh(:,n+1)/cosh(n*a));
        T_modD(:,n+1) = (1/Pr)*((temp(1,(n+no_modes)+1)-
temp(2,(n+no_modes)+1))*0.5*n*a*T_cosh(:,n+1)/sinh(n*a)+(temp(1,(n+no_m
odes)+1)+temp(2,(n+no_modes)+1))*0.5*n*a*T_sinh(:,n+1)/cosh(n*a));
    end
end

%Recombine paired real function values into complex function values
fp =
complex(fn(1:(mode_size)*6,:),fn((mode_size*6)+1:2*(mode_size*6),:));
fp(1,:) = real(fp(1,:));
tempr = [];
tempi = tempr;
temp1 = tempi;
temp2 = temp1;

%Create Differential equations for each mode
for n = 0:no_modes
    moden = (n)*6+1;
    %Linear terms
    a1 = (2*n^2*a^2+i*n*a*(Re*(1-x.^2)-c).')*fp(moden+2,:);
    a2 = (-n^4*a^4-i*n^3*a^3*(Re*(1-x.^2)-c).'+i*n*a*Re^2)*fp(moden,:);
    a3 = (Ra*i*n*a)*fp(moden+4,)+(Ra*i*n*a)*T_mod(:,n+1).';
    temp1 = [diag(a1 + a2).'+ a3];
    if (Ra==0) || (temp(1,no_modes+1)==0 && temp(2,no_modes+1)==0)
        T = 0;
    else
        T = 1;
    end
    a4 = (n^2*a^2+i*n*a*Pr*(Re*(1-x.^2)-c).')*fp(moden+4,:);
    a5 = (0.5*i*n*a*T).'*fp(moden,:);
    a6 = (i*n*a*Pr*Re*(1-x.^2).')*T_mod(:,n+1).';
    temp2 = [diag(a4 + a6).'+ a5];
    %Non-linear terms - interdependence between modes
    for l = -no_modes:no_modes
        model = (abs(l))*6+1;
        modenl = (abs(n-l))*6+1;
        abnl = abs(n-l);
        %Only accept modes within series truncation bounds
        if abnl<=no_modes
            if (l>=0) && ((n-l)>=0)
                t1 = fp(modenl+1,:).*(fp(model+2,:)-
l^2*a^2*fp(model,:));
                t2 = fp(modenl,:).*(fp(model+3,:)-
l^2*a^2*fp(model+1,:));
                temp1 = [temp1+i*a*(l*(t1)-(n-l)*(t2))];
                t3 =
fp(modenl+1,:).*(fp(model+4,)+T_mod(:,abs(l)+1).');
                t4 =
fp(modenl,:).*(fp(model+5,)+T_modD(:,abs(l)+1).');
                temp2 = [temp2+i*a*Pr*(l*(t3)-(n-l)*(t4))];
            elseif (l<0) && ((n-l)>=0)
                t1 = fp(modenl+1,:).*(conj(fp(model+2,:))-
l^2*a^2*conj(fp(model,:)));

```

```

                t2 = fp(modenl, :).*(conj(fp(model+3, :))-
1^2*a^2*conj(fp(model+1, :)));
                temp1 = [temp1+i*a*(1*(t1)-(n-1)*(t2))];
                t3 =
fp(modenl+1, :).*(conj(fp(model+4, :))+conj(T_mod(:, abs(l)+1)'));
                t4 =
fp(modenl, :).*(conj(fp(model+5, :))+conj(T_modD(:, abs(l)+1)'));
                temp2 = [temp2+i*a*Pr*(1*(t3)-(n-1)*(t4))];
                elseif (l>=0) && ((n-1)<0)
                t1 = conj(fp(modenl+1, :)).*(fp(model+2, :)-
1^2*a^2*fp(model, :));
                t2 = conj(fp(modenl, :)).*(fp(model+3, :)-
1^2*a^2*fp(model+1, :));
                temp1 = [temp1+i*a*(1*(t1)-(n-1)*(t2))];
                t3 =
conj(fp(modenl+1, :)).*(fp(model+4, :)+T_mod(:, abs(l)+1)');
                t4 =
conj(fp(modenl, :)).*(fp(model+5, :)+T_modD(:, abs(l)+1)');
                temp2 = [temp2+i*a*Pr*(1*(t3)-(n-1)*(t4))];
                else
                t1 = conj(fp(modenl+1, :)).*(conj(fp(model+2, :))-
1^2*a^2*conj(fp(model, :)));
                t2 = conj(fp(modenl, :)).*(conj(fp(model+3, :))-
1^2*a^2*conj(fp(model+1, :)));
                temp1 = [temp1+i*a*(1*(t1)-(n-1)*(t2))];
                t3 =
conj(fp(modenl+1, :)).*(conj(fp(model+4, :))+conj(T_mod(:, abs(l)+1)'));
                t4 =
conj(fp(modenl, :)).*(conj(fp(model+5, :))+conj(T_modD(:, abs(l)+1)'));
                temp2 = [temp2+i*a*Pr*(1*(t3)-(n-1)*(t4))];
                end
            end
        end
        tempr = [tempr; real(fp(moden+1, :)); real(fp(moden+2, :));
real(fp(moden+3, :)); real(temp1); real(fp(moden+5, :)); real(temp2)];
        tempi = [tempi; imag(fp(moden+1, :)); imag(fp(moden+2, :));
imag(fp(moden+3, :)); imag(temp1); imag(fp(moden+5, :)); imag(temp2)];
    end
    dydx = [tempr; tempi];

function res = alttempbc(fna, fnb);
%Loads Boundary Conditions
global no_modes a Re Ra Pr c no_pts temp vsuc tempscale

mode_size = (no_modes+1);
modezero = 1;
ind = [];
%Recombine paired real BCs into complex BCs
fpa =
complex(fna(1:(6*mode_size)), fna((6*mode_size+1):(6*mode_size*2)));
fpb =
complex(fnb(1:(6*mode_size)), fnb((6*mode_size+1):(6*mode_size*2)));
%Create suction and temperature boundary conditions from applied
suctions
%and temperatures
bc = zeros(size(fpa));
bcu = zeros(1, 3*mode_size);

```

```
bcl = bcu;
for n = 0:no_modes
    modebc = (n)*6+1;
    %Create reference index
    ind = [ind modebc modebc+1 modebc+4];
    %Load suction and temperatures in correct modes
    if n~=0
        bcu(3*(n)+1) = 0;
        bcl(3*(n)+1) = 0;
        bcu(3*(n)+2) = 0;
        bcl(3*(n)+2) = 0;
        bcu(3*(n)+3) = 0;
        bcl(3*(n)+3) = 0;
    else
        bcu(3*(n)+1) = 0;
        bcl(3*(n)+1) = 0;
        bcu(3*(n)+2) = 0;
        bcl(3*(n)+2) = 0;
        bcu(3*(n)+3) = 0;
        bcl(3*(n)+3) = 0;
    end
end

end
%Apply to existing Boundary Conditions using indices to identify proper
modes
bc(1:(mode_size*3)) = fpa(ind)-bcu.';
bc((mode_size*3+1):(mode_size*6)) = fpb(ind)-bcl.';
res = [real(bc).' imag(bc).'].';
```

Alttempinit_Mk4s_Mk3sf.m

```
function [x,fn] = alttempinit_Mk4s_Mk3sf(no_modes, a, Re, Ra, Pr, c,
no_pts, temp, vsuc, tempscale);
%Linear solution of channel with periodic Temperature & Suciton at
Boundary
%Initial Conditions for non-linear solution
%Point Spacing and Derivative Coefficient Matrix
x = zeros(no_pts,1);
D = zeros(no_pts,no_pts,4);
[x,D] = chebdif(no_pts,4);

%U = Velocity Distribution across Channel
%Poiseuille Flow
U = zeros(no_pts,no_pts,3);
U(:,1) = 1-x.^2;
U(:,2) = -2*x;
U(:,3) = -2;
%T = Temperature Distribution across Channel
T = zeros(no_pts,no_pts,2);
T(:,1) = -0.5*(x-1)/Pr;
T(:,2) = -0.5/Pr;
%T_Mod = Temperature Distribution due to conduction of modulated
heating
T_mod = zeros(no_pts,2*no_modes+1);
T_sinh = zeros(size(T_mod));
T_cosh = zeros(size(T_mod));
for n = -no_modes:no_modes
    if n ~= 0
        for m = 1:no_pts
            T_sinh(m,n+no_modes+1) = sinh(n*a*x(m));
            T_cosh(m,n+no_modes+1) = cosh(n*a*x(m));
        end
    end
end
for n = -no_modes:no_modes
    if n ~= 0
        T_mod(:,n+no_modes+1) = (1/Pr)*((temp(1,(n+no_modes)+1)-
temp(2,(n+no_modes)+1))*0.5*T_sinh(:,(n+no_modes)+1)/sinh(n*a)+(temp(1,
(n+no_modes)+1)+temp(2,(n+no_modes)+1))*0.5*T_cosh(:,(n+no_modes)+1)/co
sh(n*a));
    end
end

%Set-up Operators
mode_size = (2*no_modes+1);
mat_size = mode_size*no_pts*2;
I = eye(no_pts);
A = zeros(mat_size,mat_size);
C = zeros(mat_size,1);
% Load Operators for each mode in Diagonal
for n = -no_modes:no_modes
    npos1 = 2*(n+no_modes)*no_pts+1;
    npos2 = 2*(n+no_modes)*no_pts+no_pts;
    npos3 = 2*(n+no_modes)*no_pts+no_pts*2;
```

```

    A(npos1:npos2,npos1:npos2) = D(:, :, 4) - 2*n^2*a^2*D(:, :, 2) + n^4*a^4*I -
    i*n*a*(Re*diag(U(:, 1)) - c)*(D(:, :, 2) - n^2*a^2*I) + i*n*a*Re*diag(U(:, 3));
    A(npos1:npos2,npos2+1:npos3) = -Ra*i*n*a*I;
    if (Ra==0) || (temp(1,no_modes+1)==0 && temp(2,no_modes+1)==0)
        Tt = 0;
    else
        Tt = 1;
    end
    A(npos2+1:npos3,npos1:npos2) = i*n*a*Pr*(diag(T(:, 2)))*Tt;
    A(npos2+1:npos3,npos2+1:npos3) = D(:, :, 2) - n^2*a^2*I -
    i*n*a*Pr*(Re*diag(U(:, 1)) - c);

    C(npos1:npos2) = i*n*a*Ra*T_mod(:, n+no_modes+1);
    C(npos2+1:npos3) = i*n*a*Pr*Re*diag(U(:, 1))*T_mod(:, n+no_modes+1);
end
%Form Dirichlet and Newmann BCs
bcindexRHS = [];
bcindexLHS = [];
for n = -no_modes:no_modes
    npos1 = 2*(n+no_modes)*no_pts+1;
    npos2 = 2*(n+no_modes)*no_pts+no_pts;
    npos5 = 2*(n+no_modes)*no_pts+no_pts*2;
    %Dirichlet BCs
    npos3 = npos1+1;
    npos4 = npos2-1;
    A(npos3,npos1:npos5) = [D(1, :, 1) zeros(1, no_pts)];
    A(npos4,npos1:npos5) = [D(no_pts, :, 1) zeros(1, no_pts)];
    bcindexRHS = [bcindexRHS, npos1, npos1+1, npos2-
    1, npos2, npos2+1, npos5];
    bcindexLHS = [bcindexLHS, (npos1+2):(npos2-2), (npos2+2):(npos5-1)];
end
%Newmann BCs
flowbc = zeros(1, 2*no_modes);
for n = -no_modes:no_modes
    tpos = n+no_modes+1;
    npos = (n+no_modes)*6+1;
    if n~=0
        flowbc(npos) = i*vsuc(1, tpos)/(n*a);
        flowbc(npos+3) = i*vsuc(2, tpos)/(n*a);
        flowbc(npos+4) = 0;
        flowbc(npos+5) = 0;
    else
        flowbc(npos) = 0;
        flowbc(npos+3) = 0;
        flowbc(npos+4) = 0;
        flowbc(npos+5) = 0;
    end
    flowbc(npos+1) = 0;
    flowbc(npos+2) = 0;
end
%Remove rows '1' and 'n' from mode matrices on diagonal
A = A(bcindexLHS, :);
%Set Right-Hand-Side to apply suction/temperature BCs
B = -A(:, bcindexRHS)*flowbc.' + C(bcindexLHS);
%Remove columns '1' and 'n' from mode matrices on diagonal
A = A(:, bcindexLHS);
%Solve

```

```

ans = A\B;
%Reform solution with suction/temperature BCs on boundary
ansRC = zeros(no_pts*2,mode_size);
for n = -no_modes:no_modes
    npos = (n+no_modes)*6+1;
    npos1 = (n+no_modes)+1;
    npos2 = (n+no_modes)*(no_pts*2-6)+1;
    npos3 = npos2+no_pts-4-1;
    npos4 = npos2+(2*no_pts-6)-1;
    ansRC(:,npos1) = [flowbc(npos);flowbc(npos); ans(npos2:npos3);
flowbc(npos3); flowbc(npos+3); flowbc(npos+4); ans(npos3+1:npos4);
flowbc(npos+5)];
end

%Breakdown solution into function and derivatives in Real and Imaginary
Components
fn = zeros(12*mode_size,no_pts);
mode_size = (2*no_modes+1);
indr = [];
indi = indr;
indtr = indi;
indti = indtr;
for n = -no_modes:no_modes
    npos = (n+no_modes)*6+1;
    npos1 = (n+no_modes)+1;
    ipos = 6*(2*no_modes+1)+npos;
    npostemp = no_pts;
    npostemp2 = no_pts*2;
    %    moder = (n)*6+1;
    %    modei = moder+mode_size*6;
    %    modetr = (n)*6+5;
    %    modeti = modetr+mode_size*6;
    %    indr = [indr moder];
    %    indi = [indi modei];
    %    indtr = [indtr modetr];
    %    indti = [indti modeti];
    fn(npos,:) = real(ansRC(1:npostemp,npos1)).';
    fn(npos+1,:) = real(D(:,:,1)*ansRC(1:npostemp,npos1)).';
    fn(npos+2,:) = real(D(:,:,2)*ansRC(1:npostemp,npos1)).';
    fn(npos+3,:) = real(D(:,:,3)*ansRC(1:npostemp,npos1)).';
    fn(npos+4,:) = real(ansRC(npostemp+1:npostemp2,npos1)).';
    fn(npos+5,:) = real(D(:,:,1)*ansRC(npostemp+1:npostemp2,npos1)).';
    fn(ipos,:) = imag(ansRC(1:npostemp,npos1)).';
    fn(ipos+1,:) = imag(D(:,:,1)*ansRC(1:npostemp,npos1)).';
    fn(ipos+2,:) = imag(D(:,:,2)*ansRC(1:npostemp,npos1)).';
    fn(ipos+3,:) = imag(D(:,:,3)*ansRC(1:npostemp,npos1)).';
    fn(ipos+4,:) = imag(ansRC(npostemp+1:npostemp2,npos1)).';
    fn(ipos+5,:) = imag(D(:,:,1)*ansRC(npostemp+1:npostemp2,npos1)).';
end

%Display Linear Streamfunction
%    x = x;
%    xx = x;
%    fr = fn([indr indtr],:);
%    fi = fn([indi indti],:);
%display_modes(x,fr,fi,xx,mode_size,no_modes,1,'Linear Solution');

```

Wall_Temp_Vort_Stab_NL_FloryanForm.m

```

function [evout] = Wall_Temp_Vort_Stab_NL_FloryanForm(Re,Ra,Pr,a,b,c,
no_pts,no_modes_mf,no_modes_stab,Tm,S,temp,vsuc,EigenFnReturn,GravDir,
mf_From_File,BC,timescale);
%Numerical solution to the Eigenvalue problem for a channel subjected
to
%modulated heating

Base_flow =
['AltTemp_',num2str(Re),'_',num2str(Ra),'_',num2str(Pr),'_',num2str(a),
'_',num2str(no_pts),'_',num2str(no_modes_mf),'_',num2str(Tm),'_',num2st
r(S),'_sin_f.mat'];

if EigenFnReturn~=2
    fprintf('\n\nWall Temperature Fourier Series Coefficients\n');
    fprintf('Mode Number');
    fprintf('%11i',-no_modes_mf);
    for n=-no_modes_mf+1:1:no_modes_mf
        fprintf('%14i',n);
    end
    fprintf('\n');
    fprintf('Upper-Wall ');
    for n=-no_modes_mf+1:1:no_modes_mf
        npos=n+no_modes_mf+1;
        fprintf('%14.8f',temp(1,npos));
    end
    fprintf('\n');
    fprintf('Lower-Wall ');
    for n=-no_modes_mf+1:1:no_modes_mf
        npos=n+no_modes_mf+1;
        fprintf('%14.8f',temp(2,npos));
    end
    fprintf('\n\n');

    fprintf('Wall Suction Fourier Series Coefficients\n');
    fprintf('Mode Number');
    fprintf('%11i',-no_modes_mf);
    for n=-no_modes_mf+1:1:no_modes_mf
        fprintf('%14i',n);
    end
    fprintf('\n');
    fprintf('Upper-Wall ');
    for n=-no_modes_mf+1:1:no_modes_mf
        npos=n+no_modes_mf+1;
        fprintf('%14.8f',vsuc(1,npos));
    end
    fprintf('\n');
    fprintf('Lower-Wall ');
    for n=-no_modes_mf+1:1:no_modes_mf
        npos=n+no_modes_mf+1;
        fprintf('%14.8f',vsuc(2,npos));
    end
    fprintf('\n\n');

    %Obtain Non-linear Profile and Temperature Distribution
    fprintf('Mean Flow Calculation: ');

```

```

end
if mf_From_File==0
    InitFn.x = [];
    InitFn.y = [];
    if S>0
        [x,umean,Dumean,vmean,Dvmean,str] = Basic_Flow_suc(a, Re, c,
no_modes_mf, no_pts, vsuc);
        InitFn.x = x;
        for n=-no_modes_mf:1:no_modes_mf
            InitFn.y =
[InitFn.y;real(str(:,(n+no_modes_mf)*4+1:(n+no_modes_mf)*4+4).');zeros(
size(x)).';zeros(size(x)).'];
        end
        for n=-no_modes_mf:1:no_modes_mf
            InitFn.y =
[InitFn.y;imag(str(:,(n+no_modes_mf)*4+1:(n+no_modes_mf)*4+4).');zeros(
size(x)).';zeros(size(x)).'];
        end
        [x,umean,Dumean,vmean,Dvmean,tmean,Dtmean,plx,str] =
Basic_Flow_Mk4sf(a, Re, Ra, Pr, c, no_modes_mf, no_pts, temp, vsuc,
InitFn);
    else
        InitFn.x = 0;
        InitFn.y = 0;
        if EigenFnReturn~=2
            tic
        end
        [x,umean,Dumean,vmean,Dvmean,tmean,Dtmean,plx,str] =
Basic_Flow_Mk4sf(a, Re, Ra, Pr, c, no_modes_mf, no_pts, temp, vsuc,
InitFn);
        %[x,umean,Dumean,vmean,Dvmean,tmean,Dtmean,plx,str] =
Basic_Flow_Mk3s(a, Re, -Ra/(64*Re^2*Pr), Pr, c, no_modes_mf, no_pts,
temp, vsuc, InitFn);
        if EigenFnReturn~=2
            toc
        end
    end
end
if EigenFnReturn~=2

save(Base_flow,'x','umean','Dumean','vmean','Dvmean','tmean','Dtmean','
str','-mat');
end
else
    load('-
mat',Base_flow,'x','umean','Dumean','vmean','Dvmean','tmean','Dtmean','
str');
    if EigenFnReturn~=2
        fprintf('From File\n');
    end
end
end
if EigenFnReturn~=2
    fprintf('Flow Stability Calculation: ');
    tic
end
%Convert and Expand/Truncate Mean Flow Data
% tmean =-0.5*tmean;
% Dtmean =-0.5*Dtmean;

```

```

if no_modes_mf>no_modes_stab
    mode_diff = no_modes_mf-no_modes_stab;
    umean = umean(:,mode_diff+1:2*no_modes_mf+1-mode_diff);
    Dumean = Dumean(:,mode_diff+1:2*no_modes_mf+1-mode_diff);
    vmean = vmean(:,mode_diff+1:2*no_modes_mf+1-mode_diff);
    Dvmean = Dvmean(:,mode_diff+1:2*no_modes_mf+1-mode_diff);
    tmean = tmean(:,mode_diff+1:2*no_modes_mf+1-mode_diff);
    Dtmean = Dtmean(:,mode_diff+1:2*no_modes_mf+1-mode_diff);
elseif no_modes_stab>no_modes_mf
    mode_diff = no_modes_stab-no_modes_mf;
    umean = [zeros(no_pts,mode_diff) umean(:, :)
zeros(no_pts,mode_diff)];
    Dumean = [zeros(no_pts,mode_diff) Dumean(:, :)
zeros(no_pts,mode_diff)];
    vmean = [zeros(no_pts,mode_diff) vmean(:, :)
zeros(no_pts,mode_diff)];
    Dvmean = [zeros(no_pts,mode_diff) Dvmean(:, :)
zeros(no_pts,mode_diff)];
    tmean = [zeros(no_pts,mode_diff) tmean(:, :)
zeros(no_pts,mode_diff)];
    Dtmean = [zeros(no_pts,mode_diff) Dtmean(:, :)
zeros(no_pts,mode_diff)];
end

%Point Spacing and Derivative Coefficient Matrix
x = zeros(no_pts,1);
D = zeros(no_pts,no_pts,4);
[x,D] = chebdif(no_pts,4);

nn = 3:(no_pts-2);    n1=no_pts-1;
M = -[D(1,2,1) D(1,n1,1) ; D(no_pts,2,1) D(no_pts,n1,1)]\ [D(1,nn,1);
D(no_pts,nn,1)];

%Uo = Velocity Distribution across Channel
%Poiseuille Flow
Uo = diag(1-x.^2);
DUo = diag(-2*x);
%T = Temperature Distribution across Channel
T = zeros(no_pts,2);
T(:,1) = -0.5*(x-1)/Pr;
T(:,2) = -0.5/Pr*ones(1,no_pts);
%T_Mod = Temperature Distribution due to conduction of modulated
heating
T_mod = zeros(no_pts,2*no_modes_stab+1);
T_modD = T_mod;
T_sinh = zeros(size(T_mod));
T_cosh = zeros(size(T_mod));
for n = -no_modes_mf:no_modes_mf
    npos = n+no_modes_stab+1;
    if n ~= 0
        for m = 1:no_pts
            T_sinh(m,npos) = sinh(n*a*x(m));
            T_cosh(m,npos) = cosh(n*a*x(m));
        end
    end
end
end
end

```

```

for n = -no_modes_mf:no_modes_mf
    npos = n+no_modes_stab+1;
    npos1 = n+no_modes_mf+1;
    if (n ~= 0)
        T_mod(:,npos) = (1/Pr)*((temp(1,npos1)-
temp(2,npos1))*0.5*T_sinh(:,npos)/sinh(n*a)+(temp(1,npos1)+temp(2,npos1)
))*0.5*T_cosh(:,npos)/cosh(n*a));
        T_modD(:,npos) = (1/Pr)*((temp(1,npos1)-
temp(2,npos1))*0.5*n*a*T_cosh(:,npos)/sinh(n*a)+(temp(1,npos1)+temp(2,n
pos1))*0.5*n*a*T_sinh(:,npos)/cosh(n*a));
    end
end
if (Ra==0) || (temp(1,no_modes_mf+1)==0 && temp(2,no_modes_mf+1)==0)
    To = 0;
else
    To = 1;
end
tmean = [zeros(no_pts,no_modes_stab) T(:,1)*To
zeros(no_pts,no_modes_stab)] + tmean + T_mod;
Dtmean = [zeros(no_pts,no_modes_stab) T(:,2)*To
zeros(no_pts,no_modes_stab)] + Dtmean + T_modD;
clear T_mod T_sinh T_cosh;
%Set-up Operators
A = zeros((3*no_pts)*(2*no_modes_stab+1));
B = A;
C = B;
AF = zeros((3*no_pts-8)*(2*no_modes_stab+1));
BF = AF;
I = eye(no_pts);
A1 = zeros(no_pts); A2 = A1; A3 = A1; A4 = A1; A5 = A1; A6 = A1; A7 =
A1; A8 = A1; A9 = A1;
B1 = A1; B2 = B1; B3 = B1; B4 = B1; B5 = B1; B6 = B1; B7 = B1; B8 = B1;
B9 = B1;

for s=-no_modes_stab:1:no_modes_stab
    %Diagonal Terms
    spos = s+no_modes_stab;
    A1 = (Re*Uo-c*I)*(i*s*a)*(1+s^2*a^2/b^2)+((1/(b^2))*(s^4*a^4*I-
s^2*a^2*D(:, :, 2))+I*(2*s^2*a^2+b^2)-D(:, :, 2)));
    A2 = (Re*Uo-
c*I)*(s^2*a^2/b^2)*D(:, :, 1)+Re*DUo+(1/(b^2))*(i*s*a*D(:, :, 3)-
i*s^3*a^3*D(:, :, 1))-i*s*a*D(:, :, 1));
    A3 = zeros(no_pts);
    A4 = (Re*Uo-
c*I)*(s^2*a^2/b^2)*D(:, :, 1)+Re*DUo*(s^2*a^2/b^2)+((1/(b^2))*(i*s*a*D(:,
:, 3)-i*s^3*a^3*D(:, :, 1))-i*s*a*D(:, :, 1));
    A5 = (Re*Uo-c*I)*(i*s*a)*(I-(1/b^2)*D(:, :, 2))-
Re*DUo*(i*s*a/b^2)*D(:, :, 1)+((1/(b^2))*(D(:, :, 4)-s^2*a^2*D(:, :, 2))-
2*D(:, :, 2)+(s^2*a^2+b^2)*I);
    A6 = -Ra*I;
    A7 = zeros(no_pts);
    A8 = zeros(no_pts);
    A9 = ((Re*Uo-c*I)*(i*s*a)+(1/Pr)*(-
D(:, :, 2)+(s^2*a^2+b^2)*I))*(1/(b^2));

    B1 = -(1+s^2*a^2/b^2)*I;
    B2 = (i*s*a/b^2)*D(:, :, 1);

```

```

B3 = zeros(no_pts);
B4 = (i*s*a/b^2)*D(:, :, 1);
B5 = -(I-(1/b^2)*D(:, :, 2));
B6 = zeros(no_pts);
B7 = zeros(no_pts);
B8 = zeros(no_pts);
B9 = -I*(1/(b^2));

A(spos*(3*no_pts)+1:(spos+1)*(3*no_pts), spos*(3*no_pts)+1:(spos+1)*(3*no
o_pts)) = [A1 A2 A3; A4 A5 A6; A7 A8 A9];

B(spos*(3*no_pts)+1:(spos+1)*(3*no_pts), spos*(3*no_pts)+1:(spos+1)*(3*no
o_pts)) = [B1 B2 B3; B4 B5 B6; B7 B8 B9];

clear A1 A2 A3 A4 A5 A6 A7 A8 A9;
clear B1 B2 B3 B4 B5 B6 B7 B8 B9;
%Off-diagonal Terms
for m = -no_modes_stab:1:no_modes_stab
    smpos = s-m+no_modes_stab+1;
    mpos = m+no_modes_stab;
    if (abs(s-m) <= no_modes_stab)
        A1 = diag(umean(:, smpos)) * (i*m*a) * (1+m^2*a^2/b^2) ...
            + i*(s-m)*a*diag(umean(:, smpos)) * (1+m^2*a^2/b^2) ...
            + diag(vmean(:, smpos)) * (1+m^2*a^2/b^2)*D(:, :, 1) ...
            - i*(s-m)*a*diag(vmean(:, smpos)) * (i*m*a/b^2)*D(:, :, 1);

        A2 = diag(umean(:, smpos)) * (m^2*a^2/b^2)*D(:, :, 1) ...
            - i*(s-
m)*a*diag(umean(:, smpos)) * (i*m*a/b^2)*D(:, :, 1) ...
            + diag(Dumean(:, smpos)) ...
            - diag(vmean(:, smpos)) * (i*m*a/b^2)*D(:, :, 2) ...
            - i*(s-m)*a*diag(vmean(:, smpos)) * (1/b^2)*D(:, :, 2);

        A3 = zeros(no_pts);
        A4 = diag(umean(:, smpos)) * (m^2*a^2/b^2)*D(:, :, 1) ...
            - diag(Dvmean(:, smpos)) * (i*m*a/b^2)*D(:, :, 1) ...
            + i*(s-m)*a*diag(vmean(:, smpos)) ...
            - diag(vmean(:, smpos)) * (i*m*a/b^2)*D(:, :, 2) ...
            + diag(Dumean(:, smpos)) * (m^2*a^2/b^2);

        A5 = diag(umean(:, smpos)) * (i*m*a) * (I-(1/b^2)*D(:, :, 2)) ...
            + diag(Dvmean(:, smpos)) * (I-(1/b^2)*D(:, :, 2)) ...
            + diag(vmean(:, smpos)) * (D(:, :, 1) - (1/b^2)*D(:, :, 3)) ...
            - diag(Dumean(:, smpos)) * (i*m*a/b^2)*D(:, :, 1);

        A6 = zeros(no_pts);
        A7 = i*(s-m)*a*diag(tmean(:, smpos)) * (1/(b^2));
        A8 = diag(Dtmean(:, smpos)) * (1/(b^2));
        A9 =
(diag(umean(:, smpos)) * (i*m*a) + diag(vmean(:, smpos)) * D(:, :, 1)) * (1/(b^2));

A(spos*(3*no_pts)+1:(spos+1)*(3*no_pts), mpos*(3*no_pts)+1:(mpos+1)*(3*no
o_pts)) =
A(spos*(3*no_pts)+1:(spos+1)*(3*no_pts), mpos*(3*no_pts)+1:(mpos+1)*(3*no
o_pts)) + [A1 A2 A3; A4 A5 A6; A7 A8 A9];

```

```

        end
    end
end

%Apply Boundary Conditions
if BC == 1
    %Use Derivative Coefficient Matrix to Apply Neumann BCs
    for s=-no_modes_stab:1:no_modes_stab
        spos = s+no_modes_stab;
        for m =-no_modes_stab:1:no_modes_stab
            mpos = m+no_modes_stab;

            A1 =
A(spos*(3*no_pts)+1:spos*(3*no_pts)+no_pts,mpos*(3*no_pts)+1:mpos*(3*no
_pts)+no_pts);
            A2 =
A(spos*(3*no_pts)+1:spos*(3*no_pts)+no_pts,mpos*(3*no_pts)+no_pts+1:mpos
s*(3*no_pts)+2*no_pts);
            A3 =
A(spos*(3*no_pts)+1:spos*(3*no_pts)+no_pts,mpos*(3*no_pts)+2*no_pts+1:m
pos*(3*no_pts)+3*no_pts);
            A4 =
A(spos*(3*no_pts)+no_pts+1:spos*(3*no_pts)+2*no_pts,mpos*(3*no_pts)+1:m
pos*(3*no_pts)+no_pts);
            A5 =
A(spos*(3*no_pts)+no_pts+1:spos*(3*no_pts)+2*no_pts,mpos*(3*no_pts)+no_
pts+1:mpos*(3*no_pts)+2*no_pts);
            A6 =
A(spos*(3*no_pts)+no_pts+1:spos*(3*no_pts)+2*no_pts,mpos*(3*no_pts)+2*n
o_pts+1:mpos*(3*no_pts)+3*no_pts);
            A7 =
A(spos*(3*no_pts)+2*no_pts+1:spos*(3*no_pts)+3*no_pts,mpos*(3*no_pts)+1
:mpos*(3*no_pts)+no_pts);
            A8 =
A(spos*(3*no_pts)+2*no_pts+1:spos*(3*no_pts)+3*no_pts,mpos*(3*no_pts)+n
o_pts+1:mpos*(3*no_pts)+2*no_pts);
            A9 =
A(spos*(3*no_pts)+2*no_pts+1:spos*(3*no_pts)+3*no_pts,mpos*(3*no_pts)+2
*no_pts+1:mpos*(3*no_pts)+3*no_pts);

            B1 =
B(spos*(3*no_pts)+1:spos*(3*no_pts)+no_pts,mpos*(3*no_pts)+1:mpos*(3*no
_pts)+no_pts);
            B2 =
B(spos*(3*no_pts)+1:spos*(3*no_pts)+no_pts,mpos*(3*no_pts)+no_pts+1:mpos
s*(3*no_pts)+2*no_pts);
            B3 =
B(spos*(3*no_pts)+1:spos*(3*no_pts)+no_pts,mpos*(3*no_pts)+2*no_pts+1:m
pos*(3*no_pts)+3*no_pts);
            B4 =
B(spos*(3*no_pts)+no_pts+1:spos*(3*no_pts)+2*no_pts,mpos*(3*no_pts)+1:m
pos*(3*no_pts)+no_pts);
            B5 =
B(spos*(3*no_pts)+no_pts+1:spos*(3*no_pts)+2*no_pts,mpos*(3*no_pts)+no_
pts+1:mpos*(3*no_pts)+2*no_pts);

```

```

        B6 =
B(spos*(3*no_pts)+no_pts+1:spos*(3*no_pts)+2*no_pts,mpos*(3*no_pts)+2*no
o_pts+1:mpos*(3*no_pts)+3*no_pts);
        B7 =
B(spos*(3*no_pts)+2*no_pts+1:spos*(3*no_pts)+3*no_pts,mpos*(3*no_pts)+1
:mpos*(3*no_pts)+no_pts);
        B8 =
B(spos*(3*no_pts)+2*no_pts+1:spos*(3*no_pts)+3*no_pts,mpos*(3*no_pts)+n
o_pts+1:mpos*(3*no_pts)+2*no_pts);
        B9 =
B(spos*(3*no_pts)+2*no_pts+1:spos*(3*no_pts)+3*no_pts,mpos*(3*no_pts)+2
*no_pts+1:mpos*(3*no_pts)+3*no_pts);

        AA = [A1 A2 A3; A4 A5 A6; A7 A8 A9];
        BB = [B1 B2 B3; B4 B5 B6; B7 B8 B9];
        if spos==mpos
            ATemp = [[AA(2:no_pts-1,no_pts+2);AA(no_pts+3:2*no_pts-
2,no_pts+2);AA(2*no_pts+2:3*no_pts-1,no_pts+2)] [AA(2:no_pts-
1,2*no_pts-1);AA(no_pts+3:2*no_pts-2,2*no_pts-
1);AA(2*no_pts+2:3*no_pts-1,2*no_pts-1)]];
            BTemp = [[BB(2:no_pts-1,no_pts+2);BB(no_pts+3:2*no_pts-
2,no_pts+2);BB(2*no_pts+2:3*no_pts-1,no_pts+2)] [BB(2:no_pts-
1,2*no_pts-1);BB(no_pts+3:2*no_pts-2,2*no_pts-
1);BB(2*no_pts+2:3*no_pts-1,2*no_pts-1)]];
        end
        A1 = A1(2:no_pts-1,2:no_pts-1);
        A2 = A2(2:no_pts-1,3:no_pts-2);
        A3 = A3(2:no_pts-1,2:no_pts-1);
        A4 = A4(3:no_pts-2,2:no_pts-1);
        A5 = A5(3:no_pts-2,3:no_pts-2);
        A6 = A6(3:no_pts-2,2:no_pts-1);
        A7 = A7(2:no_pts-1,2:no_pts-1);
        A8 = A8(2:no_pts-1,3:no_pts-2);
        A9 = A9(2:no_pts-1,2:no_pts-1);

        B1 = B1(2:no_pts-1,2:no_pts-1);
        B2 = B2(2:no_pts-1,3:no_pts-2);
        B3 = B3(2:no_pts-1,2:no_pts-1);
        B4 = B4(3:no_pts-2,2:no_pts-1);
        B5 = B5(3:no_pts-2,3:no_pts-2);
        B6 = B6(3:no_pts-2,2:no_pts-1);
        B7 = B7(2:no_pts-1,2:no_pts-1);
        B8 = B8(2:no_pts-1,3:no_pts-2);
        B9 = B9(2:no_pts-1,2:no_pts-1);
        if spos==mpos
            AF(spos*(3*no_pts-8)+1:(spos+1)*(3*no_pts-
8),mpos*(3*no_pts-8)+1:(mpos+1)*(3*no_pts-8)) = [A1 A2 A3; A4 A5 A6; A7
A8 A9] + ATemp*[zeros(2,no_pts-2) M zeros(2,no_pts-2)];
            BF(spos*(3*no_pts-8)+1:(spos+1)*(3*no_pts-
8),mpos*(3*no_pts-8)+1:(mpos+1)*(3*no_pts-8)) = [B1 B2 B3; B4 B5 B6; B7
B8 B9] + BTemp*[zeros(2,no_pts-2) M zeros(2,no_pts-2)];
        else
            AF(spos*(3*no_pts-8)+1:(spos+1)*(3*no_pts-
8),mpos*(3*no_pts-8)+1:(mpos+1)*(3*no_pts-8)) = [A1 A2 A3; A4 A5 A6; A7
A8 A9];

```

```

                BF(spos*(3*no_pts-8)+1:(spos+1)*(3*no_pts-
8),mpos*(3*no_pts-8)+1:(mpos+1)*(3*no_pts-8)) = [B1 B2 B3; B4 B5 B6; B7
B8 B9];
            end
        end
    end
else
    %Substitute Rows with Derivative Coefficients to Apply Neumann BCs
    for s=-no_modes_stab:1:no_modes_stab
        spos = s+no_modes_stab;
        for m =-no_modes_stab:1:no_modes_stab
            mpos = m+no_modes_stab;

            A1 =
A(spos*(3*no_pts)+1:spos*(3*no_pts)+no_pts,mpos*(3*no_pts)+1:mpos*(3*no
_pts)+no_pts);
            A2 =
A(spos*(3*no_pts)+1:spos*(3*no_pts)+no_pts,mpos*(3*no_pts)+no_pts+1:mpos
s*(3*no_pts)+2*no_pts);
            A3 =
A(spos*(3*no_pts)+1:spos*(3*no_pts)+no_pts,mpos*(3*no_pts)+2*no_pts+1:m
pos*(3*no_pts)+3*no_pts);
            A4 =
A(spos*(3*no_pts)+no_pts+1:spos*(3*no_pts)+2*no_pts,mpos*(3*no_pts)+1:m
pos*(3*no_pts)+no_pts);
            A5 =
A(spos*(3*no_pts)+no_pts+1:spos*(3*no_pts)+2*no_pts,mpos*(3*no_pts)+no_
pts+1:mpos*(3*no_pts)+2*no_pts);
            A6 =
A(spos*(3*no_pts)+no_pts+1:spos*(3*no_pts)+2*no_pts,mpos*(3*no_pts)+2*no
o_pts+1:mpos*(3*no_pts)+3*no_pts);
            A7 =
A(spos*(3*no_pts)+2*no_pts+1:spos*(3*no_pts)+3*no_pts,mpos*(3*no_pts)+1
:mpos*(3*no_pts)+no_pts);
            A8 =
A(spos*(3*no_pts)+2*no_pts+1:spos*(3*no_pts)+3*no_pts,mpos*(3*no_pts)+n
o_pts+1:mpos*(3*no_pts)+2*no_pts);
            A9 =
A(spos*(3*no_pts)+2*no_pts+1:spos*(3*no_pts)+3*no_pts,mpos*(3*no_pts)+2
*no_pts+1:mpos*(3*no_pts)+3*no_pts);

            B1 =
B(spos*(3*no_pts)+1:spos*(3*no_pts)+no_pts,mpos*(3*no_pts)+1:mpos*(3*no
_pts)+no_pts);
            B2 =
B(spos*(3*no_pts)+1:spos*(3*no_pts)+no_pts,mpos*(3*no_pts)+no_pts+1:mpos
s*(3*no_pts)+2*no_pts);
            B3 =
B(spos*(3*no_pts)+1:spos*(3*no_pts)+no_pts,mpos*(3*no_pts)+2*no_pts+1:m
pos*(3*no_pts)+3*no_pts);
            B4 =
B(spos*(3*no_pts)+no_pts+1:spos*(3*no_pts)+2*no_pts,mpos*(3*no_pts)+1:m
pos*(3*no_pts)+no_pts);
            B5 =
B(spos*(3*no_pts)+no_pts+1:spos*(3*no_pts)+2*no_pts,mpos*(3*no_pts)+no_
pts+1:mpos*(3*no_pts)+2*no_pts);

```

```

        B6 =
        B(spos*(3*no_pts)+no_pts+1:spos*(3*no_pts)+2*no_pts,mpos*(3*no_pts)+2*no
        o_pts+1:mpos*(3*no_pts)+3*no_pts);
        B7 =
        B(spos*(3*no_pts)+2*no_pts+1:spos*(3*no_pts)+3*no_pts,mpos*(3*no_pts)+1
        :mpos*(3*no_pts)+no_pts);
        B8 =
        B(spos*(3*no_pts)+2*no_pts+1:spos*(3*no_pts)+3*no_pts,mpos*(3*no_pts)+n
        o_pts+1:mpos*(3*no_pts)+2*no_pts);
        B9 =
        B(spos*(3*no_pts)+2*no_pts+1:spos*(3*no_pts)+3*no_pts,mpos*(3*no_pts)+2
        *no_pts+1:mpos*(3*no_pts)+3*no_pts);

        if spos==mpos
            A1(2,:) = zeros(1,no_pts);
            A2(2,:) = D(1,:,1);
            A3(2,:) = zeros(1,no_pts);
            A1(no_pts-1,:) = zeros(1,no_pts);
            A2(no_pts-1,:) = D(no_pts,:,1);
            A3(no_pts-1,:) = zeros(1,no_pts);
        else
            A1(2,:) = zeros(1,no_pts);
            A2(2,:) = zeros(1,no_pts);
            A3(2,:) = zeros(1,no_pts);
            A1(no_pts-1,:) = zeros(1,no_pts);
            A2(no_pts-1,:) = zeros(1,no_pts);
            A3(no_pts-1,:) = zeros(1,no_pts);
        end

        B1(2,:) = zeros(1,no_pts);
        B2(2,:) = zeros(1,no_pts);
        B3(2,:) = zeros(1,no_pts);
        B1(no_pts-1,:) = zeros(1,no_pts);
        B2(no_pts-1,:) = zeros(1,no_pts);
        B3(no_pts-1,:) = zeros(1,no_pts);

        A1 = A1(2:no_pts-1,2:no_pts-1);
        A2 = A2(2:no_pts-1,2:no_pts-1);
        A3 = A3(2:no_pts-1,2:no_pts-1);
        A4 = A4(2:no_pts-1,2:no_pts-1);
        A5 = A5(2:no_pts-1,2:no_pts-1);
        A6 = A6(2:no_pts-1,2:no_pts-1);
        A7 = A7(2:no_pts-1,2:no_pts-1);
        A8 = A8(2:no_pts-1,2:no_pts-1);
        A9 = A9(2:no_pts-1,2:no_pts-1);

        B1 = B1(2:no_pts-1,2:no_pts-1);
        B2 = B2(2:no_pts-1,2:no_pts-1);
        B3 = B3(2:no_pts-1,2:no_pts-1);
        B4 = B4(2:no_pts-1,2:no_pts-1);
        B5 = B5(2:no_pts-1,2:no_pts-1);
        B6 = B6(2:no_pts-1,2:no_pts-1);
        B7 = B7(2:no_pts-1,2:no_pts-1);
        B8 = B8(2:no_pts-1,2:no_pts-1);
        B9 = B9(2:no_pts-1,2:no_pts-1);

```

```

        AF(spos*(3*no_pts-6)+1:(spos+1)*(3*no_pts-
6),mpos*(3*no_pts-6)+1:(mpos+1)*(3*no_pts-6)) = [A1 A2 A3; A4 A5 A6; A7
A8 A9];
        BF(spos*(3*no_pts-6)+1:(spos+1)*(3*no_pts-
6),mpos*(3*no_pts-6)+1:(mpos+1)*(3*no_pts-6)) = [B1 B2 B3; B4 B5 B6; B7
B8 B9];
    end
end
clear AA A BB B;
A = AF;
B = BF;
clear AF BF;

if EigenFnReturn ~=1
    %Solve for Eigenvalues
    ev = eig(A,B);
    %ev = eig(A,B,25,0+0*i);
    %Sort
    egs = -real(ev);
    [egs,ii] = sort(egs);
    ev = ev(ii);
    ef = 0;
    ef2 = 0;

elseif EigenFnReturn == 1;
    n4 = no_pts-4;
    %Solve for Eigenvalues and Eigenfunctions
    [ef,ev] = eig(A,B);

    efu = zeros(no_pts,(3*no_pts-
8)*(2*no_modes_stab+1),2*no_modes_stab+1);
    efv = zeros(no_pts,(3*no_pts-
8)*(2*no_modes_stab+1),2*no_modes_stab+1);
    eft = zeros(no_pts,(3*no_pts-
8)*(2*no_modes_stab+1),2*no_modes_stab+1);
    %Reconstruct Eigenfunctions (Fn + bc)
    n8 = (3*no_pts-8)*(2*no_modes_stab+1);
    for s=-no_modes_stab:1:no_modes_stab
        spos = s+no_modes_stab;
        tu = ef(spos*(3*no_pts-8)+1:spos*(3*no_pts-8)+(no_pts-2),:);
        efu(:, :, spos+1) = [zeros(1,(3*no_pts-
8)*(2*no_modes_stab+1));tu;zeros(1,(3*no_pts-8)*(2*no_modes_stab+1))];
        tt = ef(spos*(3*no_pts-8)+2*no_pts-6+1:spos*(3*no_pts-
8)+2*no_pts-6+(no_pts-2),:);
        eft(:, :, spos+1) = [zeros(1,(3*no_pts-
8)*(2*no_modes_stab+1));tt;zeros(1,(3*no_pts-8)*(2*no_modes_stab+1))];
        ef1 = zeros(no_pts,(3*no_pts-8)*(2*no_modes_stab+1));
        for m = 1:n8
            tv = ef(spos*(3*no_pts-8)+no_pts-2+1:spos*(3*no_pts-
8)+no_pts-2+(no_pts-4),m);
            int_points = M * tv;
            ef1(:,m) = [0; int_points(1); tv; int_points(2); 0];
            [fmax,mm] = max(ef1(:,m));
            %ef1(:,m) = ef1(:,m)/ef1(mm,m);
        end;
        efv(:, :, spos+1) = ef1;
    end;
end;

```

```

end
clear tu tv tt;
ev = diag(ev);

%Sort
egs = -real(ev);
[egs,ii] = sort(egs);
ev = ev(ii);
for s=-no_modes_stab:1:no_modes_stab
    spos = s+no_modes_stab;
    for m = 1:n8
        ef3(:,m,spos+1)=efv(:,ii(m),spos+1);
    end
    efv(:, :, spos+1) = ef3(:, :, spos+1);
    for m = 1:n8
        ef3(:,m,spos+1)=efu(:,ii(m),spos+1);
    end
    efu(:, :, spos+1) = ef3(:, :, spos+1);
    for m = 1:n8
        ef3(:,m,spos+1)=eft(:,ii(m),spos+1);
    end
    eft(:, :, spos+1) = ef3(:, :, spos+1);
end
%for s=-no_modes_stab+1:1:no_modes_stab
%   efv(:, :, 1)=efv(:, :, 1)+efv(:, :, spos);
%   efu(:, :, 1)=efu(:, :, 1)+efu(:, :, spos);
%   eft(:, :, 1)=eft(:, :, 1)+eft(:, :, spos);
%end
end

%Output to File
fid = fopen('spectrum_FloryanForm_NL','w');
%write calculation conditions
fprintf(fid,'Floryan Formulation NL\n');
fprintf(fid,'Eigenvalue Spectrum\n\n');
fprintf(fid,'%12.5e Reynolds Number\n',Re);
fprintf(fid,'%12.5e Rayleigh Number\n',Ra);
fprintf(fid,'%12.5e Pradtle Number\n',Pr);
fprintf(fid,'%12.5e Alpha Wave Number\n',a);
fprintf(fid,'%12.5e Beta Wave Number\n\n',b);
fprintf(fid,'%4i Collocation Points Used in Solution\n',no_pts);
fprintf(fid,'%4i Modes Retained in Stability
Calculations\n',no_modes_stab);

fprintf(fid,'%4i Modes Used to Represent Mean-Flow\n\n',no_modes_mf);
fprintf(fid,'Wall Temperature Fourier Series Coefficients\n');
fprintf(fid,'Mode Number');
fprintf(fid,'%11i',-no_modes_mf);
for n=-no_modes_mf+1:1:no_modes_mf
    fprintf(fid,'%14i',n);
end
fprintf(fid,'\n');
fprintf(fid,'Upper-Wall ');
for n=-no_modes_mf:1:no_modes_mf
    npos=n+no_modes_mf+1;
    fprintf(fid,'%14.8f',temp(1,npos));
end

```

```

fprintf(fid,'\n');
fprintf(fid,'Lower-Wall  ');
for n=-no_modes_mf:1:no_modes_mf
    npos=n+no_modes_mf+1;
    fprintf(fid,'%14.8f',temp(2,npos));
end
fprintf(fid,'\n');
fprintf(fid,'\n');

%Remove Complex Conjugate Eigenvalues
% s = 2;
% while s <= size(ev,1)
%     if imag(ev(s-1))>10^(-8)
%         ev = [ev(1:s-2); ev(s+1:end)];
%         s = s-1;
%     end
%     s = s+1;
% end
% ev = ev(1:15).';
ev=ev.';
if timescale==1
    fprintf(fid,'Thermal Diffusion Time Scale\n');
    ev = ev.*Pr;
elseif timescale==2
    fprintf(fid,'Dynamic Time Scale\n');
    %Kelly to Floryan(Suction
    ev = ev.*(1/(Pr*Re));
elseif timescale==3
    fprintf(fid,'Viscous Time Scale\n');
    %Kelly to Clever&Busse
end

fprintf(fid,'\n');

evout = [real(ev);imag(ev)];
fprintf(fid,'%20.12e %20.12e\n',evout);
fclose(fid);

if EigenFnReturn == 1
    %Output to File
    fid = fopen('eigenfunction_FloryanForm_NL','w');
    %write calculation conditions
    fprintf(fid,'Kelly Formulation NL\n');
    fprintf(fid,'Eigenfunctions\n');
    fprintf(fid,'%12.5e Reynolds Number\n',Re);
    fprintf(fid,'%12.5e Rayleigh Number\n',Ra);
    fprintf(fid,'%12.5e Pradtle Number\n',Pr);
    fprintf(fid,'%12.5e Alpha Wave Number\n',a);
    fprintf(fid,'%12.5e Beta Wave Number\n\n',b);
    fprintf(fid,'%4i Collocation Points Used in Solution\n',no_pts);
    fprintf(fid,'%4i Modes Retained in Stability
Calculations\n',no_modes_stab);

    fprintf(fid,'%4i Modes Used to Represent Mean-
Flow\n\n',no_modes_mf);
    fprintf(fid,'Wall Temperature Fourier Series Coefficients\n');
    fprintf(fid,'Mode Number');

```

```

fprintf(fid,'%11i',-no_modes_mf);
for n=-no_modes_mf+1:1:no_modes_mf
    fprintf(fid,'%14i',n);
end
fprintf(fid,'\n');
fprintf(fid,'Upper-Wall  ');
for n=-no_modes_mf:1:no_modes_mf
    npos=n+no_modes_mf+1;
    fprintf(fid,'%14.8f',temp(1,npos));
end
fprintf(fid,'\n');
fprintf(fid,'Lower-Wall  ');
for n=-no_modes_mf:1:no_modes_mf
    npos=n+no_modes_mf+1;
    fprintf(fid,'%14.8f',temp(2,npos));
end
fprintf(fid,'\n');
fprintf(fid,'\n');

fprintf(fid,'Wall Temperature Fourier Series Coefficients\n');
fprintf(fid,'Mode Number');
fprintf(fid,'%11i',-no_modes_mf);
for n=-no_modes_mf+1:1:no_modes_mf
    fprintf(fid,'%14i',n);
end
fprintf(fid,'\n');

fprintf(fid,'Vertical Eigenfunctions\n\n');
for m=1:1:(no_pts-4)
    for k=1:1:no_pts
        for n=-no_modes_stab:1:no_modes_stab
            npos =n+no_modes_stab+1;
            efout = [real(efv(k,m,npos));imag(efv(k,m,npos))];
            fprintf(fid,'%14.6e %14.6e ',efout);
        end
        fprintf(fid,'\n');
    end
    fprintf(fid,'\n\n');
end
fprintf(fid,'Horizontal Eigenfunctions\n\n');
for m=1:1:(no_pts-4)
    for k=1:1:no_pts
        for n=-no_modes_stab:1:no_modes_stab
            npos =n+no_modes_stab+1;
            efout = [real(efu(k,m,npos));imag(efu(k,m,npos))];
            fprintf(fid,'%14.6e %14.6e ',efout);
        end
        fprintf(fid,'\n');
    end
    fprintf(fid,'\n\n');
end
fprintf(fid,'Temperature Eigenfunctions\n\n');
for m=1:1:(no_pts-4)
    for k=1:1:no_pts
        for n=-no_modes_stab:1:no_modes_stab
            npos =n+no_modes_stab+1;
            efout = [real(eft(k,m,npos));imag(eft(k,m,npos))];

```

```
                fprintf(fid,'%14.6e %14.6e ',efout);
            end
            fprintf(fid,'\n');
        end
        fprintf(fid,'\n\n');
    end
    fclose(fid);
end
if EigenFnReturn~=2
    toc
end
```

WT_EigenFnReturn_FloryanForm_NL.m

```

function [x,efu,efv,eft,D] = WT_EigenFnReturn_FloryanForm_NL(Re,Ra,Pr,
a,b,c,no_pts,no_modes_mf,no_modes_stab,Tm,S,temp,vsuc,ev_input,
EigenFnReturn,GravDir,mf_From_File);
%Returns the eigenfunction for a particular eigenvalue for a channel
%subjected to modulated heating

Base_flow =
['AltTemp_',num2str(Re),'_',num2str(Ra),'_',num2str(Pr),'_',num2str(a),
'_',num2str(no_pts),'_',num2str(no_modes_mf),'_',num2str(Tm),'_',num2st
r(S),'_sin_f.mat'];

%Obtain Non-linear Profile and Temperature Distribution
if mf_From_File==0
    InitFn.x = [];
    InitFn.y = [];
    if S>0
        [x,umean,Dumean,vmean,Dvmean,str] = Basic_Flow_suc(a, Re, c,
no_modes_mf, no_pts, vsuc);
        InitFn.x = x;
        for n=-no_modes_mf:1:no_modes_mf
            InitFn.y =
[InitFn.y;real(str(:,(n+no_modes_mf)*4+1:(n+no_modes_mf)*4+4).')];zeros(
size(x)).';zeros(size(x)).'];
        end
        for n=-no_modes_mf:1:no_modes_mf
            InitFn.y =
[InitFn.y;imag(str(:,(n+no_modes_mf)*4+1:(n+no_modes_mf)*4+4).')];zeros(
size(x)).';zeros(size(x)).'];
        end
        [x,umean,Dumean,vmean,Dvmean,tmean,Dtmean,plx,str] =
Basic_Flow_Mk4sf(a, Re, Ra, Pr, c, no_modes_mf, no_pts, temp, vsuc,
InitFn);
    else
        InitFn.x = 0;
        InitFn.y = 0;
        [x,umean,Dumean,vmean,Dvmean,tmean,Dtmean,plx,str] =
Basic_Flow_Mk4sf(a, Re, Ra, Pr, c, no_modes_mf, no_pts, temp, vsuc,
InitFn);
    end

save(Base_flow,'x','umean','Dumean','vmean','Dvmean','tmean','Dtmean','
str','-mat');
else
    load('-
mat',Base_flow,'x','umean','Dumean','vmean','Dvmean','tmean','Dtmean','
str');
end

%Convert and Expand/Truncate Mean Flow Data

if no_modes_mf>no_modes_stab
    mode_diff = no_modes_mf-no_modes_stab;
    umean = umean(:,mode_diff+1:2*no_modes_mf+1-mode_diff);
    Dumean = Dumean(:,mode_diff+1:2*no_modes_mf+1-mode_diff);
    vmean = vmean(:,mode_diff+1:2*no_modes_mf+1-mode_diff);

```

```

    Dvmean = Dvmean(:,mode_diff+1:2*no_modes_mf+1-mode_diff);
    tmean = tmean(:,mode_diff+1:2*no_modes_mf+1-mode_diff);
    Dtmean = Dtmean(:,mode_diff+1:2*no_modes_mf+1-mode_diff);
elseif no_modes_stab>no_modes_mf
    mode_diff = no_modes_stab-no_modes_mf;
    umean = [zeros(no_pts,mode_diff) umean(:,,:)]
zeros(no_pts,mode_diff)];
    Dumean = [zeros(no_pts,mode_diff) Dumean(:,,:)]
zeros(no_pts,mode_diff)];
    vmean = [zeros(no_pts,mode_diff) vmean(:,,:)]
zeros(no_pts,mode_diff)];
    Dvmean = [zeros(no_pts,mode_diff) Dvmean(:,,:)]
zeros(no_pts,mode_diff)];
    tmean = [zeros(no_pts,mode_diff) tmean(:,,:)]
zeros(no_pts,mode_diff)];
    Dtmean = [zeros(no_pts,mode_diff) Dtmean(:,,:)]
zeros(no_pts,mode_diff)];
end

%Point Spacing and Derivative Coefficient Matrix
x = zeros(no_pts,1);
D = zeros(no_pts,no_pts,4);
[x,D] = chebdif(no_pts,4);

%Basic Flow
Uo = diag(1-x.^2);
DUo = diag(-2*x);
%T = Temperature Distribution across Channel
T = zeros(no_pts,2);
T(:,1) = -0.5*(x-1)/Pr;
T(:,2) = -0.5/Pr*ones(1,no_pts);
%T_Mod = Temperature Distribution due to conduction of modulated
heating
T_mod = zeros(no_pts,2*no_modes_stab+1);
T_modD = T_mod;
T_sinh = zeros(size(T_mod));
T_cosh = zeros(size(T_mod));
for n = -no_modes_mf:no_modes_mf
    npos = n+no_modes_stab+1;
    if n ~= 0
        for m = 1:no_pts
            T_sinh(m,npos) = sinh(n*a*x(m));
            T_cosh(m,npos) = cosh(n*a*x(m));
        end
    end
end
for n = -no_modes_mf:no_modes_mf
    npos = n+no_modes_stab+1;
    npos1 = n+no_modes_mf+1;
    if (n ~= 0)
        T_mod(:,npos) = (1/Pr)*((temp(1,npos1)-
temp(2,npos1))*0.5*T_sinh(:,npos)/sinh(n*a)+(temp(1,npos1)+temp(2,npos1)
))*0.5*T_cosh(:,npos)/cosh(n*a));
        T_modD(:,npos) = (1/Pr)*((temp(1,npos1)-
temp(2,npos1))*0.5*n*a*T_cosh(:,npos)/sinh(n*a)+(temp(1,npos1)+temp(2,n
pos1))*0.5*n*a*T_sinh(:,npos)/cosh(n*a));
    end
end

```

```

end
if (Ra==0) || (temp(1,no_modes_mf+1)==0 && temp(2,no_modes_mf+1)==0)
    To = 0;
else
    To = 1;
end
tmean = [zeros(no_pts,no_modes_stab) T(:,1)*To
zeros(no_pts,no_modes_stab)] + tmean + T_mod;
Dtmean = [zeros(no_pts,no_modes_stab) T(:,2)*To
zeros(no_pts,no_modes_stab)] + Dtmean + T_modD;
clear T_mod T_sinh T_cosh;

%Set-up Operators
A = zeros((3*no_pts)*(2*no_modes_stab+1));
B = A;
AF = zeros((3*no_pts-6)*(2*no_modes_stab+1));
BF = AF;
I = eye(no_pts);
A1 = zeros(no_pts); A2 = A1; A3 = A1; A4 = A1; A5 = A1; A6 = A1; A7 =
A1; A8 = A1; A9 = A1;
B1 = A1; B2 = B1; B3 = B1; B4 = B1; B5 = B1; B6 = B1; B7 = B1; B8 = B1;
B9 = B1;

for s=-no_modes_stab:1:no_modes_stab
    %Diagonal Terms
    spos = s+no_modes_stab;
    A1 = (Re*Uo-c*I)*(i*s*a)*(1+s^2*a^2/b^2)+((1/(b^2)))*(s^4*a^4*I-
s^2*a^2*D(:, :, 2))+I*(2*s^2*a^2+b^2)-D(:, :, 2));
    A2 = (Re*Uo-
c*I)*(s^2*a^2/b^2)*D(:, :, 1)+Re*DUo+(1/(b^2))*(i*s*a*D(:, :, 3)-
i*s^3*a^3*D(:, :, 1))-i*s*a*D(:, :, 1);
    A3 = zeros(no_pts);
    A4 = (Re*Uo-
c*I)*(s^2*a^2/b^2)*D(:, :, 1)+Re*DUo*(s^2*a^2/b^2)+((1/(b^2))*(i*s*a*D(:,
:, 3)-i*s^3*a^3*D(:, :, 1))-i*s*a*D(:, :, 1));
    A5 = (Re*Uo-c*I)*(i*s*a)*(I-(1/b^2)*D(:, :, 2))-
Re*DUo*(i*s*a/b^2)*D(:, :, 1)+((1/(b^2))*(D(:, :, 4)-s^2*a^2*D(:, :, 2))-
2*D(:, :, 2)+(s^2*a^2+b^2)*I);
    A6 = -Ra*I;
    A7 = zeros(no_pts);
    A8 = zeros(no_pts);
    A9 = ((Re*Uo-c*I)*(i*s*a)+(1/Pr)*(-
D(:, :, 2)+(s^2*a^2+b^2)*I))*(1/(b^2));

    B1 = -(1+s^2*a^2/b^2)*I;
    B2 = (i*s*a/b^2)*D(:, :, 1);
    B3 = zeros(no_pts);
    B4 = (i*s*a/b^2)*D(:, :, 1);
    B5 = -(I-(1/b^2)*D(:, :, 2));
    B6 = zeros(no_pts);
    B7 = zeros(no_pts);
    B8 = zeros(no_pts);
    B9 = -I*(1/(b^2));

A(spos*(3*no_pts)+1:(spos+1)*(3*no_pts),spos*(3*no_pts)+1:(spos+1)*(3*n
o_pts)) = [A1 A2 A3; A4 A5 A6; A7 A8 A9];

```

```

B(spos*(3*no_pts)+1:(spos+1)*(3*no_pts),spos*(3*no_pts)+1:(spos+1)*(3*no
o_pts)) = [B1 B2 B3; B4 B5 B6; B7 B8 B9];

clear A1 A2 A3 A4 A5 A6 A7 A8 A9;
clear B1 B2 B3 B4 B5 B6 B7 B8 B9;
%Off-diagonal Terms
for m =-no_modes_stab:1:no_modes_stab
    smpos = s-m+no_modes_stab+1;
    mpos = m+no_modes_stab;
    if (abs(s-m)<=no_modes_stab)
        A1 = diag(umean(:,smpos))*(i*m*a)*(1+m^2*a^2/b^2)...
            + i*(s-m)*a*diag(umean(:,smpos))*(1+m^2*a^2/b^2)...
            + diag(vmean(:,smpos))*(1+m^2*a^2/b^2)*D(:, :, 1)...
            - i*(s-m)*a*diag(vmean(:,smpos))*(i*m*a/b^2)*D(:, :, 1);

        A2 = diag(umean(:,smpos))*(m^2*a^2/b^2)*D(:, :, 1)...
            - i*(s-
m)*a*diag(umean(:,smpos))*(i*m*a/b^2)*D(:, :, 1)...
            + diag(Dumean(:,smpos))...
            - diag(vmean(:,smpos))*(i*m*a/b^2)*D(:, :, 2)...
            - i*(s-m)*a*diag(vmean(:,smpos))*(1/b^2)*D(:, :, 2);

        A3 = zeros(no_pts);
        A4 = diag(umean(:,smpos))*(m^2*a^2/b^2)*D(:, :, 1)...
            - diag(Dvmean(:,smpos))*(i*m*a/b^2)*D(:, :, 1)...
            + i*(s-m)*a*diag(vmean(:,smpos))...
            - diag(vmean(:,smpos))*(i*m*a/b^2)*D(:, :, 2)...
            + diag(Dumean(:,smpos))*(m^2*a^2/b^2);

        A5 = diag(umean(:,smpos))*(i*m*a)*(I-(1/b^2)*D(:, :, 2))...
            + diag(Dvmean(:,smpos))*(I-(1/b^2)*D(:, :, 2))...
            + diag(vmean(:,smpos))*(D(:, :, 1) - (1/b^2)*D(:, :, 3))...
            - diag(Dumean(:,smpos))*(i*m*a/b^2)*D(:, :, 1);

        A6 = zeros(no_pts);
        A7 = i*(s-m)*a*diag(tmean(:,smpos))*(1/(b^2));
        A8 = diag(Dtmean(:,smpos))*(1/(b^2));
        A9 =
(diag(umean(:,smpos))*(i*m*a)+diag(vmean(:,smpos))*D(:, :, 1))*(1/(b^2));

A(spos*(3*no_pts)+1:(spos+1)*(3*no_pts),mpos*(3*no_pts)+1:(mpos+1)*(3*n
o_pts)) =
A(spos*(3*no_pts)+1:(spos+1)*(3*no_pts),mpos*(3*no_pts)+1:(mpos+1)*(3*n
o_pts)) + [A1 A2 A3; A4 A5 A6; A7 A8 A9];
    end
end
end

%Apply Boundary Conditions
%Substitute a First-Derivative Condition with a Second-Derivative
Condition
%to creat an Inhomogenous problem
for s=-no_modes_stab:1:no_modes_stab
    spos = s+no_modes_stab;
    for m =-no_modes_stab:1:no_modes_stab

```

```

mpos = m+no_modes_stab;

A1 =
A(spos*(3*no_pts)+1:spos*(3*no_pts)+no_pts,mpos*(3*no_pts)+1:mpos*(3*no
_pts)+no_pts);
A2 =
A(spos*(3*no_pts)+1:spos*(3*no_pts)+no_pts,mpos*(3*no_pts)+no_pts+1:mpos
s*(3*no_pts)+2*no_pts);
A3 =
A(spos*(3*no_pts)+1:spos*(3*no_pts)+no_pts,mpos*(3*no_pts)+2*no_pts+1:m
pos*(3*no_pts)+3*no_pts);
A4 =
A(spos*(3*no_pts)+no_pts+1:spos*(3*no_pts)+2*no_pts,mpos*(3*no_pts)+1:m
pos*(3*no_pts)+no_pts);
A5 =
A(spos*(3*no_pts)+no_pts+1:spos*(3*no_pts)+2*no_pts,mpos*(3*no_pts)+no_
pts+1:mpos*(3*no_pts)+2*no_pts);
A6 =
A(spos*(3*no_pts)+no_pts+1:spos*(3*no_pts)+2*no_pts,mpos*(3*no_pts)+2*n
o_pts+1:mpos*(3*no_pts)+3*no_pts);
A7 =
A(spos*(3*no_pts)+2*no_pts+1:spos*(3*no_pts)+3*no_pts,mpos*(3*no_pts)+1
:mpos*(3*no_pts)+no_pts);
A8 =
A(spos*(3*no_pts)+2*no_pts+1:spos*(3*no_pts)+3*no_pts,mpos*(3*no_pts)+n
o_pts+1:mpos*(3*no_pts)+2*no_pts);
A9 =
A(spos*(3*no_pts)+2*no_pts+1:spos*(3*no_pts)+3*no_pts,mpos*(3*no_pts)+2
*no_pts+1:mpos*(3*no_pts)+3*no_pts);

B1 =
B(spos*(3*no_pts)+1:spos*(3*no_pts)+no_pts,mpos*(3*no_pts)+1:mpos*(3*no
_pts)+no_pts);
B2 =
B(spos*(3*no_pts)+1:spos*(3*no_pts)+no_pts,mpos*(3*no_pts)+no_pts+1:mpos
s*(3*no_pts)+2*no_pts);
B3 =
B(spos*(3*no_pts)+1:spos*(3*no_pts)+no_pts,mpos*(3*no_pts)+2*no_pts+1:m
pos*(3*no_pts)+3*no_pts);
B4 =
B(spos*(3*no_pts)+no_pts+1:spos*(3*no_pts)+2*no_pts,mpos*(3*no_pts)+1:m
pos*(3*no_pts)+no_pts);
B5 =
B(spos*(3*no_pts)+no_pts+1:spos*(3*no_pts)+2*no_pts,mpos*(3*no_pts)+no_
pts+1:mpos*(3*no_pts)+2*no_pts);
B6 =
B(spos*(3*no_pts)+no_pts+1:spos*(3*no_pts)+2*no_pts,mpos*(3*no_pts)+2*n
o_pts+1:mpos*(3*no_pts)+3*no_pts);
B7 =
B(spos*(3*no_pts)+2*no_pts+1:spos*(3*no_pts)+3*no_pts,mpos*(3*no_pts)+1
:mpos*(3*no_pts)+no_pts);
B8 =
B(spos*(3*no_pts)+2*no_pts+1:spos*(3*no_pts)+3*no_pts,mpos*(3*no_pts)+n
o_pts+1:mpos*(3*no_pts)+2*no_pts);
B9 =
B(spos*(3*no_pts)+2*no_pts+1:spos*(3*no_pts)+3*no_pts,mpos*(3*no_pts)+2
*no_pts+1:mpos*(3*no_pts)+3*no_pts);

```

```

if spos==mpos
    A4(2,:) = zeros(1,no_pts);
    A5(2,:) = D(1,:,1);
    A6(2,:) = zeros(1,no_pts);
    A4(no_pts-1,:) = zeros(1,no_pts);
    A5(no_pts-1,:) = D(no_pts,:,1);
    A6(no_pts-1,:) = zeros(1,no_pts);
else
    A4(2,:) = zeros(1,no_pts);
    A5(2,:) = zeros(1,no_pts);
    A6(2,:) = zeros(1,no_pts);
    A4(no_pts-1,:) = zeros(1,no_pts);
    A5(no_pts-1,:) = zeros(1,no_pts);
    A6(no_pts-1,:) = zeros(1,no_pts);
end
if (s==0)&&(m==0)
    A4(2,:) = zeros(1,no_pts);
    A5(2,:) = D(1,:,1);
    A6(2,:) = zeros(1,no_pts);
    A4(no_pts-1,:) = zeros(1,no_pts);
    A5(no_pts-1,:) = D(no_pts,:,2);
    A6(no_pts-1,:) = zeros(1,no_pts);
end

B4(2,:) = zeros(1,no_pts);
B5(2,:) = zeros(1,no_pts);
B6(2,:) = zeros(1,no_pts);
B4(no_pts-1,:) = zeros(1,no_pts);
B5(no_pts-1,:) = zeros(1,no_pts);
B6(no_pts-1,:) = zeros(1,no_pts);

A1 = A1(2:no_pts-1,2:no_pts-1);
A2 = A2(2:no_pts-1,2:no_pts-1);
A3 = A3(2:no_pts-1,2:no_pts-1);
A4 = A4(2:no_pts-1,2:no_pts-1);
A5 = A5(2:no_pts-1,2:no_pts-1);
A6 = A6(2:no_pts-1,2:no_pts-1);
A7 = A7(2:no_pts-1,2:no_pts-1);
A8 = A8(2:no_pts-1,2:no_pts-1);
A9 = A9(2:no_pts-1,2:no_pts-1);

B1 = B1(2:no_pts-1,2:no_pts-1);
B2 = B2(2:no_pts-1,2:no_pts-1);
B3 = B3(2:no_pts-1,2:no_pts-1);
B4 = B4(2:no_pts-1,2:no_pts-1);
B5 = B5(2:no_pts-1,2:no_pts-1);
B6 = B6(2:no_pts-1,2:no_pts-1);
B7 = B7(2:no_pts-1,2:no_pts-1);
B8 = B8(2:no_pts-1,2:no_pts-1);
B9 = B9(2:no_pts-1,2:no_pts-1);

AF(spos*(3*no_pts-6)+1:(spos+1)*(3*no_pts-6),mpos*(3*no_pts-6)+1:(mpos+1)*(3*no_pts-6)) = [A1 A2 A3; A4 A5 A6; A7 A8 A9];
BF(spos*(3*no_pts-6)+1:(spos+1)*(3*no_pts-6),mpos*(3*no_pts-6)+1:(mpos+1)*(3*no_pts-6)) = [B1 B2 B3; B4 B5 B6; B7 B8 B9];
end

```

```

end

clear AA A BB B;
A = AF;
B = BF;
clear AF BF;

%Set-Up Left-Hand-Side of equation
C = (A-ev_input/Pr*B);

%Define Right-Hand-Side of Equation with Inhomogenous BC
lnfn = [zeros(no_pts-2,1);zeros(no_pts-2,1);zeros(no_pts-2,1)];
for s=-no_modes_stab+1:1:no_modes_stab
    if s == 0
        %tpm = [zeros(round((no_pts-2)/2)-1,1);1;zeros(round((no_pts-
2)/2)-1,1)];
        %lnfnout = [zeros(no_pts-2,1);tpm;zeros(no_pts-2,1)];
        lnfnout = [zeros(no_pts-2,1);zeros(no_pts-3,1);1;zeros(no_pts-
2,1)];
    else
        lnfnout = [zeros(no_pts-2,1);zeros(no_pts-2,1);zeros(no_pts-
2,1)];
    end
    lnfn = [lnfn;lnfnout];
end

%Solve for Eigenfunction
ef = (C)\lnfn;

%Recover Eigenfunctions
efu = 0;
efv = 0;
eft = 0;
for s=-no_modes_stab:1:no_modes_stab
    %s=0;
    spos = s+no_modes_stab;
    xpos = 0;
    expo = exp(i*s*a*xpos);
    efu = efu + [0;ef(spos*(3*no_pts-6)+1:spos*(3*no_pts-6)+no_pts-
2);0]*expo;
    efv = efv + [0;ef(spos*(3*no_pts-6)+no_pts-2+1:spos*(3*no_pts-
6)+no_pts-2+no_pts-2);0]*expo;
    eft = eft + [0;ef(spos*(3*no_pts-6)+2*no_pts-4+1:spos*(3*no_pts-
6)+2*no_pts-4+no_pts-2);0]*expo;
end

```